1-1-2011

Mechanisms of persistent translation arrest following global brain ischemia and reperfusion

Jill Theresa Jamison
Wayne State University,

MECHANISMS OF PERSISTENT TRANSLATION ARREST FOLLOWING GLOBAL BRAIN ISCHEMIA & REPERFUSION

by

JILL T. JAMISON

DISSERTATION

Submitted to the Graduate School

of Wayne State University,

Detroit, Michigan

in partial fulfillment of the requirements

for the degree of

DOCTOR OF PHILOSOPHY

2012

MAJOR: PHYSIOLOGY

Approved by:

_____

Advisor Date

_____

_____

_____

DEDICATION

This dissertation is dedicated to the family and friends who have supported me throughout this journey.

To Dave Sheldon, my husband, best friend and "funny guy", it has been your constant support from the very beginning that has allowed me to follow my dreams. Thank you for your love, patience, and kindness. Thanks for always providing a space for me to be myself. I love you and thank you for marrying me.

To my beautiful parents, Larry and Polly Jamison. I love you both so much. It is because of you that I am the person I am today. Any achievements in my life are simply because you did such a great job as parents.

To Dr. DeGracia, I truly feel if it were not for you, this experience would not be possible. It is not a secret that I think you are the most amazing mentor, I think I have thanked you every day for the last four years. You are an extraordinary teacher. You have a gift of explaining complex ideas, thoughts, and feelings in ways that people from all backgrounds can interpret the meaning for their own understanding. Thank you for your patience and all the incredible opportunities I have been able to experience since becoming your student. I look forward to the many years ahead of being your life-long student and friend.

To Rainey, Noah, Nicholas and Alex, you can be whatever you want to be. Just remember to follow your dreams, work hard, and always surround yourself with positive people that you know care, love and believe you.

To my dear friends:

Leah and Ben Zhang, there are no words that can express how thankful and appreciative I am for opening your house to me. Leah, you are an amazing friend, thank you for keeping me sane, introducing me to kimchi and Niki, and being my Mecca companion. You inspire me.

Colleen and Ron Borghi, my home away from home. I owe the physiology department, if for only one thing, it would be introducing me to you. I truly feel as though I am an extension of your family and so happy to finally have a sister!

Ruth Watts, thank you for being an amazing study buddy and always getting my jokes.

"The Physiology Girls", you all know who you are, I am so glad to have met you and have enjoyed our many food/wine related events.

Christine Cupps, thank you for helping me with whatever crisis that has arisen over the last four years and knowing what to do to fix it.

ACKNOWLEDGMENTS

I would like to thank the members of my dissertation committee, Dr. Donald DeGracia, Dr. Joseph Dunbar, Dr. Janice Schwartz and Dr. Jinsheng Zhang, as well as the entire Physiology department for their time and support of my education and research.

I want to especially thank Jie Wang, to whom I am indebted for her skillful and meticulous work in performing the 2VO/HT surgeries. She is not only a skillful surgeon, but the "right hand" to most day-to-day activities that take place within our laboratory. I am grateful for her support, hard work and most of all friendship.

I want to also thank Jeffrey Szymanski. We have been working in the lab together for about 3 years and he has been a great support to me; whether it is technical training, providing a wide-range of factoids, or moral support on the slopes of Boyne. Although we are very different in many ways, I think we work well together and I hope, with everything he has taught me, I have been able to reciprocate over the years.

I want to thank Dr. Foaz Kayali for all of the initial work he did developing the techniques for FISH and IF, as well as taking the time to teach me. In addition, I would like to thank Monique Lewis, Jennifer Rudolph and Dr. George Roberts who have all offered invaluable technical support. Finally, I would also like to say thanks to Dr. Christian Kreipke and Dr. Jose Rafols for their collaboration on the ET-1 project. Both Drs. Kreipke and Rafols were instrumental in my attending the 2010 International Stroke Conference. Special thanks to Steve Schafer, Michael Fronczak and Christian Reynolds for their technical support with the ET-1 model.

This work was supported by grants from the National Institutes of Health (NIGMS 2 R25 GM58905-10 IMSD and NINDS NS057167 DJD).

TABLE OF CONTENTS

LIST OF TABLES

LIST OF FIGURES

LIST OF ABBREVIATIONS

2VO/HT,	Bilateral Carotid Artery Occlusion Plus Hypotension Ischemia
40S,	Small Ribosomal Subunit
4E-BPs,	eIF4E- Binding Proteins
60S,	Large Ribosomal Subunit
ARE,	AU- Rich Elements
ATP,	Adenosine Triphosphate
CAr,	Cardiac Arrest
CA/R,	Cardiac Arrest and Resusitation
CA1,	Cornu Ammonis 1
CA3,	Cornu Ammonis 3
CamKII,	Ca2+ Calmodulin Kinase II
CHX,	Cycloheximide
CNS,	Central Nervous System
COX IV,	Cytochrome C Oxidase Subunit IV
COX-2,	Cyclooxygenase-2
CPR,	Cardiopulmonary Resuscitation
CVA,	Cerebrovascular Accident
DG,	Dentate Gyrus
DNA,	Deoxyribonucleic Acid
DND,	Delayed Neuronal Death
eIF2,	Eukaryotic Initiation Factor 2
eIF2α(P),	Phosphorylated form of Eukaryotic Initiation Factor 2 Alpha
eIF4,	Eukaryotic Initiation Factor 4
eIFs,	Eukaryotic Initiation Factors
ELAV/Hu granules,	Embryonic Lethal Abnormal Vision
EM,	Electron Microscope
ER,	Endoplasmic Reticulum
ET-1,	Endothelin-1
FISH,	Fluorescent in situ Hybridization
GAPDH,	Glyceraldehyde-3-Phosphate Dehydrogenase
GDP,	Guanosine Diphosphate
GEF,	Guanine Nucleotide Exchange Factor
GM130,	Cis-Golgi Matrix Marker 130 kilodaltons
GTP,	Guanosine Triphosphate
hnRNP,	Heavy Nuclear Ribonucleoprotein Complexes
hr,	Hours
HSC-70,	Constitutive Heat Shock Protein 70
HSP,	Heat Shock Protein
I/R,	Ischemia and Reperfusion
IEG,	Immediate Early Genes
IF,	Immunofluorescence
IPC,	Ischemic Precondition
IRES,	Internal Ribosome Entry Sites
m7G,	7-Methylguanylate Cap
MAP,	Mean Arterial Pressure
Met,	Methionine

min,	Minutes
MRI,	Magnetic Resonance Imaging
mRNA,	Messenger Ribonucleic Acid
mRNPs,	Messenger Ribonucleoprotein Particles
NC,	Nitrocellulose
NeuN,	Neuronal Nuclei
NF H/M,	Neurofilament Heavy and Medium Weight Chains
NIC	Nonischemic Control
NO,	Nitric Oxide
PABP,	Polyadenylated Binding Protein
PAs,	Protein Aggregates
P-bodies,	Processing Bodies
PBS,	Phosphate Buffered Saline
PDI,	Protein Disulfide Isomerase
PDVF,	Polyvinylflouride
PFA,	Paraformaldehyde
PIC,	Pre-initiation Complex
PKC,	Protein Kinase C
PLA2,	Phospholipase A2
poly(A),	Poly-Adenylated mRNA
PTRO,	Post Transcriptional RNA Operon
RBP,	RNA Binding Proteins
ROS,	Reactive Oxygen Species
RPA,	Large 60S Ribosomal Subunit P Antigen
S6,	40 S Ribosomal Subunit Antisera
sec,	Seconds
SGs,	Stress Granules
SSC,	Saline- Sodium Citrate
TA,	Translation Arrest
TCA,	Trichloroacetic Acid
TGN38,	Trans-Golgi Network 38 kilodalton antigen
TIA-1,	T-Cell Internal Antigen-1
TNF-α,	Tumor Necrosis Factor alpha
tRNA,	Transfer Ribonucleic Acid
TTBS,	Tween 20 + Tris Buffered Saline
TTP,	Tristetraprolin
UTR,	Untranslated Region
α,	Alpha
β,	Beta
γ,	Gamma

CHAPTER 1

Background

Introduction

The topic of this dissertation is brain ischemia and reperfusion (I/R) injury. Brain I/R manifests clinically as stroke and cardiac arrest and resuscitation (CA/R). The clinical relevance of brain I/R injury is significant, affecting millions of individuals each year and costing billions of dollars worldwide in healthcare costs and lost productivity. However, the underlying causes of neuronal death are still unknown. To date, there are no effective clinical treatments to halt morbidity and mortality following brain ischemia. This work investigates novel mechanisms of I/R injury in the hope of contributing to the development of effective therapies against this devastating disease.

This work focuses specifically on the inhibition of protein synthesis (or translation arrest, TA) in neurons following global brain I/R. I do so because the inhibition of protein synthesis in neurons is one of the most reliable predictors of outcome: recovery of protein synthesis indicates survival; lack of recovery of neuronal protein synthesis always accompanies neuronal death. In spite of being a well-studied aspect of brain I/R injury, the exact mechanism of TA is unknown and thus, so is the link between TA and neuronal death. In this chapter, I discuss existing studies of TA following brain I/R in the context of advances in the molecular biology of protein synthesis. These include: (1) phenomenological relationship of TA to cell death, (2) studies of initiation factors and TA and (3) TA and stress responses. These investigations however, provide an incomplete understanding of the process. Important questions remain regarding the mechanisms and role of TA in the post-ischemic response.

Data collected from our lab, as well as others in the field, indicates that post-ischemic TA may be a marker of the genetic reprogramming of post-ischemic neurons to a stress response

phenotype dedicated to exclusive translation of stress-induced mRNAs. Based on the current understanding of the molecular biology of translation regulation, I present a novel hypothesis of post-ischemic TA that involves the regulation of mRNA, or ribonomics, in the control of protein synthesis. In subsequent chapters, I present data showing persistent inhibition of protein synthesis, in vulnerable post-ischemic neurons, is due to a ribonomic mechanism. This dissertation is therefore significant for solving the problem of why protein synthesis remains inhibited in a prolonged fashion in post-ischemic neurons destined to die.

Brain Ischemia and Reperfusion

Ischemia is the pathological reduction or cessation of blood flow to a tissue. Reperfusion is the restoration of blood. Specific forms of cell damage are induced by either ischemia or reperfusion as discussed below. This damage differentially affects various neuronal types where some are able to recover and others die.

There are two types of brain ischemia: focal and global. Focal ischemia involves a circumscribed area of the brain, whereas global ischemia involves the entire brain. Both forms of ischemia negatively affect brain structure and function ranging from serious brain damage to mortality.

Focal Brain Ischemia

The most important clinical manifestation of focal brain ischemia is stroke. Also known as cerebrovascular accident or CVA, stroke is the leading cause of adult disability and the third cause of death worldwide following heart disease and cancer. Ischemic stroke occurs when the blood supply to an isolated area of the brain is restricted or eliminated. Focal ischemic injury consists of a core region of dead cells surrounded by a zone of hypoperfused cells called the penumbra region (Muir et al., 2006). The core is closest to the occluded vessel; consequently, this will result in death of all cells in that region. The cells defining the penumbra die hours to

days after the initial insult. Neuronal death of the penumbra that occurs in a delayed fashion, following ischemia, is referred to as delayed neuronal death (DND).

Global Brain Ischemia

Global ischemia involves cessation of blood flow to the entire brain. Clinically, global ischemia manifests during cardiac arrest (CAr). CAr occurs when the mechanical activity of the heart ceases and is commonly confirmed by the absence of circulation (Roger et al., 2011). In cases in which life saving maneuvers are administered through techniques like cardiopulmonary resuscitation (CPR), defibrillation and/or administration of various pharmacologic agents, these acts of resuscitation, if successful, reintroduce brain blood flow (this process of reperfusion is further discussed below).

The anatomy of damage after global ischemia is different from that of focal ischemia. For example, the pattern or morphological alterations of brain damage in global ischemia are highly dependent on time. Less than 4 minutes (min) of ischemia results in no obvious brain damage. With 30 min or more of global ischemia, widespread necrosis results in brain death. Within the window of approximately 4 to 30 min, a gradation of ischemic impact occurs within specific neuronal populations (Hossmann and Kleihues, 1973; White et al., 1985). Neurons most vulnerable are those of the Cornu Ammonis 1 (CA1) layer of the hippocampus, followed by layers III and V of the cerebral cortex, cerebellar Purkinje cells, thalamic and striatal regions (Jenkins et al., 1981; White et al., 1993). Selectively vulnerable neurons die by DND between 24-72 hours (hr) following reperfusion, whereas glia and vascular cells survive (Kirino, 1982).

The mechanisms underlying DND are unknown. Some investigators have associated DND with apoptosis (Nitatori et al., 1995), but if this were true, then apoptosis inhibitors would prevent DND, which they do not (Deshpande et al., 1992; Gillardon et al., 1999). The nature of DND is considerably more complex than classical apoptosis (MacManus and Buchan, 2000).

The present dissertation will investigate mechanisms involving TA believed to play a critical role in DND.

Clinical Significance of Global Brain Ischemia

Sudden CAr is the leading cause of death for adults forty years and older (American Heart Association, 2009; Roger et al., 2011). It is estimated that roughly 250,000 Americans die every year from CAr (Forcina et al., 2009). Figure 1 reflects the number of fatalities contributed by house fire, prostate cancer, breast cancer and automobile accidents; the sum of these contributes only half of the total lives lost to CAr each year (Temecula, 2009).

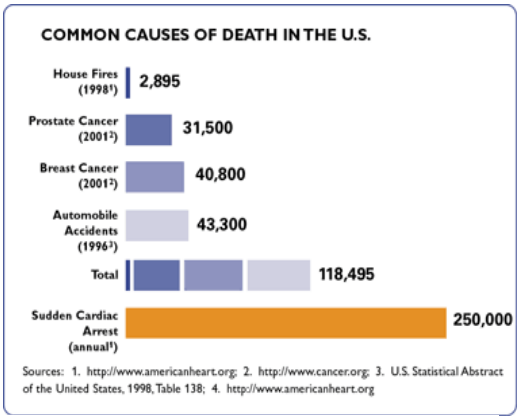

Figure 1. Common causes of death in the U.S. From the Temecula, CAr website. Used under the Fair Use in Copyright Law (Temecula, 2009).

The rate of patient survival after an in-hospital CA/R is 27% in children and 18% in adults (Lloyd-Jones et al., 2009). Those individuals resuscitated following CAr, who are not diagnosed brain dead, often suffer serious brain damage. The extent of damage correlates with the duration of ischemic insult. In an observational cohort study, of the 1700 adults diagnosed with primary CAr, only 1.4% of those individuals had intact neurologic faculties (Eckstein et al., 2005). Roughly, 70,000 patients a year survive from CAr through life saving resuscitation technologies. Of these, only 3-10% maintains their quality of life. A staggering 60% die in the hospital, as a consequence of brain damage. The remaining individuals require some form of assistance to maintain a standard quality of life (Lloyd-Jones et al., 2009).

Established Mechanisms Underlying Brain Ischemia/Reperfusion Injury

Since no effective clinical therapies exist to halt DND, this suggests our understanding of the process is not fully known. However, many injury mechanisms have been identified and

collectively are referred to as the "ischemic cascade", represented in Figure 2 (Lyden and Wahlgren, 2000). Brain damage following I/R results from: (1) damage that is initiated during the ischemic period and (2) damage initiated during reperfusion (each is discussed in turn).

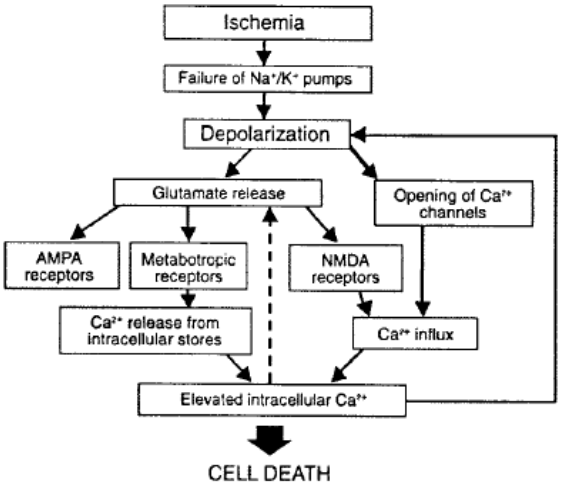

Figure 2. Overview of ischemic cascade. (Lyden and Wahlgren, 2000).

Overview of Ischemic Injury

Ischemic injury begins when levels of glucose and oxygen dramatically decrease following loss of blood to the brain. The immediate consequence is a depletion of adenosine triphosphate (ATP). The loss of ATP occurs rapidly with a 50% decrease in the first min of ischemia and complete depletion by 4 min (Krause et al., 1988). This in turn activates a cascade of events, with the loss of ATP inhibiting all ATP dependent processes within the brain. The primary response of ATP loss is the inhibition of Na^+-K^+ ATPase. This pump functions to regulate electrochemical gradients and membrane potentials that are crucial for promoting optimal neuronal function. Without the activity of the Na^+-K^+ ATPase, Na^+ and K^+ begin to equilibrate and the required ion gradients needed to maintain homeostasis are lost. This effect triggers the loss of the Na^+ gradient; further affecting other processes that are dependent upon Na^+, such as glucose and amino acid transport. Perhaps most important, the Ca^{2+} gradient, also begins to dissipate. The result of ion equilibration across the membrane is an overall net depolarization that causes release of neurotransmitters and further stimulates depolarization of the cell (Simon et al., 1984). The consequence of these events produces a state of excitotoxicity.

Excitotoxicity

In normal situations, release of glutamate from presynaptic neurons binds to NMDA (N-

methyl-D-asparate) and AMPA (α-amino-3-hydroxy-5-methyl-4-isoxazole propionic acid) receptors on postsynaptic neurons (Sattler and Tymianski, 2001). Binding of these receptors causes rapid influx of Na^+ and Ca^{2+} via receptor operated ion channels, which in turn, causes depolarization (Xie et al., 1995). Depolarization further induces Ca^{2+} influx through voltage gated Ca^{2+} channels as well as the release of Ca^{2+} from intracellular compartments (Lipton, 1999). Increases in intracellular Ca^{2+} causes further neurotransmitter release thus perpetuating the cycle.

During ischemia, this highly regulated system is forced into an uncontrolled state. Without ATP-dependent mechanisms to reset the cell back to normal, excitotoxicity continues until either reperfusion reintroduces necessary metabolic demands, or the cell dies by bursting due to massive ion influx. These factors are linked to the necrotic death of neurons during ischemia (Hertz, 2008). However, with moderate ischemic durations (~10-20 min), similar to those seen clinically with CA/R, the ionic influx of Na^+ is not great enough to burst the cell. Rather, it is thought that the unregulated state of intracellular Ca^{2+} may be one of many factors contributing to DND.

Consequence of Increased Intracellular Ca^{2+} During Ischemia

The Ca^{2+} ion plays a critical and central role in cell physiology; therefore, its intracellular concentration must be tightly regulated. Some examples of Ca^{2+} regulated processes are: signal transduction pathways, action as a second messenger, release of neurotransmitters, participation in enzymatic activity, calcium-induced calcium release, and contribution to membrane potentials across excitable membranes. As such, multiple regulatory systems are involved in the control of Ca^{2+} in order to properly facilitate these functions (Boron, 2005). In ischemia, Ca^{2+} concentrations are uncontrolled and without intervention, this state activates a number of pathological processes.

During ischemia, large concentration changes in Ca^{2+} affect both extracellular and intracellular compartments. Specifically, during global ischemia, at the time of anoxic depolarization, extracellular levels of Ca^{2+} abruptly fall from normal concentrations of ~1.2 mM to ~0.1 mM, roughly 60-90 seconds (sec) after the start of ischemia (Siemkowicz and Hansen, 1981; Benveniste et al., 1988; Xie et al., 1995). It has further been shown, that Ca^{2+} moves into the intracellular space at a higher rate, increasing 70% during anoxia in the vulnerable CA1 region of the hippocampus; as compared to 30% in ischemia resistant dentate gyrus (Kass and Lipton, 1986). Large increases in intracellular levels of Ca^{2+} were recorded by microelectrodes in the CA1 and Cornu Ammonis 3 (CA3) hippocampal neurons. Initially, small increases of 10-30 nM were seen in the first minute of ischemia. Within the next 2-3 min, cytosolic Ca^{2+} within CA1 hippocampal neurons raised from 90 nM to 30 μM. These results were further verified with incorporation of MK801, a blocking agent that binds to NMDA receptors. By blocking NMDA receptors, Ca^{2+} channels could not open and Ca^{2+} influx was inhibited (Silver and Erecińska, 1990). In another study using a Confocal Laser Scanning Microscope, a low affinity Ca^{2+} dye was applied to brain slices and a rapid increase in intracellular Ca^{2+} from 60 nM to 24 μM was detected (Grøndahl and Langmoen, 1998). These results further substantiate the findings that increases in intracellular Ca^{2+} concentrations occur during ischemia.

With these dramatic changes in Ca^{2+}, normal homeostatic regulation and the functions associated with Ca^{2+}, are drastically altered causing deleterious effects to the cell. One example, is represented by a family of Ca^{2+}-activated intracellular cysteine proteases called calpains. There are two main classes of calpains that have been isolated in protein form: μ-calpain (micromolar Ca^{2+}- requiring) and m-calpain (millimolar Ca^{2+}- requiring) (Saido et al., 1994). Calpains are located exclusively within the intracellular compartment and seem to associate with subcellular organelles such as the cytoskeleton, vesicles and the plasma membrane (Goll et al.,

2003). Mechanisms for the activation of calpain have not been clearly established, however initial activation of μ- and m- calpain (10μM and 1mM, respectively) have shown to be associated with high concentrations of Ca^{2+} (Lipton, 1999). Localization of calpain has been found in neuronal populations that have selective vulnerability. μ-calpain has been found to be distributed throughout the neuron including spines, dendrites, cell somata and axons (Perlmutter et al., 1988; Rami, 2003). Within the rabbit, μ-calpain was found in the pyramidal neurons, whereas m-calpain, which is far less sensitive, was localized within interneurons, which are known typically for showing greater resistance to ischemic damage (Fukuda et al., 1990). Additionally, calpain activity increases in neurons during both global and focal ischemia (Neumar et al., 2001). Important substrates of calpain include eIF-4G and eIF4E (Neumar et al., 1998; DeGracia, 2004) which are two examples of eukaryotic initiation factors (eIFs) that are important for translation (discussed in detail below).

Increased intracellular Ca^{2+} is also involved in the activation of phospholipase A_2 (PLA_2) (Sun et al., 2004). Phospholipases are enzymes that release fatty acids and are involved in cell signaling processes (Dennis, 1994). PLA_2 is involved in the conversion of free fatty acids either into arachidonic acid, a proinflammatory mediator, or in the reincorporation of fatty acids into the plasma membrane (Cummings et al., 2000). In the unregulated environment caused by ischemia, PLA_2 leads to increased production of proinflammatory mediators through which arachidonic acid is converted into leukotrienes or prostaglandins (Murakami et al., 1997). Cyclooxygenase-2 or COX-2 is the enzyme responsible for arachidonic acid conversion (Cummings et al., 2000) into prostanoids, a well-known biochemical event associated with cerebral ischemia, edema and other central nervous system (CNS) disorders (Sairanen et al., 1998). Sairanen et al. (1998) found that initial responses of COX-2 following focal ischemia were predominantly in neurons at the site of the core. This localization correlates with the idea

that production of prostanoids and free radicals aggravate tissue injury during cerebral ischemia. This suggests that the proinflammatory responses of COX-2, in addition to other deleterious effects previously mentioned, contribute to excitotoxicity.

Other factors associated with abnormal increases in intracellular Ca^{2+} concentration include kinases, such as protein kinase C (PKC) and Ca^{2+}-calmodulin kinase II (CamKII) (Matsumoto et al., 2004). The altered regulatory state of these systems upsets the integrity of neuronal signaling. Consequently, there is an overproduction of neuronal nitric oxide synthase resulting in overproduction of nitric oxide (NO) (Beckman et al., 1990). Finally, increased concentration levels of Ca^{2+}, up regulates deoxyribonucleic acid (DNA) degradation through activation of DNA endonucleases (McCabe et al., 1992).

Each of the affects listed above share a similar quality; altered Ca^{2+} regulation resulted in their initial activation. Currently, we have a better understanding on the effects of altered Ca^{2+} regulation in neurons; following ischemia, Ca^{2+} regulation depends largely on duration of ischemia followed by subsequent reperfusion. In cases in which ischemia durations are shorter, followed subsequently by reperfusion, Ca^{2+} levels have been shown to return to resting levels. Yet, selectively vulnerable neurons still go on to die by 48-72 hr (Silver and Erecińska, 1992) . This work, along with the many others involved in studying the mechanisms of the ischemic cascade, all provided significant contributions regarding the fate of the cell. However, it still did not explain DND of selective neurons following reperfusion. I now turn to details related to reperfusion injury.

Overview of Reperfusion Injury

Upon the return of blood flow following ischemia (reperfusion), blood enters a massively altered system that further compounds the ischemic damage. Following reperfusion, there is an initial increase in blood flow (hyperemia) that is due to the buildup of vasodilating metabolites.

ATP levels recover relatively rapidly, within the first 10 min. Recovery of ~70-80% occurs throughout the reperfusion period (Pulsinelli and Duffy, 1983; Cardell et al., 1991). With the increase in ATP, ion gradients are re-established by 20 min of reperfusion (Hoehner et al., 1987). However, a hypoperfusion occurs within ~60 min of reperfusion (Krause et al., 1988). At this point the metabolic demand of the brain is very high, and the actual metabolic rate is depressed roughly 50% or more for at least 6 hr after ischemia (Mies et al., 1990). This reflects an uncoupling of blood flow with the metabolic need of the brain during reperfusion. Although (Mies et al., 1990) were able to show long lasting regional disturbances in regional flow and metabolism coupling, they were not able to establish a relationship between these differences and post-ischemic hypoperfusion. Thus this reveals that DND is not a consequence of hypoperfusion mediated through secondary tissue hypoxia.

Following the post-ischemic response, further damage ensues during reperfusion that compounds the initial injuries, originally fostered by ischemia. Damages associated with reperfusion injury include reactive oxygen species, lipid peroxidation, further altercations in cell signaling pathways and persistent TA.

Reactive Oxygen Species

Following reperfusion there is a large burst of free radical production with the rerelease of oxygen. Reintroducing oxygen in the presence of xanthine oxidase and cyclooxygenase produces free radicals or reactive oxygen species (ROS) (McCord, 1993). Formation of ROS produces numerous consequences that are detrimental to the cell.

As previously mentioned, an increase in intracellular Ca^{2+} concentration triggers the increase in arachidonic acid. As seen in Figure 3, cyclooxygenase catalyzes arachidonic acid producing prostaglandin G (Ulrich et al., 2006). Prostaglandin G is peroxidized further, producing a free radical and prostaglandin H (Krause et al., 1988). This results in the oxidative

degradation of plasma membranes whereby free radicals strip electrons from membrane phospholipids. This process of lipid peroxidation causes drastic changes to both the permeability and fluidity of the plasma membrane (Farber, 1982). These effects alter fatty acid side chains causing cross-linking, in addition to polymerization of membrane lipids and proteins (Freeman and Crapo, 1982). Lipid peroxidation has also been shown to inhibit Na^+-K^+ ATPase (Demopoulos et al., 1980). In the CA/R model (15 min ischemia, 4 and 8 min reperfusion), there was an inability to regulate Na^+, K^+, and Ca^{2+} across cellular membranes. This effect was thought to be attributed to lipid peroxidation (Hoehner et al., 1987).

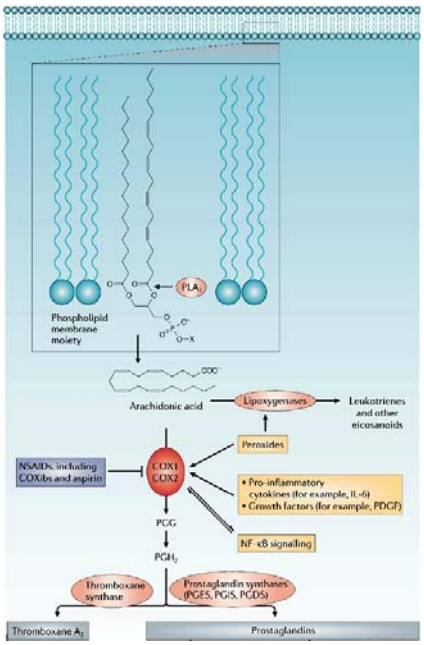

Figure 3. Role of COX enzymes in the formation of prostanoids. (Ulrich et al., 2006)

While there seems to be a strong association between ROS formation and lipid peroxidation evoking cell death, experimental evidence has altered this concept. NB-104 cells were given anti-radical strategies along with arachidonate or a lipid peroxidizing promoting agent (CumOOH). In control studies, both arachidonate and CumOOH induced similar forms of cell death in NB-104 cells, but with anti-radicals, only arachidonate was able to induce cell death (O'Neil et al., 1999). These results indicate arachidonate has effects, not involving radicals, which provide an alternate pathway leading to cell death. Thus, this indicates ROS are not the sole contributing factor, but rather part of a larger cell death response system.

Translation Arrest During Reperfusion

(Kleihues and Hossmann, 1971) first discovered inhibition in protein translation during reperfusion. Through a series of experiments they were able to show: (1) a decrease of

incorporated radioactive leucine in an *in vitro* translation reaction using 30 min reperfused brain homogenates compared to controls and (2) during reperfusion a dissaggregation of polysomes both visually using an electron microscope (EM) and biochemically through running polysome profiles using a sucrose density gradient.

From this work, Kleihaus and Hossman were able to demonstrate that during ischemia, ribosomes remained attached to messenger ribonucleic acid (mRNA) with no evidence of increased monomeric subunits. This contributed to the idea that during ischemia there is a complete breakdown of energy producing metabolism, one consequence of which is to "freeze" polyribosomes. Thus, there is a halt in protein synthesis, by which both initiation and elongation are in an arrested state during ischemia. Following reperfusion, the number of polyribosomes began to decrease significantly. This observation suggested that inhibition of protein synthesis during reperfusion could be attributed to the inhibition of translation initiation (Kleihues and Hossmann, 1971).

Following this initial study, many labs confirmed these findings and characterized the fact that protein synthesis is inhibited in the brain for several hours following reperfusion. A very important discovery was made at this stage; specific brain regions survive and recover from TA, whereas vulnerable brain regions do not recover from TA and invariably die by DND (Hossmann, 1993). This event is represented in Figure 4, in which autoradiographs of *in vivo* protein translation was taken in gerbils following global brain I/R.

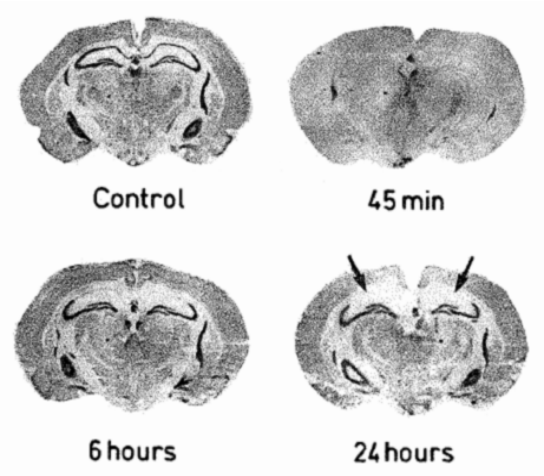

Figure 4. Autoradiographs of radioactive amino acid incorporation into brains of reperfused animals. Arrows identifying failed recovery of translation within CA1 neurons (Hossmann, 1993).

Notice at 5 min ischemia and 45 min reperfusion there is a complete inhibition of translation throughout the brain. Within 6 hr of reperfusion the vast majority of protein translation is recovered with the exception of the CA1 hippocampal region. Continuing through 24 hr of reperfusion, CA1 failed to recover translation (identified in Figure 4 by arrows) and this region will go on to die by 72 hr reperfusion.

The discovery that cell death correlates with TA suggests that the mechanisms of TA play a causal role in cell death. As a result, understanding the mechanisms involving this process became a considerable goal for many laboratories including our own. To better understand the results and knowledge acquired thus far, it is first necessary to summarize information regarding the process of translation initiation and its regulatory elements.

Protein Translation

Protein translation is comprised of three stages: initiation, elongation, and termination. Initiation involves a number of factors that function collectively to promote assembly of mRNA, small 40S ribosomal subunit, large 60S ribosomal subunit and methionine conjugated initiator transfer ribonucleic acid (tRNA) (Met-$tRNA_i$), represented in Figure 5. Once the complex is produced, factors involved in elongation begin to move the ribosome along mRNA, attaching the appropriate amino acids as each triplet codon is read. As the nucleotide sequence is read in the 5' to 3' direction the translated polypeptide sequence elongates. Termination proceeds once tRNA binds to a stop codon, signaling elongation is complete. Along the way, chaperones are involved in folding proteins into their functional three dimensional conformations. The remainder of this topic will focus on the initiation factors involved in translation initiation.

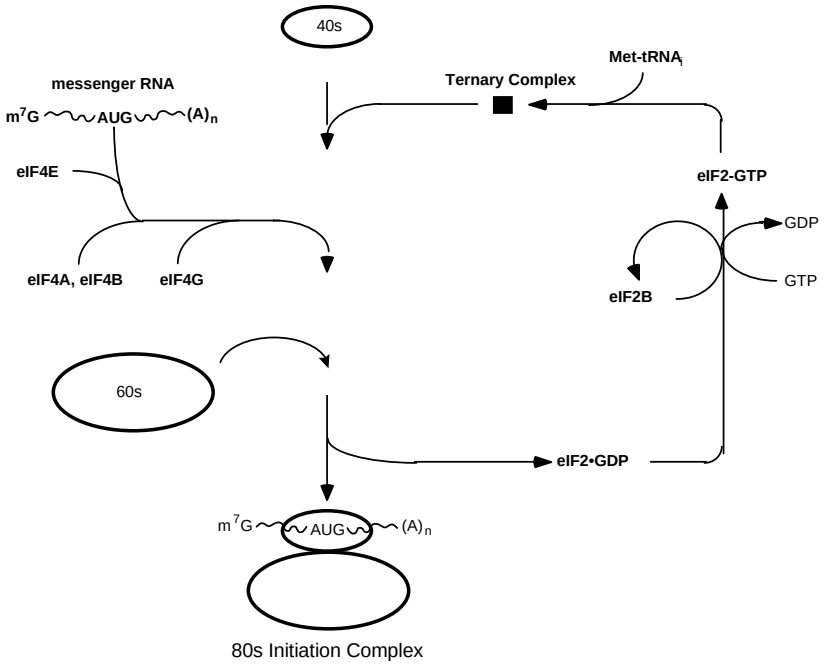

Figure 5. Abbreviated steps in translation initiation.

Rate-Limiting Steps of Translation Initiation

Two rate limiting steps are involved in translation initiation (Merrick, 1990). The first step involves eukaryotic initiation factor 2 (eIF2) catalyzing the delivery of the first amino acid, methionine (Met). The second rate limiting step involves the eukaryotic initiation factor 4 (eIF4) catalyzing the delivery of mRNA to the initiation complex. By altering the activity of eIF2, the cell controls the global rate of total protein synthesis. Without eIF2, the initiator Met, is not delivered. Altering the activity of eIF4, fine tunes how much mRNA and specifically, which mRNA will be tranlated. Thus, the regulation of translation initiation is highly dependent on the activity of eIF2 and eIF4.

Function and Regulation of eIF2

eIF2 is a heterotrimer comprised of three subunits: alpha (α), beta (β) and gamma (γ). The β and γ subunits function as catalytic sites, whereas the α subunit functions as a regulatory component. To begin initiation, eIF2 must first form a complex with guanosine triphosphate

(GTP). Once bound to GTP, eIF2 can then bind to Met-tRNAi to form the ternary complex (eIF2-GTP-Met-tRNAi). The ternary complex then binds the small ribosomal subunit (40S) to form the 43S pre-initiation complex (PIC). The 43S PIC is recruited to the capped 5' end of mRNA which it then partners to the eIF4F complex to form the 48S PIC. The Met-tRNAi is tethered to the PIC by the GTP bound eIF2 complex. The PIC scans the mRNA from the 5' end to the 3' end for the start codon, AUG. Once AUG is found, scanning stops, and hydroylsis of GTP within the ternary complex occurs. eIF2 is now bound to guanosine diphosphate (GDP), which is released along with other initiation factors. With the loss of these factors the 48S PIC is available to bind with the large 60S ribosomal subunit forming the completed 80S complex. This step marks the end of initiation and the beginning of elongation (Merrick, 1990; Sonenberg and Hinnebusch, 2009).

Previously, it was mentioned that overall rate of protein synthesis is regulated by eIF2. This is accomplished when the alpha subunit on eIF2 (eIF2α) becomes phosphorylated [eIF2α(P)] on Serine 51. Upon phosphorylation, the alpha subunit binds eIF2B with a 150-fold greater affinity as compared to its unphosphorylated counterpart eIF2α (Rowlands et al., 1988). Thus eIF2α(P) sequesters eIF2B, inhibiting its normal role as a GEF. Inhibition of eIF2B results in accumulation of eIF2-GDP which prevents ternary complex formation and thereby renders ribosomes inactive by preventing delivery of Met-tRNAi. The inability of eIF2-GTP to form is the cause of eIF2α becoming phosphorylated. This phosphorylated event is responsible for inhibiting protein synthesis. With a molar concentration of 5:1 between eIF2 and eIF2B respectively, it would only take about 20% of eIF2α(P) to cause an almost complete TA (Oldfield et al., 1994; Burda et al., 1994).

In order for subsequent rounds of initiation to occur, GDP must be replaced with GTP on eIF2. Consequently, a guanine nucleotide exchange factor (GEF), eIF2B functions to exchange

GDP for GTP, and in so doing, recycles eIF2-GTP. The role of eIF2B is crucial for eIF2 to properly function and thus resets the stage for further initiation. The stoichiometry of eIF2 to eIF2B is a factor of 5:1 in most cells (Oldfield et al., 1994). Thus for initiation to continue there must be an adequate quantity of eIF2B available.

Function and Regulation of eIF4F

eIF4F is a heterotetramer comprised of: eIF4A, eIF4B, eIF4E and eIF4G. As a complex, the function of eIF4F is to deliver mRNA to the 43S PIC. eIF4F binds directly to the 7-methyl guanylate cap (m7G) at the 5' end of mRNA via eIF4E. eIF4A in conjunction with eIF4B, has RNA helicase activity that promotes unwinding the mRNA secondary structure at the 5' untranslated region (UTR) in order to promote the ribosome to bind and scan mRNA for the initiation codon. eIF4G is a large scaffolding protein that, in concert with other subunits on eIF4F, binds directly to the ribosome. In additon, eIF4G also interacts with polyadenylated binding protein (PABP), a protein that binds with high affinity to the 3' end of the polyadenylated (pA) tail of mRNA. Thus this interaction between eIF4G and PABP (Figure 6) influences the circularization of mRNA (Sonenberg and Dever, 2003). Regulating eIF4F promotes regulation of a variety of mRNAs that are being delivered to the ribosomes. The main targets in alterring eIF4F activity focus on individually regulating eIF4E and eIF4G directly. Table 1 reviews each of the eukaryotic initiation factors involved in the initiation of translation (Hellen and Sarnow, 2001).

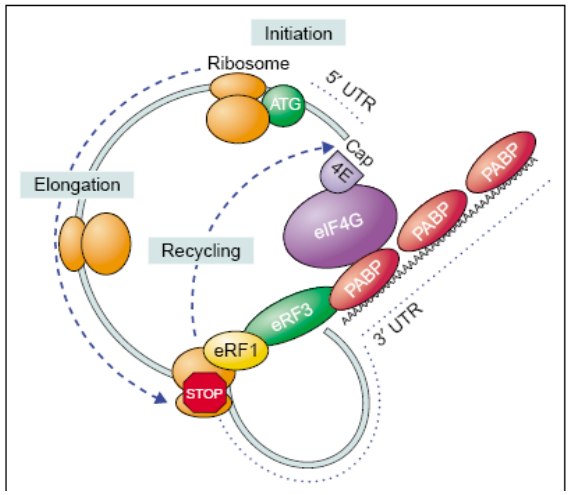

Figure 6. Diagram depicting the circularization of mRNA. (Sonenberg and Dever, 2003)

Table 1. Characteristics of translation initiation factors.

Name	Function
eIF1	Enables ribosomes to scan; destabilizes aberrant initiation complexes
eIF1A	Promotes binding of Met-tRNA$_i$ to 40S subunit; promotes ribosomal scanning
eIF2	GTP-dependent binding of Met-tRNA$_i$ to 40S subunit; GTPase
eIF2B	Guanine nucleotide exchange factor for elF2
eIF3	Ribosomal dissociation; promotes binding mRNA and Met-tRNA$_i$ to 40S
eIF4A	RNA-dependent ATPase; RNA helicase
eIF4B	Promotes RNA helicase activity of elF4A, elF4F
eIF4E	m^{7}G cap-binding subunit
eIF4G	Binds RNA, PABP, elF4E, elF4A, elF3
eIF4F	elF4E/4A/4G heterotrimer: binds m^{7}G caps, RNA helicase
eIF5	Activates GTPase activity of elF2
eIF5B	Ribosomal subunit joining; GTPase

Simplified from Hellen & Sarnow, 2001.

Regulation of eIF4E

The regulation of eIF4E occurs in at least three ways: transcription, phosphorylation and binding of inhibitory proteins. There are several forms of evidence indicating that eIF4E is regulated by gene transcription (Gingras et al., 1999). There is correlational evidence linking overexpressed MYC cells (protooncogenes) with an increase level of eIF4E mRNA (Rosenwald et al., 1993b, 1993a). Evidence linking MYC to the upregulation of eIF4E transcription was established by identifying two MYC binding sites in the promoter region of eIF4E (Jones et al., 1996). These results are interesting in that MYC is a potent regulator of cellular growth. The extent of how MYC and eIF4E are involved together in regulating cellular growth are undetermined at this time.

Regulation of eIF4E through phosphorylation is influenced by extracellular stimuli such as hormones, growth factors, and mitogens. Each of these promote cellular growth and enhance protein translation rates. Patterns of eIF4E phosphorylation occur during the G1 and S phases of the cell cycle that coincidentally correlate with translation activity (Fan and Penman, 1970; Bonneau and Sonenberg, 1987). Notably, eIF4E becomes dephosphorylated after heat shock in

concordance with a decrease in the global rate of translation (Duncan and Hershey, 1989).

There is not always a direct connection between eIF4E phosphorylation and increases in translation rate. For instance, cells introduced to certain forms of stress, i.e. arsenite or anisomycin, actually induce increases in eIF4E phosphorylation and decreases in protein translation (Morley and McKendrick, 1997; Wang et al., 1998). It may be suggested that in such circumstances, other factors like eIF2α(P) may be involved. It could be possible that certain stress responses trigger the phosphorylation of eIF4E in order to stimulate translation of stress induced proteins as a compensatory mechanism.

eIF4E is also regulated by a family of repressor proteins called eIF4E-binding proteins (4E-BPs). 4E-BPs do not appear to inhibit cap binding to eIF4E but rather inhibit the activity of eIF4E to associate with eIF4G, thus preventing formation of eIF4F complex. 4E-BP binding to eIF4E is highly regulated upon 4E-BP phosphorylation. In cases when 4E-BP is phosphorylated, it is unable to bind to eIF4E, permitting formation of the eIF4F complex (Haghighat et al., 1995). However, in cases of hypophosphorylation or dephosphorylation, 4E-BP has sites available to bind to eIF4E, blocking the binding of eIF4G and decreasing the rate of translation. Certain extracellular stimuli have been found to increase phosphorylation of 4E-BPs: hormones, growth factors, mitogens, cytokines and G-protein receptor agonists (Gingras et al., 1999). In certain cell types, it has been shown that certain forms of heat shock can reduce phosphorylation of 4E-BPs (Feigenblum and Schneider, 1996; Vries et al., 1997).

Regulation of eIF4G

Several studies have addressed phosphorylation as a mechanism involved in the regulation of eIF4G (Morley and Traugh, 1990, 1993; Morley and Pain, 1995). However, the stimuli that induce phosphorylation, the pathways involved, the sites of phosphorylalation and the functional consequences are not clearly identified (Gingras et al., 1999). There is evidence

that increases in phosphorylation of eIF4G correlate to increases in eIF4F complex formation. This suggests that phosphorylation of eIF4G is involved not only in the regulation of eIF4F formation, but also controlling the actual amount of complex (Bu et al., 1993).

Picornaviruses induce proteolysis of eIF4G in order to both enhance viral translation and inhibit the host cell from performing normal protein synthesis. The viral action appears to mimic normal physiological mechanisms of eIF4G cleavage (Svitkin et al., 2001) and thus provides further evidence in the characterization and regulation of eIF4G.

Reperfusion Induced Changes in Initiation Factors

eIF2 and eIF4 have been extensively investigated following brain I/R. Evidence highlighting this body of work is provided below.

Changes in eIF2 During Reperfusion

The first body of molecular study of translation initiation was performed by Drs. (Hu and Wieloch, 1993). This paper was the first to measure eIF2 activity following brain I/R. In this study, rat brain homogenates demonstrated inhibition of ternary complex formation following 15 min of ischemia and either 30 min or 1 hr reperfusion. They found that adding eIF2B could improve ternary complex formation and concluded that eIF2B was inhibited, providing a mechanism of overall translation inhibition following brain I/R (Hu and Wieloch, 1993).

However, the work done by Burda and colleagues challenged the conclusion of Hu and Wieloch (1993), by showing a large increase in the phosphorylation of eIF2α following brain I/R (Burda et al., 1994). This also would result in decreased ternary complex formation; phosphorylatioon of eIF2□ was not measured in the Hu and Wieloch (1993) study.

Following these initial studies, DeGracia et al. (1996) confirmed the results of Burda et al. (1994), finding 30% of eIF2α was phosphorylated 90 min following reperfusion (DeGracia et al., 1996). In 1997, (DeGracia et al., 1997) was the first to develop a phospho-specific antibody

against Serine 51 phosphorylated eIF2α. They were able to immuno-map the distrubution of eIF2α(P) throughout the reperfused brain. Their results showed eIF2α(P) in all post-ischemic neurons, with levels of eIF2α(P) returning to control values by 4 hr reperfusion. (DeGracia et al., 1997) revealed the peak of eIF2α phosphorylation at 10 min reperfusion, with subsequent dephosphorylation over a time course of 6 hr returning back to basal conditions. These results indicated that TA caused by eIF2α(P) was a transient event that did not directly correlate with cell death.

In support of this line of thinking, (García et al., 2004) found animals showed rapid phosphorylation of eIF2α during reperfusion, whether or not they had been subjected to ischemic preconditioning (IPC). IPC is a phenomena in which an animal is exposed to a sublethal ischemic insult which subsequently protects it from a lethal dose of ischemia (Zhao et al., 2006). Since IPC does not evoke cell death, but eIF2α(P) was expressed, this would again support the idea that eIF2α(P) is not directly related to cell death (Davis and Patel, 2003).

Both results present a clear line of evidence that phosphorylation of eIF2α is not directly involved with cell death. Instead it appears to be responsible for an acute TA located throughout the brain that does not correlate with cell death of any kind. In a later section, we will further discuss what the acute phosphorylation of eIF2α may mean in the reperfused brain.

Changes in eIF4

The first evaluation of eIF4F following brain I/R showed no change in eIF4E, however there was evidence of eIF4G degradation (DeGracia et al., 1996). The degradation of eIF4G was verified by the Burda laboratory (Martín de la Vega et al., 2001). In additon they showed eIF4G degradation was highest in the CA1 region of the hippocampus. These authors also found eIF4E was degraded after prolonged ischemia (30 min), but no long term change in 4E-BP phosphorylation occured. (Neumar et al., 1998) showed μ-calpain or calpain I, was responsible

for the loss of eIF4G, which was confirmed by Garcia et al. (2004). The latter showed that phosphorylation of eIF4G decreased during ischemia but rapidly renormalized during reperfusion.

Interpretting the role of eIF4G is more challenging as compared to eIF2. The function and regulation of eIF2 during translation is more straight-forward because it is a well understood system; however, the regulation of eIF4G via phosphorylation and proteolysis, is not well understood. (DeGracia et al., 2002) speculated that changes in eIF4G following I/R would involve internal ribosome entry site (IRES)-based initiaton that occurs when eIF4G is degraded. IRES located on the mRNA are internal initiation sites that do not require normal cap binding in order to initiate protein translation (Hellen and Sarnow, 2001). However, a study by (MacManus et al., 2004) ruled out this possiblity by showing that mRNAs on ribosomes following brain I/R are not enriched in IRES. Clearly, the role of eIF4G in I/R is under-determined and significant questions remain as to its role, if any, in post-ischemic neuronal death.

Protein Aggregates

Dr. Hu has presented an alternative hypothesis that he calls cotranslation aggregation, to explain prolonged TA following brain I/R. It is well known that ubiquitin, a small highly conserved regulatory protein, is covalently bond to proteins that are "marked" for protein degradation or proteolysis by the proteosome (DeGracia and Hu, 2007). If ubiquinated, proteins accumulate at a rate that exceeds the rate of proteosome degradation. The result is an accumulation of abnormal proteins clumping together throughout the cytoplasm. During brain reperfusion, free ubiquitin levels drop very rapidly with the onset of blood flow (Hu et al., 2001). Dr. Hu discovered that free ubiquitin declines because cell proteins are rapidly tagged with ubiquitin early in reperfusion, forming large clusters of ubiquitinated proteins. He has identified

two types of structures that contain ubiquinated proteins in reperfused neurons. The initial large clusters he calls ubiquinated protein clusters or "ubi particles;" are relatively large structures (~2 μm) located in the cytoplasm visible under the light microscope. These particles are found in all post ischemic neurons following reperfusion (Hu et al., 2000, 2001). The second particle he calls protein aggregates (PAs). These are small structures (~250 nm) found to persist in CA1 after 24 hr reperfusion and be absent in resistant neurons. Dr. Hu surmises that the ubi protein clusters transform into PAs in vulnerable neurons, but are clear from resistant neurons.

Identification of PAs showed an accumulation of: constitutive chaperones such as constitutive heat shock protein 70 (HSC70); initiation factors (eIF2, eIF4E) as well as both large and small ribosomal subunits (Zhang et al., 2006). These accumulations were then collected as cortical homogenates, subjected to 20 min global ischemia and found to produce DND (Liu et al., 2005). Therefore, Dr. Hu has concluded that an irreversible sequestration of ribosomes and associated proteins occurs within PAs and this is what he terms cotranslational aggregation. Thus, loss of ribosomes and initiaiton factors in PAs can also cause prolonged TA within selectively vulnerable cells destined for DND. With these findings, Dr. Hu has proposed a mechanism by which PAs could be involved in prolonged TA in post-ischemic CA1 neurons. First, I/R causes misfolded nascent peptides to accumulate during the elongation process of translation. Nascent peptides can then become the target of ubiquination and clump together. As nascent peptides clump, they also accumulate ribsomes and various other translational protein modifiers, disrupting normal ribosomal functions. These events establish a process, which has been coined "cotranslational aggregation". This was the first alternative pathway, following eIF2α phosphorylation, as a potential explanation for irreversible prolonged TA of neurons, which later undergo DND.

There is clear evidence to support the Hu model, however there are some weaknesses.

First, the stoichiometry suggests that only a small percent of ribosomes are trapped in PAs (DeGracia et al., 2007b). Second, the pathological process of protein aggregation does not account for the physiological regulatory changes in translation, either the phosphorylation of eIF2α, nor the degradation of eIF4G. The ideas that will be developed in the following sections, will propose an alternative model that does not exclude Dr. Hu's model, but instead incorporates PAs into a larger framework of regulatory sequestration of various ribonomic agents.

Subcellular Structures Involved in mRNA Regulation

Throughout the life cycle, mRNA molecules associate with various proteins, generating what is referred to as messenger ribonucleoprotein particles or mRNPs (Anderson and Kedersha, 2006). In cells, mRNPs can form relatively large structures that are often visualized using a light microscope. Figure 7 highlights a few of these structures, revealing an integrated dynamic in the flow and function of mRNA, from synthesis to degradation (DeGracia et al., 2008a). Here I will describe how these subcellular structures are intricately involved in mRNA related functions. This is referred to as the ribonomic network.

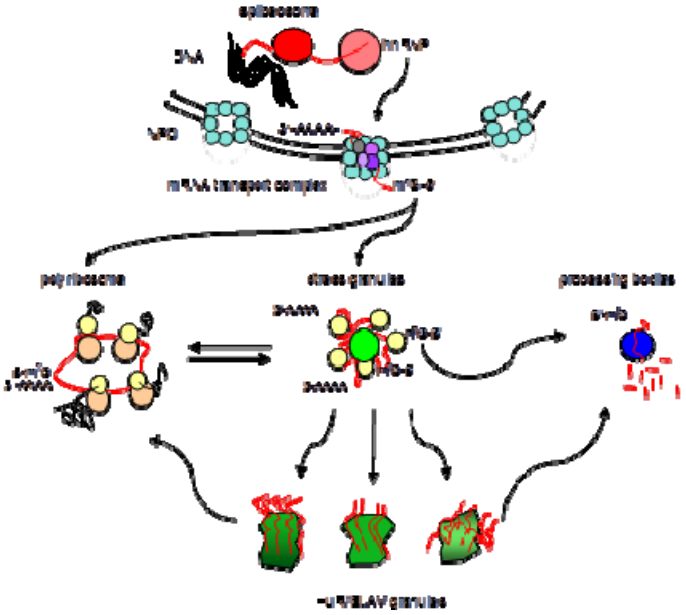

Figure 7. Diagram depicting the ribonomic network. (DeGracia et al., 2008)

Ribonomics

The ribonomic network first described by (Tenenbaum et al., 2002), identified mRNAs as being a significant aspect of regulatory control. mRNAs organized into structural and functional

groups provided a mechanism that could not only affect gene expression but also affect the control and regulation of translated proteins. Rather than the classic linear view where DNA transcribes RNA and RNA translates into protein; the ribonome is represented by the fact that levels of proteins within the proteome do not precisely correlate with levels of mRNAs within the transcriptome (Keene, 2001). This finding alone suggests that additional regulation must be involved. mRNA that was once thought of as a simple, passive, transitory state between DNA and protein, is now thought of as a dynamic and complex regulatory unit. The ribonome consists of thousands of RNA binding proteins (RBPs) along with their associated mRNAs, non-coding regulatory RNAs as well as associated proteins; together these are all contained in mRNPs (Mansfield and Keene, 2009). The major theme of the ribonome (also referred to as post-transcriptional RNA operon or PTRO) involves mRNPs at the center of mRNA regulatory processes. The major functions of the ribonomic network include: (1) mRNA biogenesis, involving transcription and processing, (2) routing or transport, (3) silencing or storage, (4) translation and (5) degradation (DeGracia et al., 2008a). Simply stated in a 2009 review, "it (referencing ribonome) is not simply a matter of controlling a single mRNA's fate, but rather the intricate harmonization of groups of messages that underlie the functioning." This quote taken from (Mansfield and Keene, 2009) reflects the coordinated, highly regulated processes involved with mRNA. Considered below, are the mRNPs located both inside and outside the nuclear compartment of the cell, intimately involved in mRNA regulation.

Regulation of Nuclear mRNAs

The biogenesis of mRNA is a result of nuclear DNA transcription along with subsequent upstream signaling pathways linked to gene transcription. Involved in this process are mRNPs, positioned at various stages along the mRNA handling process. **Spliceosomes** are but one example that excises introns and piece together exons of newly synthesized mRNAs (Valadkhan,

2007). Another example, **heavy nuclear ribonucleoprotein complexes (hnRNPs)** are involved with polyadenylation, capping and transport of mRNAs from the nucleus out to the cytoplasm (Carpenter et al., 2006).

Regulation of mRNAs Outside the Nucleus

Once transcribed, mRNA is routed from the nucleus to the cytoplasm. In some situations, heat shock-induced mRNAs have been shown to be transported via specific complexes, whereas in more common cases, general mRNA transport complexes are involved. Once outside the nucleus, mRNA is shuttled to any one of the various mRNPs discussed below, based on the various role(s) needing to be served (DeGracia et al., 2008c).

Polysomes are one of the classic cytoplasmic structures; involved in translation, genetic information contained within mRNA is converted into the functional form, protein. As one of the structures in the ribonomic network, polysomes are seen as an mRNP that forms and unforms depending on the needs of the cell (Anderson and Kedersha, 2006). Thus, whether or not translation occurs, depends upon the cellular needs at a specific point in time.

Both **processing bodies** and **exosomes** serve roles as mRNA degradation complexes. Within these two ribonomic structures, they may contain initiation factors, however neither structure contains ribosomal subunits (Anderson and Kedersha, 2006). Processing bodies or P-bodies serve a dual function as a site of mRNA silencing or decay (Brengues et al., 2005; Teixeira and Parker, 2007). Exosomes serve solely as degradative complexes, by which mRNAs uncapped and deadenylated are broken down (Schwartz and Parker, 2000).

The formation of another ribonomic complex, the embryonic lethal abnormal vision or **ELAV/Hu granules** are examples of mRNPs that follow major cell physiological changes, such as those seen during differentiation or under cell stress (Antic and Keene, 1998a). Hu proteins are mammalian homologs of the Drosophila ELAV. Those Hu proteins found to be ubiquitously

expressed are known as HuR or HuA, whereas HuB, HuC and HuD are specific to neurons (Burry and Smith, 2006). Hu proteins are involved in partitioning functionally related or structurally organized groups of mRNA into set cohorts. This has been thought to be important for the coordinated and highly regulated fate of the mRNA, in terms of targeting them for simultaneous translation, silencing or degradation (Keene, 2007). The ELAV/Hu granule is a unique structure that offers speed and flexibility in regards to genetic reprogramming that could not be achieved with the same efficiency through transcriptional regulation. The composition of these structures are far less characterized as compared to stress granules(discussed below), however Hu granules have been found to contain eIF4G, eIF4E, PABP, Hu proteins and mRNA (Tenenbaum et al., 2002).

Thus far, I have presented examples of complex structures found to be intimately involved in the regulation of mRNA and have further substantiated the unique and dynamic functionality of the ribonomic network. The last example, stress granules (SGs), has been studied a great deal in our own laboratory under the direction of Dr. Donald DeGracia. Below I will provide a brief background on SGs, followed by the work of Dr. Foaz Kayali conducted in Dr. DeGracia's laboratory.

Stress Granules and Evoked Stress Responses

In order to better understand the functionality of SGs, one must first understand the cellular environment and induced stress response mechanisms that surrounds their activitity. Environmental stress is a transient occurance that forces cells to adapt in order to remain viable. Some examples of environmental stress include: oxidative stress; heat shock; UV radiation; osmotic shock; endplasmic reticulum (ER) stress and viral infection. In order for cells to combat the changes evoked by stress, cells must continuously modify the types of proteins they synthesize. Thus, cells have evolved a wide range of post-transcriptional modifications to

regulate gene expression.

One example, where this is of critical importance, is during a stress response involving global TA. In such a situation, cells must set priority on the specific stressed-induced transcripts needed for cellullar survival. One multifunctional protein that has been found to be an important translational regulator during the stress response is TIA-1 (T-cell internal antigen-1) (Kedersha and Anderson, 2002). TIA-1 acts as translational silencer in the expression of TNF-α in macrophages. TIA-1 can bind with high affinity to AU – rich elements (AREs) along the TNF-α mRNA. By binding to the ARE sequence it diverts RNAs from polysomes to mRNPs (Dember et al., 1996; Gueydan et al., 1999). In stressed environments, TIA-1 proteins exhibit an altered, subcellular distribution, moving from the nucleus out into the cytoplasm where they can accumulate at "phase-dense subcellular cites". These cites are SGs (Kedersha et al., 1999).

Structures analogous to SGs were first described in heat shocked tomato cells. These cells were found to express small heat shock proteins (HSP) and pA mRNAs; however HSP mRNAs were excluded. mRNAs sequestered in SGs were translationally inactive, but could be translated upon dissociation of SGs; which correlates with initiation of protein synthesis just following recovery from heat stress (Nover et al., 1983). From this initial work, it was proposed that SGs were sites that stored mRNA during stress and could make mRNA available for translation, once the initial stress was removed.

Through a number of studies the following conclusions could be drawn in regard to exogenous stress: cells can shut off protein synthesis and form SGs (Harding et al., 2001). Initially, SGs were thought to house mRNA, thereby regulating stress induced TA directly. However, it now appears that the mechanisms involved in the formation of SGs are intimately linked to both the control and regulation of protein synthesis.

Stress Granule Structure and Dynamics

One of the main techniques used to determine the compositional structure and dynamics of SGs was through the use of immunofluorescence (IF) (Kedersha et al., 2005). This technique (shown in Figure 8) allows characterization of an unknown structure through direct visual analysis. SGs can be easily dectected by performing immunostaining using either TIA-1 or PABP antibodies. *In situ* IF has also been used to show poly(A) mRNA within SGs (Kedersha and Anderson, 2002).

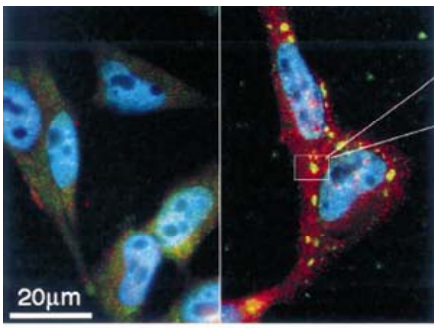

Figure 8. Heat shocked HeLa cells, revealing stress granules. (Kedersha and Anderson, 2002)

It was introduced previously that the dynamics of SGs are linked to the inhibition of protein synthesis in a response to some form of exogenous stress. Upon stress, TIA-1 proteins travel from the nucleus out to the cytoplasm, where they form SGs. If the stress response is removed, SGs will continue to increase in size, but are found to decrease in number, contributing to the fusion of smaller SGs. As the severity of the stress declines, the cell begins to recover and SGs suddenly disperse. Thus, the formation and recession of SGs correlates with recovery of protein synthesis as well as the state of enduring viability expressed by the cell. In cases in which cell stress exceeds a point to which SGs perpetuate, this irreversible response leads to cell death (Kedersha and Anderson, 2002).

It has been shown that the presense of SGs correspond to increases in eIF2α(P) levels. However, treating cells with inhibitors of translational elongation (cyclohexamide), causes the assembly of SGs to decline despite the elevated levels of eIF2α(P). This response suggests that SGs and the mRNA they contain, move in equilibrium with polysomes (Kedersha et al., 2000). However, agents that promote premature termination or evoke energy depletion, can cause a

state in which SGs are elevated and eIF2α(P) is low (Kedersha et al., 2002). This dynamic behavior of SGs appears to be maintained through the regulation of mRNA metabolism. Thus, SGs are transient, cytoplasmic compartments, whose ebb and flow rests on the homestatic environment of the cell.

In 1999, Anderson and Kedersha isolated some key components in understanding the structural make-up of SGs. In addition to TIA-1, they showed SGs contained the 40S ribosomal subunit (using S6 antisera) and a number of initiation factors including eIF4E and eIF4G and mRNA binding factors. Factors, which were excluded from SGs, included the large ribosomal subunits, stressed-induced mRNAs and eIF2 and eIF5 (Kedersha et al., 2002). This classification of identity and association implied that the compartmentalization and exclusion of key factors (i.e. ribsomal units), made it almost impossible for protein translation to occur in the presence of SGs. Thus, the line between TA and cell stress began to become more evident with the knowledge gained regarding SGs.

Using the evidence gained through their work and others, Anderson and Kedersha developed a model that illustrates the formation of SGs. It states that anything that promotes dissociation of polysomes can lead to the progressive state of TIA-1 migrating from the nucleus to the cytoplasm. TIA-1 is characterized by a set of properties that make it critical for the formation of SGs: (1) it can bind mRNAs nonspecifically and (2) it self-aggregates. Thus, Anderson and Kedersha illustrate a scenario by which TIA-1 is bound to mRNA and mRNA is bound within the 48S preinitiation complex. This association of TIA-1-mRNA-48S PIC aggregates with other such complexes, subsequently forming SGs (Anderson and Kedersha, 2002a).

Over time, the knowledge of SG composition has become quite developed. In addition to the initation factors and proteins previously introduced, there are a number of RNA binding

proteins associated with SGs such as tristetraprolin (TTP) and HuR (Anderson and Kedersha, 2006). For convenience and practicality, I have only introduced a few of the key proteins and factors associated with SGs. At the 2006, Translational Control Meeting, held in Cold Spring Harbor, NY, Dr. Nancy Kedersha presented 50 known factors that were associated and identified with SGs. Current data, presented by Dr. Kedersha in 2009, at a seminar held in the Physiology department at Wayne State University School of Medicine, revealed an even more elaborate, detailed categorization of SG proteins. Thus, within a brief period of time, the characterization of SGs has grown rapidly. At one time, SGs were considered static compartments that held and protected mRNAs during cell stress. With more recent evidence, SGs are now characterized as dynamic structures, that not only protect mRNAs (and various other proteins, factors, etc.), but also provide the appropriate environment for the transient flux of mRNAs throughout the cell

Stress Granules and Post-Ischemic Translation Arrest

In 1984, Kirino et al. studied dying CA1 reperfused neurons by using EM. They observed an accumulation of particles located in the cytoplasm of the dying cell that appeared as electron dense substances. It was noted that these electron dense substances correlated exactly with hippocampal CA1 neurons that would later die following I/R (Kirino et al., 1984). Dr. Hu and his laboratory propose that these particles described by Kirino et al. are the protein aggregates previously discussed; however those of the DeGracia laboratory, we have offered a different interpretation. Following I/R, neuronal death correlates with: (1) prolonged inhibition of protein synthesis and (2) irreversible accumulation of cytoplasmic granules within vulnerable neurons (CA1). We propose that these particles are one of the ribonomic complexes discussed above or a variant form of them.

A similar hypothesis was presented by Dr. Foaz Kayali, at the time a Ph.D. student working in the laboratory of Dr. Donald J. DeGracia. As presented in his published work

(Kayali et al., 2005), Dr. Kayali mapped out SGs using the CA/R model following 10 min global brain ischemia and 10 min, 90 min and 4 hr of reperfusion using double labeling IF with two SG markers: S6 and TIA-1. This was the first *in vivo* description of SGs in any whole animal model. The results revealed a complete sequestration (colocalization) of the 40S ribosomal subunit (anti-S6 antibody) that was isolated within SGs (anti-TIA-1 antibody) at a time when levels of eIF2α(P) was dephosphorylated 80% from its peak. These results provided a plausible explanation for prolonged TA and DND. In 2006, the DeGracia laboratory immunomapped eIF4G following CA/R in order to further resolve key issues of eIF4G functinality and regulation that to date had not been resolved. This study identified eIF4G aggregates that formed in the cytoplasm that were more pronounced in vulnerable CA1 neurons as compared to CA3.

However, these studies had two main weaknesses, (1) in Kayali et al. resistant brain regions showed a rapid and transient increase in SGs that paralleled the phosphorylation of eIF2α, but this did not occur in CA1 and (2) within both studies the reperfusion durations were limited to 4 hr using the CA/R model. As reported earlier, cell death occurs at 72 hr reperfusion, by not observing the full duration of time, no definitive correlation with selective vulnerability could be drawn.

Thus, it became apparent that the CA/R model was itself a limitation to the lab. To alleviate this obsticle, Dr. DeGracia's laboratory switched the global brain model to bilateral carotid artery occlusion plus hypotension ischemia or 2VO/HT, a model shown to cause DND in CA1 neurons (Smith et al., 1984). The main advantage to using 2VO/HT is the high survival rate of >85% (Smith et al., 1984), whereas the CA/R model has a low survival rate of ~25% (Montie et al., 2005). Further, with 2VO/HT, animals can be reperfused for any duration of reperfusion; with CA/R, animals exponentially die as a function of reperfusion duration. CA/R not only affects the brain, but generates significant peripheral organ damage in the heart, lungs,

kidneys and GI tract (Montie et al., 2005). As highlighted in Smith et al.(1984), 2VO/HT produces well-defined patterns of neuronal death based on the specific duration of ischemia given. Additionally, less than 1% of animals display seizure activity following or during surgery; in contrast, up to 25% of animals display seizures after CA/R. Circulation to the brainstem via the vertebral arteries, is preserved using the 2VO/HT; thereby maintaining brainstem regulation of visceral pulmonary and cardiovascular function, which means the animal can spontaneously breathe without a ventilator. For these reasons, 2VO/HT is superior to CA/R and is the sole model used in my work to induce global forebrain ischemia.

In a 2007 study, using the 2VO/HT model 10 min of ischemia was induced in male rats followed by 1, 2 and 3 days reperfusion. IF was used to study colocalization patterns of TIA-1/S6, ubiquitin/S6 and ubiquitin/TIA-1 in order to observe possible interactions between SGs and Dr. Hu's ubi protein clusters. The results from this study found, (1) S6 staining does not significantly decrease in CA1 and in fact could still be detected at 24 and 48 hr reperfusion, and (2) at 48 hr reperfusion, SGs colocalized with protein aggregates in vulnerable neurons (DeGracia et al., 2007b).

Unexpectedly, CA/R and 2VO/HT revealed distinct differences in S6 staining patterns; S6 is not soley sequestered into SGs in post-ischemic CA1 neurons. This finding altered the role that SGs played in the post-ischemic stress response, but it did not rule out the functional role SGs have in translation regulation. Thus, this left the lab to question the role of ribonomics and complex structures in post-ischemic TA.

Ribonomics and Post-Ischemic Translation Arrest

Summary and Proposed Hypothesis

I have reviewed and presented information that demonstrates that prolonged inhibition in protein synthesis arrest correlates with DND of selectively vulnerable neurons following brain

I/R. I presented information showing that there is an altered state of regulation involved with initiation factors that occur during the stress response that promotes subcelluar compartmentalization of translational elements into ribonomic complexes. I reviewed studies that described the mechanisms involved in post-ischemic inhibition of protein synthesis. In spite of the complexity of the studies I reviwed, taken as a whole, they have not revealed why protein synthesis inhibition persists in vulnerable neurons such as CA1, but recovers in cells that will survive, such as within the CA3 region of the hippocampus. In all post-ischemic brain regions, protein translation is initially inhibited by the phosphorylation of eIF2α; however, this global response is both acute and transient. Regardless, the relationship between TA and DND must be: (1) selective for the vulnerable neurons (CA1) and not for the cells that recover from I/R (CA3) and (2) the response must persist through the time course leading up to vulnerable cell death. This, therefore leads, to my proposing the following three hypotheses for my dissertation:

Hypothesis #1: **Prolonged translation arrest is caused by a sequestration of translational machinery following global brain ischemia and reperfusion.**

Hypothesis #2: The sequestration is physiological, involving one or more ribononomic structures.

Hypothesis #3: Formation of ribonomic structures are causally linked to post-ischemic translation arrest.

The above hypotheses were tested in a whole animal (male Long Evans rats) model of global brain I/R using *in situ* antibodies and mRNA staining methods, *in vivo* protein synthesis and Western blots, which are collectively presented in the following chapters.

CHAPTER 2

Prolonged Translation Arrest is caused by a Sequestration of Translational Machinery

Overview

Hypothesis #1: Ribonomic complexes are involved in the sequestration of translational machinery following global brain ischemia and reperfusion.

Rationale

Prolonged translation arrest defines the fate of specific cell populations; vulnerable neurons (CA1) die by 72 hours, whereas resistant neurons (CA3) eventually return to active protein translation and survive. I therefore hypothesize that sequestration of mRNA will correlate to TA in CA1 and CA3, at time courses out to 48 hr reperfusion.

Experimental Overview

Using the 2VO/HT model in male Long Evans rats, the experimental groups included 10 mins ischemia followed by reperfusion times of: 1 hr (1hR), 8 hours (8hR), 16 hours (16hR), 36 hours (36hR), 48 hours (48hR) and 72 hours (72hR). The specific number of animals per experimental group used for a given study are listed below. Animals were perfusion fixed and tissue slices prepared. All I/R groups were compared to the nonischemic controls (NIC). Tissue slices were double labeled using fluorescent *in situ* hybridization (FISH) to detect poly(A) mRNAs and immunofluorescence histochemistry (IF) at reperfusion times 1-48hR for the following ribosomal antigens, S6 and RPA. Experimental groups were repeated (including the 72hR group) and *in vivo* translation rates were measured by incorporation of ^{35}S-methionine/^{35}S-cysteine into CA1 and CA3; phosphorylation of eIF2α was assessed by Western blot in the same samples. Hypothesis 1 was tested by correlating histological mRNA distributions throughtout the same time courses of *in vivo* translation and eIF2α phosphorylation.

Experimental Procedures

Materials

Glyceraldehyde-3-phosphate dehydrogenase (GAPDH) (sc-25778) was purchased from Santa Cruz Biotechnology, Inc. (Santa Cruz, CA). Mouse monoclonal (2317) S6 ribosomal protein antisera was purchased from Cell Signaling Technology, Inc. (Danvers, MA.). Ribosome P antigen, a marker of the 60S ribosomal subunit (RPA; HPO-0100) was purchased from ImmunoVision (Springdale, AR). Antisera for phospho-specific (AHO1492) and total (AHO 1182) eIF2α were purchased from Invitrogen (Carlsbad, CA). Alexa FluorR 488 donkey anti-goat IgG, Alexa FluorR 555 donkey anti-human IgG and Alexa FluorR 555 anti-mouse IgG, used for IF histochemistry were purchased from Molecular Probes (Eugene, OR). Fluoro-Jade was purchased from Histochem, Inc. (Jefferson, AR). All other chemicals were reagent grade.

Animal Model

All animal experiments were approved by the Wayne State University Animal Investigation Committee and were conducted following the *Guide for the Care and Use of Laboratory Animals* (National Research Council, revised 1996). Global forebrain ischemia was induced in male Long Evans rats using the bilateral carotid artery (two-vessel) occlusion and hypovolemic hypotension (2VO/HT) model of (Smith et al., 1984).

All animals using the 2VO/HT model, are first anesthetized with 5% halothane. Anesthesia is then maintained at 2% halothane in 100% O_2 using a facemask, used throughout the duration of the surgery. Rectal temperature probes were used to measure body temperature. Based on the rectal body temperature readings, a homeostatic blanket system was used to maintain body temperature (37 ± 0.5^{o} C) throughout the ischemic period, and for the first hour of reperfusion. Mean arterial pressure (MAP) was monitored in real time via tail artery access. The common carotids were isolated and lassoed bilaterally. Blood gas measurements were

maintained at pH = 7.4 ± 0.1, pO_2 = 80 mmHg and pCO_2 = 35 ± 5 mmHg immediately prior to the initation of ischemia. Blood was withdrawn from the femoral artery into a 10 ml syringe until a MAP of 50 mmHg was reached. Following the withdrawl of blood, the common carotids were clamped using microaneurysm clips. Additional blood was withdrawn to maintain a MAP at 40 mmHg for a 10 min duration of time to induce ischemia. Following ischemia for 10 min, the microaneurysm clips were released, blood was reinfused at a rate of 5 ml/min. All wounds were sutured and anesthesia and temperature control was maintained for 1 hr following the surgery. All post-surgical animals were housed in a 12-hr light/dark cycle and provided food and water access during their reperfusion periods. Reperfusion times for each animal was assigned prior to surgery. Once animals had reached their set reperfused times, they were sacrificed and the brain dissected. Tissue processing and brain dissection is further described below.

Rats were maintained normothermic during the entire ischemia period and for the first hour of reperfusion. Post-surgical animals displaying frank necrosis, weight loss > 15% initial body weight/day, or sustained seizure activity were excluded from the study. Overall survival rate for the reperfusion groups was 75%. Experimental groups were: sham-operated, NICs, 10 min ischemia and reperfusion duration of 1 hr (1hrR), 8hr (8hR), 16hr (16hR), 24 hr (24hR), 36 hr (36hR), 48 hr (48hR) and 72 hr (72hR). For microscopy, there were 5–6 animals per each experimental group. For *in vivo* translation and Western blotting, there were four animals per each experimental group.

Perfusion Fixation/Tissue Slicing

Rats were transcardially perfused with 250 ml of ice cold 0.9% NaCl solution at a rate of 20.8 ml/min. Following the NaCl solution, 300 ml of 4% paraformaldehyde (PFA) in 0.1M phosphate buffered saline (PBS) solution was perfused at a flow rate of 10 ml/min. Once perfusion was complete, brains were excised and post-fixed by immersion in 4% PFA/0.1M

PBS. The amount of time dedicated to the post-fix process was determined based on results of the perfusion fixation. Therefore, post-fixed immersion ranged from 1-3 days. Following post-fixation, coronal slices, at widths of 50 μm, were made through the dorsal hippocampus via a vibratome. The tissue was sectioned in 0.1M PBS. Each 50 μm slice was collected and stored in cryostat solution at -20^{o} C until used for staining.

Cell Death Measurements

Toluidine blue and Fluoro-Jade staining were performed exactly as described in (DeGracia et al., 2007b).

Toluidine Blue Staining: Once brain slices were mounted unto the slide they were washed 3 times in 1% PBS and air-dried overnight. The next day, slices were dehydrated in a series of graded ethanol solutions, followed by incubating the tissue in 10% Toluidine Blue/100% ethanol for 1 hr at room temperature. Sections were then washed in a graded ethanol series and 100% xylene. Slides were complete once mounting media (Vectashield) and coverslip were in place.

Fluoro-Jade Procedure: Brain sections were mounted with gelatin, onto slides and allowed to dry. Once dry, the tissue was immersed in 100% ethyl alcohol for 3 min. This was followed by a 1 min immersion in 70% alcohol and a 1 min immersion in distilled water. Slides were then transferred to 0.06% potassium permanganate solution for 15 min while gently shaking on a rotating platform. During this period, the Fluoro-Jade solution was prepared: 0.01% stock solution was prepared by dissolving 10 mg of Fluoro-Jade into 100 ml of distilled water. The working solution (0.001% Fluoro-Jade) was prepared using 10 ml of the previously prepared stock Fluoro-Jade with 90 ml of 0.1% acetic acid in distilled water. Following the immersion of potassium permanganate solution, slides were rinsed for 1 min in distilled water and then transferred to the already prepared 0.001% Fluoro-Jade staining solution, where they

gently agitated on the rotating platform for 30 min. After staining, the sections were rinsed for 1 min each in three separate distilled water washes. Excess water was drained, slides air dried and were applied with mounting media and a coverslip (Schmued et al., 1997). Fluoro-Jade slides were examined using excitation at 488 nm and emission at 518 nm.

Microscopic Analysis

Data Acquisition

For analysis, an Apotome was used, which is similar to a laser scanning confocal microscope. The Apotome focuses on a specific plane in the tissue and can acquire optical sections moving up or down from the original plane of focus. The microscope is controlled via a computer that is programmed to acquire optical sections of consecutive focal planes marked by a defined distance (the software sets this distance to meet Nyquist sampling requirements). The set of sequential optical sections are referred to as a z-stack.

All slides were examined on an Axioplan 2 Imaging System (Carl Zeiss, Oberkochen, Germany) equipped with an ApoTome. Excitation at 488 nm and 568 nm, and emission at 518 nm and 600 nm are used for Alexa 488 (green) and Alexa 555 (red) respectively. Optical sectioning was performed using 63X oil immersion objective to generate z-stacks.

Data Analysis

The qualitative descriptions can be directly observed from digital images (as previously shown in (Kayali et al., 2005)). The Zeiss Axiovision software (ver 4.2) can generate both 3D reconstructions and 2D "cut views". These can then be used for further qualitative descriptions. The orthographic projections of the 63X z-stacks can be used to quantify the number, size and intensity of subcellular structures. The orthographic projections can be used to amplify the signals from the individual optical sections and imported into Adobe Photoshop where the red and green channels are multiplied. The results can be exported to a gray scale channel that

represents overlap between both red and green channels. This overlap is referred to as the yellow channel (red + green = yellow). The yellow channels can then be exported as gray scale TIFF files that can be imported into BioImage Intelligent Quantifier ver 4 software (an image depicting each step of channel manipulation is found in Chapter 3, Figure 18). This software is typically used for counting spots on 2D gels with the capacity of performing automatic spot detection, counting and densitometry. This system can be used to count "spots" in the yellow channel. In order to normalize the gray scale ranges for each separate image to allow for direct comparison of each image acquired, a standard set of 12 6X6 pixel "marker spots" that covers the entire gray scale range were served to normalize the ranges of each individual image. The output from BioImage for each orthographic projection was contained within an Excel spreadsheet; its contents included: (1) each detected "spot", (2) its coordinates within the image, (3) the size or area (pixels) and (4) the density.

Statistics

The analysis of the yellow channels was normalized to the total number of cells in the image, which then produced a comparison from one image to the next. The averages were normalized from the experimental groups and compared by a one-way ANOVA and post hoc test to determine the *p* values (parameters set at $p < 0.05$) between the individual pairs of means.

Immunofluorescence (IF)

Brain slices were washed for 10 min in 0.1M PBS X4. Following the last wash, a preblock step including 0.1M PBS containg 0.3% Triton X-100 (PBS-Tx) was mixed in solution with 10% seurm (in the same species as the secondary antibody), and remained on tissue (~300µl is applied per tissue slice) for 25 min. Three washes in PBS followed (10 min/wash). Slices were then immersed in primary antibody (at specific concentration/antibody solution) in 1% serum and PBS-Tx solution, at room temperature left to rock overnight. The following day,

samples were washed three times in 0.1M PBS, for 10 min each. The secondary antibody was prepared in 0.1M PBS- 0.3% Tx- 10% serum and left on the tissue for 2 hr. The final 10 min wash was performed with 0.1M PBS X3. Slices are then mounted onto glass slides, sealed under coverslips and stored at -20^{o} C.

The primary and secondary antibody concentrations are decided based on dilution series that are done prior to the start of immunolabeling. This process is very similar to the steps involved above, used for immunolabeling. Each new antibody is processed the same, with a series of dilutions tested on control and experimental animals; in order to determine the concentration that limits background and provides the best overall signal.

Fluorescent *in situ* Hybridization (FISH)

Double IF/FISH was performed in a two stage procedure in which the FISH procedure was a modification of that described in (Bessert and Skoff, 1999). The first stage, the IF procedure, was performed, as described above. The second stage, FISH, was performed under low light illumination or in the dark. At the end of the IF procedure, slices were mounted on lysine-coated slides. IF-stained sections were fixed in 3.6 % formaldehyde in PBS for 10 min at room temperature and then drained and blotted. Prehybridization was carried out in a box humidified with 50% formamide/4X saline-sodium citrate (SSC) inside an incubator at 32^{o}C for 3 hr in prehybridization buffer (mRNAlocator *In Situ* Hybridization Kit, Ambion, Austin, TX). Slides were then incubated overnight in the same apparatus in a solution of 50 ng/ml of a 5'-biotinylated 50-mer oligo-dT probe (Integrated DNA Technologies, Inc., Coralville, IA), dissolved in hybridization buffer (mRNA Locator In Situ Hybridization Kit). The next day, all subsequent processing was performed at room temperature. Slides were washed three times in 2X SSC for 10 min and then incubated in the dark at 1:500 Alexa 488-labeled streptavidin (S32354, Invitrogen, Carlsbad, California) in 4X SSC/0.1% Triton X-100 for 60 min. Slides

were then washed once in 4X SSC for 10 min followed by incubation in 2X SSC/0.1% Triton X-100 containing 1:667 of biotinylated goat anti-streptavidin (BA-0500, Vector Laboratories, Burlingame, CA) for 60 min. Slides were again washed once in 4X SSC for 10 min and then incubated in 1:667 Alexa 488-labeled streptavidin in 2X SSC/0.1% Triton X-100 for 60 min. Slides were then washed sequentially in 4X SSC for 10 min and 2X SSC for 10 min, and then coverslipped for viewing. Pair wise stainings were performed for: poly(A) mRNA with, S6 (1:25) and RPA (1:5000).

In all cases, the poly(A) staining pattern obtained, by performing IF/FISH double-labeling, was identical to that obtained by performing FISH by itself. Validation of the specificity of the poly(T) probe for binding RNA was accomplished by preincubating NIC brain slices in 10 U/ml DNAse I (Invitrogen, Carlsbad, CA) or 10 U/ml DNAse-free RNAse (Roche AppliedScience, Indianapolis, IN) at 37^{o}C, or 0.1M NaOH at 50^{o}C, for 2 hr prior to performing FISH (Martone et al., 1996a).

Validation of antisera stainings included (not shown): (1) loss of signal with omission of primary antisera, (2) graded loss of signal with antisera dilution, and (3) agreement with published descriptions of antisera staining patterns where available. We previously validated the specificity of the S6 and RPA staining (Kayali et al., 2005).

***In Vivo* Translation**

Measurement of *in vivo* protein synthesis was performed as previously described (Kumar et al., 2003), with n =4 animals per each experimental group. Briefly, 1 mCi ^{35}S-methionine/^{35}S-cysteine (Trans ^{35}S-Label^{TM}, ICN Biomedicals, Inc., Irvine, CA) was administered IV through the femoral vein, 60 min prior to sacrifice. After 60 min, brains were rapidly but carefully dissected on ice, and CA1, CA3 and cerebellum were further microdissected, as shown in Figure 9 (DeGracia et al., 2007b). Regions CA1 and CA3 were pooled bilaterally (recovered wet

weights of each region were between 7-10 mg) and then sonicated at 1:10 wt:vol in buffer containing 7 M urea, 2 M thiourea, 0.4% CHAPS (3-[(3-Cholamidopropyl)dimethylammonio]-1-propanesulfonate), 10 mM DTT (dithiothreitol), 1 mM PMSF (phenylmethylsulfonyl fluoride), 4 μg/ml aprotinin, 4 μg/ml leupeptin, and 2 μg/ml pepstatin A. Thirty-five microliters of each homogenate were spotted onto individual Whatmann GF-A glass fiber filters that had been prewet in 10% trichloroacetic acid (TCA), 1.6 % unlabeled methionine and 0.4 % unlabeled cysteine. Filters were incubated in this same solution for 15 min at 4°C with rocking, washed twice with cold 5% TCA, and sequentially dried in 100% ethanol and 100% acetone. ^{35}S incorporation into TCA-precipitable material was quantified by liquid scintillation counting. Protein concentrations were determined in homogenate aliquots using the Folin phenol reagent method.

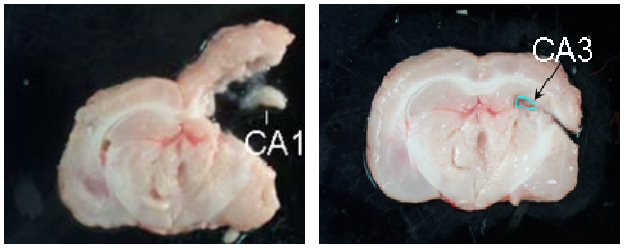

Figure 9. Microdissecting CA1 and CA3 of a rat hippocampus.

To account for slight animal-to-animal variations of *in vivo* specific activity, incorporation, in dpm/μg protein/min, for the CA1 and CA3 regions of each animal were normalized and expressed as a percentage of incorporation in the cerebellum. This procedure was feasible because cerebellum does not undergo ischemia in the 2VO/HT model (Smith et al., 1984). Pilot studies showed that total *in vivo* incorporation in cerebellum, CA1 and CA3 were statistically indistinguishable in NIC rats (average of all three brain regions was 0.26 +/- 0.08 dpm/μg protein/min, ANOVA $p = 0.564$). Normalized translation rates were compared amongst groups by ANOVA, followed by Tukey post hoc testing to show $P < 0.05$ compared to the NIC groups for each region.

Western Blotting

Fifty microgram samples of CA1, CA3 or cerebellum homogenates were run per lane on 10% SDS-PAGE gels, electroblot transferred to nitrocellulose, and Western blotted for phosphospecific (1:750) or total (1:1000) eIF2α, or GAPDH (1:1000) as previously described (Roberts et al., 2007). Thapsigargin treated NB104 cells were used as a positive control for eIF2α(P), as described previously (Kumar et al., 2003). Band densitometry was quantified in BioImage Intelligent Quantifier (Jackson, MI), and groups compared by ANOVA and Tukey Post hoc with $p < 0.05$.

Results

Cell Death and Model Validation

Figure 10 shows representative micrographs of cell staining for CA1 and CA3 over the reperfusion durations used in the present studies. As per previous reports (Smith et al., 1984; Hu et al., 2000; Liu et al., 2005; DeGracia et al., 2007b), cell death was observed exclusively in CA1 at 72hR after 10 min 2VO/HT ischemia. No changes in cell numbers were observed at 24 hR or 48 hR in CA1 or CA3. The bottom panels of Figure 10 show that Fluoro-Jade staining was observed only in 72hR CA1,

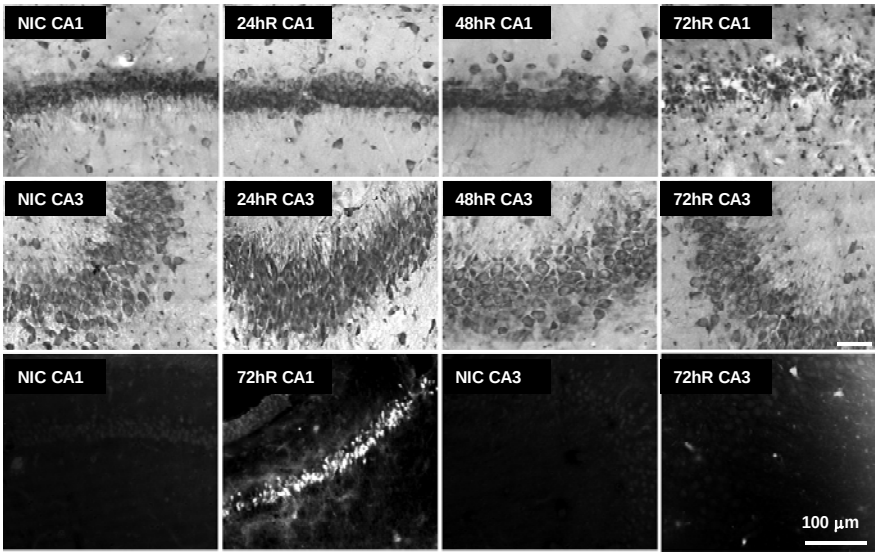

Figure 10. Cell staining of hippocampal CA1 and CA3 following I/R. Toluidine blue staining of 50 µm sections through dorsal hippocampus as indicated (Rows 1 and 2). Fluoro-jade labeling of NIC and at 72 hr reperfusion (72hR) as indicated (Row 3). Scale bar is 100 µm and applies to all panels

consistent with the loss of toluidine blue staining in this group. This data validates that the 2VO/HT model leads to the selective vulnerability of CA1 pyramidal neurons.

***In Vivo* Translation**

Figure 11A shows results of *in vivo* translation measurements in microdissected CA1 and CA3 normalized to cerebellum. Evaluation went only to 48 hR to avoid the possibility of cell death being a contributor to decreased *in vivo* translation rates. Cerebellum showed no change in translation compared to NICs during the entire reperfusion time course. TA was observed in both CA1 and CA3 with early reperfusion. However, translation gradually recovered in reperfused CA3. At 36hR and 48hR, translation in CA3 averaged ~80% of NICs, although statistically indistinguishable from NICs. In CA1, there was a recovery to about 35% of controls at 8hR, which declined after this time. Translation in CA1 after 8hR was indistinguishable from the 1hR samples. This data illustrates the well-established correlation between CA1 selective vulnerability (Figure 11) and persistent TA (Hossmann, 1993).

Phosphorylation of eIF2*α*

Phosphorylation of the alpha subunit of eIF2 was assessed in the same samples used for *in vivo* translation (Figure 11B). There was no change in the levels of total eIF2α (ANOVA p = 0.761) or GAPDH (ANOVA p = 0.586), the latter used as a normalizer (Figure 11B). We observed a statistically significant ~2.3-fold increase in eIF2α(P) only in CA1 and CA3 in the 1hR samples (Figure 11C, ANOVA p = 0.021 and 0.017 for CA1 and CA3, respectively). Levels of eIF2α(P) in cerebellum did not change (ANOVA p = 0.718). Hence, phosphorylation of eIF2α would be expected to contribute to TA at 1hR, but cannot account for the persistent TA at reperfusion durations > 1hr.

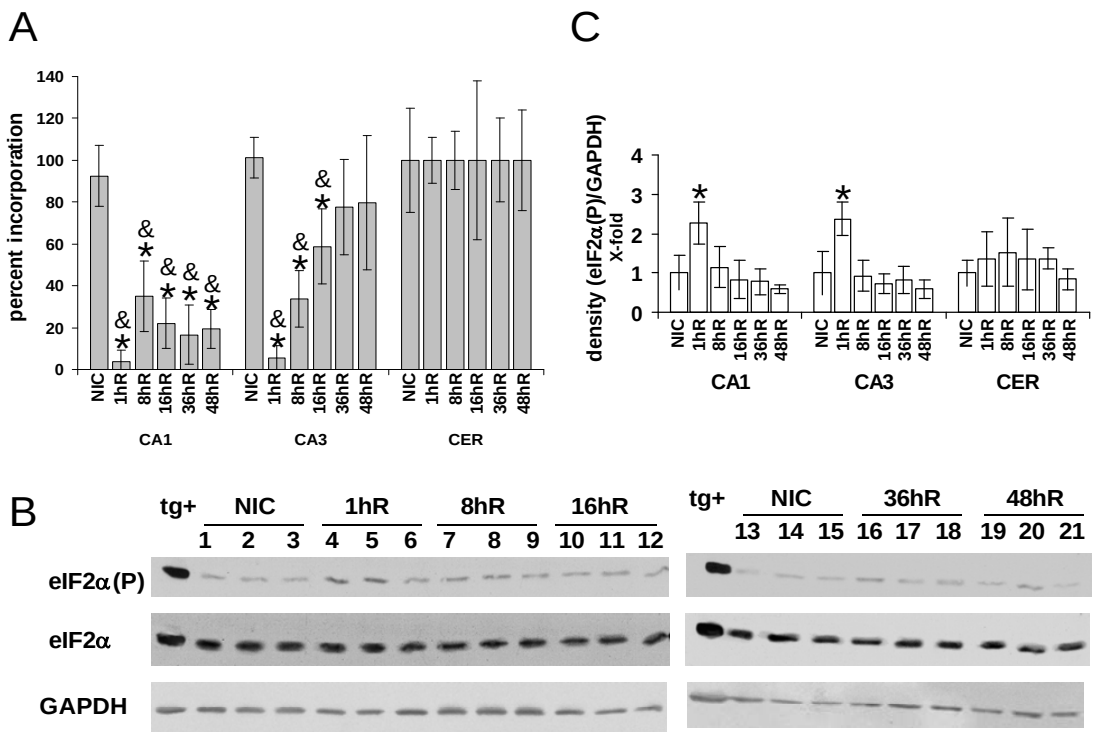

Figure 11. *In vivo* protein synthesis and eIF2α(P) following I/R. (A) *In vivo* translation in NICs, and from 1 to 48hR expressed as a percentage of incorporation in cerebellum at each time point for each animal (n=4 per group, mean ± standard deviation). *Tukey post hoc $P<0.05$ as compared with respective NICs. ANOVA P for cerebellum=0.381. & indicates samples in which respective brain regions showed mRNA clumping in their cytoplasm. (B) Western blots of microdissected brain regions (50μg/lane) for eIF2α(P), total eIF2α and GAPDH, the latter used as a normalize. Experimental groups as indicated. Lanes 1, 4, 7, 10, 13, 16, 19 representative samples of CA1. Lanes 2, 5, 8, 11, 14, 17, 20 representative samples of CA3. Lanes 3, 6, 9, 12, 15, 18, 21 representative samples of cerebellum (CER). Lane tg+ is thapsigargin-treated NB104 cells, used as a positive control for eIF2α(P) as described previously (Kumar et al., 2003). (C) Densitometry of eIF2α(P) Westerns normalized to GAPDH levels (n=4 per group, mean ± standard deviation). *Tukey post hoc $P<0.05$ as compared with respective NICs for CA1 and CA3. ANOVA P for cerebellum=0.711.

Microscope Observations

The description of the microscopy results below occurred at 100% frequency in each group. The exact number of animals in each group (in parentheses) were: NIC(six),1hR(six), 8hR (six), 16hR (six), 36hR (five) and 48hR (five). Here hippocampal regions CA1 and CA3 are compared systematically. Throughout the course of observations made, the hippocampal hilus, dentate gyrus and cerebral cortex were evaluated. Because these other brain regions: (1) did not

show cell death in the ischemia model, and (2) behaved identically to CA3 as described below, we show only CA3 results as representative of an ischemia-resistant brain region.

FISH Detection of Poly-Adenylated mRNA

FISH signal for poly(A) mRNA was eliminated when slices were pretreated with 10 U/ml RNAse or 0.1 M NaOH, but not 10U/ml DNAse, for 60 min at 37^{o}C, prior to FISH (Figure 12), providing evidence that the poly(T) probe detected RNA and not DNA.

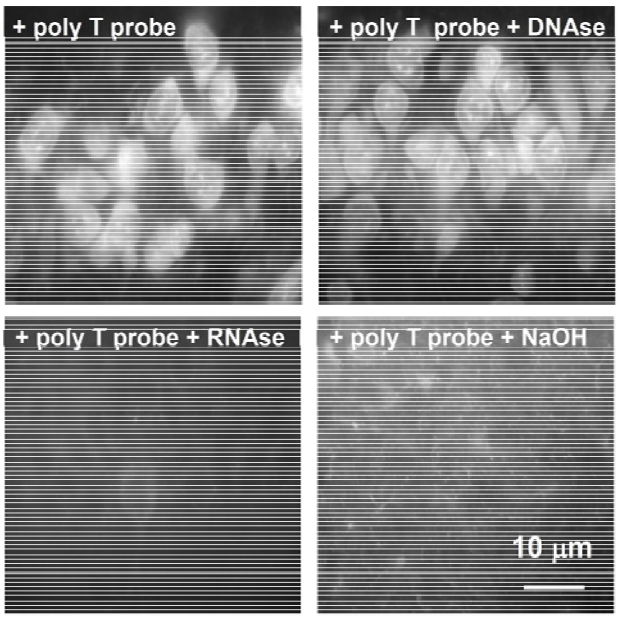

Figure 12. Validation of FISH. Fluorescence photomicrographs of NIC CA1 following treatments as indicated in labels. Probe for detecting poly(A) mRNAs was a biotinylated 50-mer poly-thymidine (poly T) probe. Treatment with 10 U RNAse A/ml or 0.1 M NaOH ablated poly(A) signal, but not treatment with 10U/ml DNAse I. Scale bar, 10 µm, applies to all panels.

Figure 13 shows poly(A) mRNA staining in CA1 and CA3 in NICs and from 1 to 48 hr reperfusion. In both regions in NIC samples, the poly(A) FISH signal showed three distinct components: (1) a diffuse homogeneous cytoplasmic staining, (2) a punctate cytoplasmic staining, and (3) staining of up to a dozen relatively large (0.5-2 µm), round bodies in the nucleus. These results are essentially identical to a previous report of poly(A) FISH staining of CA1 pyramidal neurons (Martone et al., 1996b). The co-staining pairs we performed (see ahead) showed that, in the NIC group, the punctate cytoplasmic poly(A) staining colocalized with S6 and RPA. Each of these components has previously been shown to be components of SGs (Anderson and Kedersha, 2006). Therefore, the punctate cytoplasmic poly(A) staining

represented SGs, supporting our previous observations of SGs in neurons of the normal brain (Kayali et al., 2005; DeGracia et al., 2006, 2007).

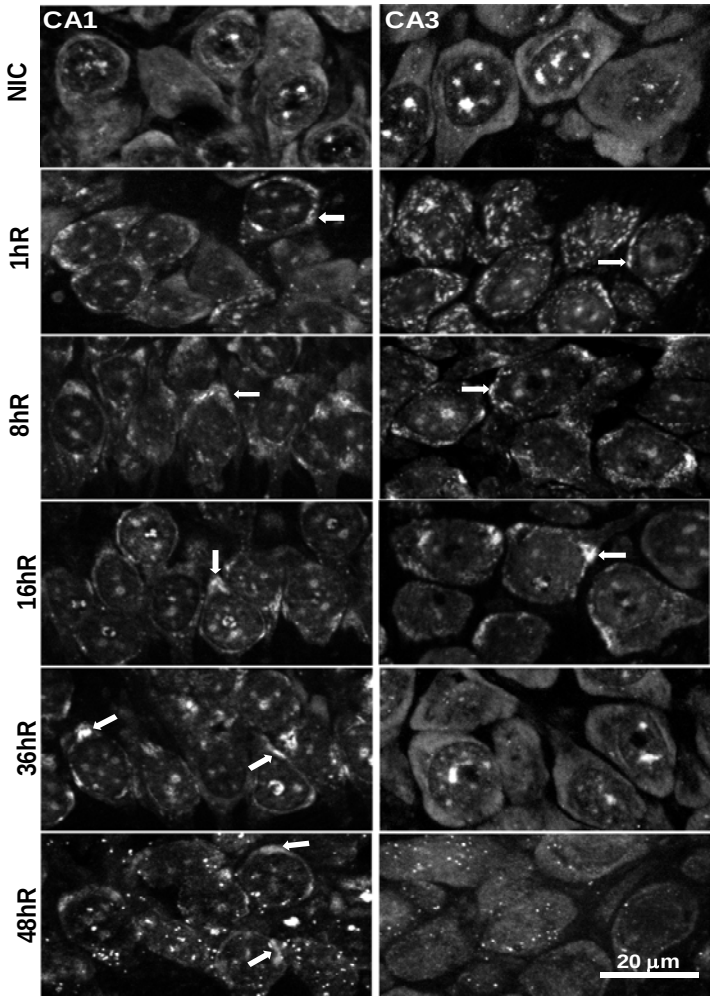

Figure 13. FISH staining of poly(A) mRNAs. In NIC and from 1-48hR respectively. Fluorescent photomicrographs of CA1 (left column) and CA3 (right column) pyramidal layer of representative samples (n= 5-6 per group) from experimental groups as indicated. Images are derived from orthographic projections of a 3.5 µm z-stack taken under 63X oil immersion. Arrows denote mRNA granules (see text). Scale bar = 20µm and applies to all panels.

Following reperfusion, there was no change in the nuclear or SG poly(A) staining components. However, at 1hR, the diffuse cytoplasmic staining underwent an apparently quantitative rearrangement in both CA1 and CA3. There was a generalized loss of diffuse cytoplasmic staining and the appearance of irregular clusters of intense, concentrated poly(A) staining. We designate these structures as "**mRNA granules**", examples of which are marked by white arrows in Figure 13. The mRNA granules were especially prominent and obvious in CA3 neurons due to their larger cytoplasmic area. The 8hR and 16hR samples showed essentially

identical staining patterns in both CA1 and CA3: the smaller mRNA granules seen at 1hR were now replaced by up to several larger concentrations of poly(A) cytoplasmic staining. After 16hR, the poly(A) staining pattern between CA1 and CA3 significantly diverged. At 36hR and 48hR, the poly(A) staining returned to a diffuse pattern in CA3, resembling NICs. However, the mRNA granules persisted in CA1 at 36hR and 48hR.

We note that the presence of the mRNA granules correlated precisely with inhibition of *in vivo* protein synthesis in CA1 and CA3. The time points in which mRNA granules were present were also the time points that showed *in vivo* translation rates statistically below controls; these groups are marked by an ampersand (&) in Figure 11. This one-to-one correlation suggests a relationship between the mRNA granules and TA.

S6 and Poly(A)

In NICs of CA1 and CA3 colocalization of S6 and poly(A) caused a diffuse yellow cytoplasm and yellow punctate cytoplasmic staining (Figure 14, NIC). The former likely represented mRNAs being translated on cytoplasmic ribosomes, the latter represented 40S subunits and mRNAs sequestered together in SGs (Figure 14, NIC, arrowhead).

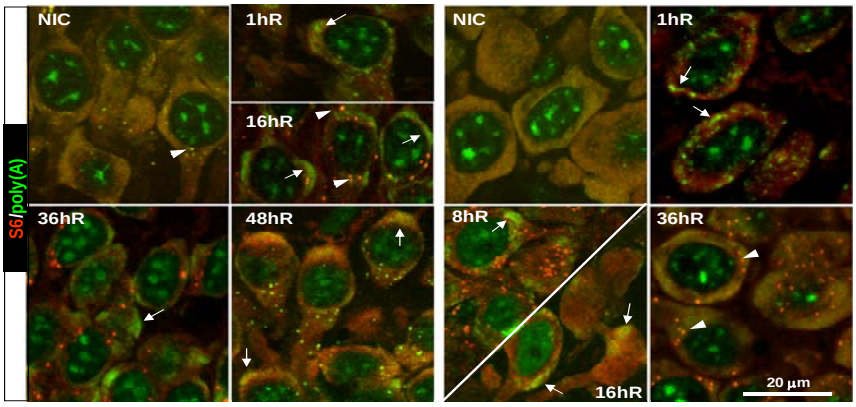

Figure 14. S6/poly(A) staining. S6 did not colocalize with mRNA granules during reperfusion. Fluorescent colors associated with each staining pair are indicated in row labels. Merged fluorescent photomicrographs of representative samples (n=5-6 per group) from experimental groups as indicated. Orthographic projections were derived as described in legend to Figure 13. Scale bar = 20 µm and applies to all panels. Arrows point to mRNA granules, arrowheads point to SGs.

During reperfusion, in CA1 from 1hR to 36hR, and in CA3 at 1hR and 8hR, the S6 did not colocalize with the mRNA granules (Figure 14). At these time points, the prominent green mRNA granules were visible against a diffuse red S6 staining in the cytoplasm. Colocalization of poly(A) and S6 in SGs were apparent (Figure 14, 16hR, arrowheads). In CA3, at 36hR (Figure 14) and 48hR (not shown), the mRNA granules were no longer observed, and S6/poly(A) costaining reverted back to that seen in NICs.

At 16hR in CA3 and 48hR in CA1, there was an increased yellow hue to the mRNA granules (Figure 14, 48hR CA1 and 16hR CA3, arrows). However, at these time points, S6 did not form distinct granular structures in the cytoplasm (Figure 14, S6 channels). To further assess the nature of this ostensible colocalization, linear densitometry was determined in both the red and green channels for CA3 at 8hR and 16hR and for CA1 at 36hR and 48hR (Figure 15). Densities were taken through individual mRNA granules (Figure15, between arrows) and plotted as a function of distance. In mRNA granules of 8hR CA3 and 36hR CA1 neurons, the density of the green channel was greater than that of the red channel (Figure 15, left graphs) and the ratio of the green to red channel densities was greater than one (Figure 15, right graphs, black curves). The opposite result occurred with 16hR CA3 and 48hR CA1 (Figure 15, middle graphs and right graphs, blue curves). Therefore, the apparently increased colocalization of S6 and poly(A) in the mRNA granules of 16hR CA3 and 48hR CA1 was not due to a concentration of S6 in the mRNA granules, but was due to a decrease in poly(A) staining intensity relative to S6 in the mRNA granules. These calculations are consistent with the interpretation that, at 16hR in CA3 and 48hR in CA1, the mRNA granules were beginning to dissipate.

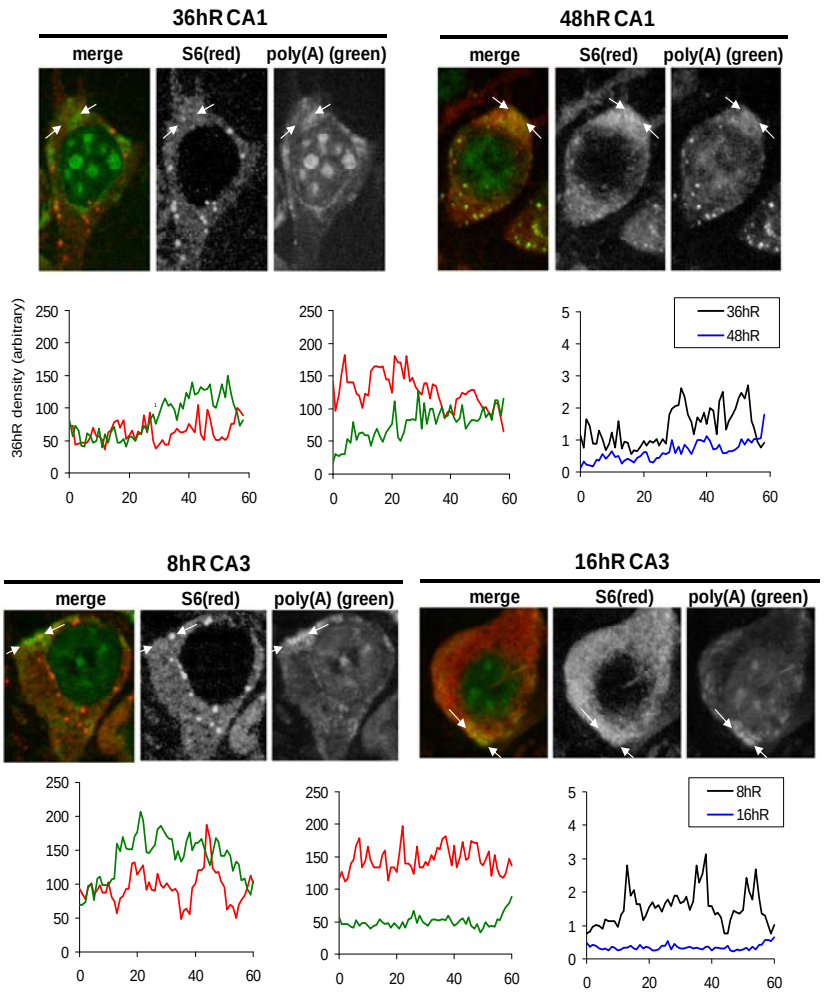

Figure 15. Linear densitometry through mRNA granules. Photomicrographs of merged, red S6 and green poly(A) channels of individual CA1 & CA3 pyramidal neurons of experimental groups as indicated. Arrows denote the start and end points for linear densitometry through individual mRNA granules. Relative location of arrows are maintained through each triplet of micrographs. Left and middle graphs are plots of channel density as a function of distance between left and right arrows. Green lines are the green poly(A) channels and red lines are the red S6 channels, and the Y axis labels identify the respective experimental groups. Right graphs are the ratio of the green to the red channels plotted as a function of distance and curves are as designated in the insets.

To get a quantitative sense of the temporal progression of S6/poly(A) double-labeling in both CA1 and CA3, we performed densitometry of the entire yellow channel as described previously (DeGracia et al., 2007a). Densitometry results, along with representative yellow channels of the CA3 samples, are shown in Figure 16. In CA1, the average density of channel overlap in NICs was higher than all the reperfusion groups, and the difference was close to being statistically significant (ANOVA p = 0.070). In CA3, a statistically significant decrease in S6/poly(A) colocalization was observed in the 1hR and 8hR groups (ANOVA p = 0.015), but from 16hR onwards was indistinguishable from NICs. Although they represent only an approximation, these results reinforce the qualitative observation that there is decreased

colocalization of S6 and poly(A) during the entire reperfusion time course in CA1, and during early reperfusion in CA3.

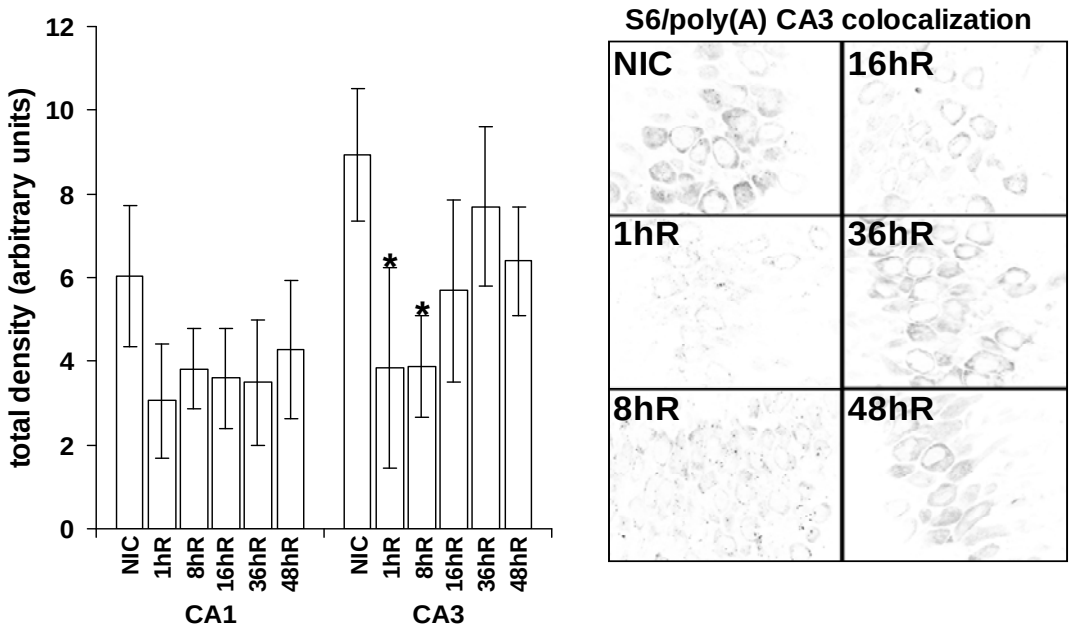

Figure 16. Semi-quantitation of colocalization. Left, integrated density (arbitrary units) of colocalization of poly(A) and S6 in CA1 and CA3 (mean ± standard deviation) of experimental groups as indicated. ANOVA *P* was 0.070 for CA1 and 0.015 for CA3. *Post hoc $P<0.05$ compared with NIC group. Right, representative yellow channels from CA3 samples.

Thus, S6 generally did not colocalize with the mRNA granules. Additionally, there was a 1:1 correlation between inhibited protein synthesis and the presence of the mRNA granules (Figures 11 & 13). Therefore, from the data it was concluded that the mRNA granules sequestered mRNA away from ribosomes. As mRNA is an essential component of protein synthesis, the compartmentalization of mRNA away from ribosomes provides a novel mechanism of prolonged TA in reperfused neurons.

Ribosomal P and Poly(A)

Figure 17 shows the large (60S) ribosomal subunit (Ribosomal P antigen), marked as RPA, double labeled with poly(A). Only 1hR samples are shown because the qualitative pattern of RPA with the mRNA granules did not change over the reperfusion time course. Additionally,

similar patterns were seen in cerebral cortical, thalamic and hilar neurons that evidenced mRNA granules following reperfusion (data not shown).

In NICs, RPA showed a diffuse cytoplasmic colocalization with poly(A) mRNAs (Figure 17A), as would be expected for cells active in protein synthesis. However, the mRNA granules did not colocalize with RPA in reperfused samples. Previously, the 40S marker S6, showed a lack of colocalization with mRNA granules following brain I/R. As it is well-known that polysomes are fully dissociated at the 1hR time point (Hossmann, 1993; Martín de la Vega et al., 2001), these results indicate that the dissociated ribosomal subunits (40S and 60S) are not associated with mRNA granules.

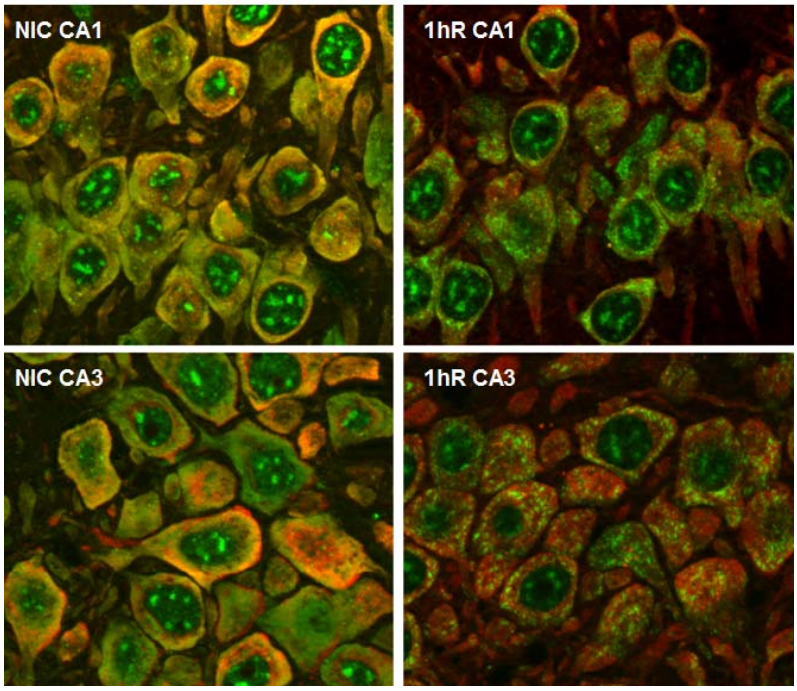

Figure 17. Representative photo-micrographs of poly(A) mRNAs and Ribosomal P antigen (RPA), as indicated in the figure for nonischemic control (NIC) and following one hour of reperfusion (1hR) in hippocampal layers CA1 and CA3. All images were acquired as described in Figure 13.

CHAPTER 3

mRNA Granules Are a Ribonomic Structure

Overview

Hypothesis #2: The sequestration is physiological, involving one or more ribononomic structures.

Rationale

In Chapter 2, using IF and FISH, I identified in both CA1 and CA3 neurons, cytoplasmic poly(A) mRNAs redistributed from a homogenous staining pattern seen in controls to granular structures we termed mRNA granules. The mRNA granules abated after 16hr reperfusion in CA3, but persisted in CA1 neurons out to 48 hr reperfusion. Protein synthesis inhibition correlated precisely with the presence of the mRNA granules. The mRNA granules did not colocalize with either small or large ribosomal subunits. This differential compartmentalization of mRNA away from both the 40S and 60S subunits correlates with translation arrest in post-ischemic neurons, thus providing a concise mechanism of persistent TA in post-ischemic CA1. Therefore, to test my hypothesis, and further elucidate and characterize mRNA granules, I will use IF/FISH to determine whether mRNA granules: (1) associate with other known ribonomic complexes, (2) are localized to any particular region of the cell, by considering possible colocalization patterns with organelles and cytoskeletal proteins, and (3) are involved with the stress response.

Experimental Overview

Using the 2VO/HT model in male Long Evans rats, the experimental groups included 10 mins ischemia followed by reperfusion times of: 1 hr (1hR), 8 hours (8hR), 16 hours (16hR), 36 hours (36hR), and 48 hours (48hR). Animals were perfusion fixed and tissue slices were prepared and stained for poly(A) mRNAs by FISH identically to Hypothesis #1. Hypothesis #2

was tested by comparing vulnerable CA1 and resistent CA3 for colocalization of poly(A) mRNA with the protein antigens listed below in Table 2. A second set of animals were used to prepare unfractionated hippocampal homogenates for Western blot to verify antibody specificity, for those antibodies not previously used in our laboratory. Using TIA-1 in this experiment also provided an opportunity to count stress granules in CA1 vs CA3 at 15 mins and 1 hr reperfusion using methods of (Kayali et al., 2005).

Table 2. Various protein antigens and they are association with a ribonomic complex (stress granules, processing bodies or ELAV/Hu granules), HuR transport protein(s), cytoskeletal protein(s) and/or organelle(s).

Protein Antigens	Detects
TIA-1	Stress Granules
TTP	Processing Bodies
PABP	ELAV/Hu granules
eIF4G	ELAV/Hu granules
HuR	ELAV/Hu granules
pp32	HuR Transport Protein
April	HuR Transport Protein
α-Tubulin	Cytoskeleton
NF H/M	Cytoskeleton
GM130	Golgi Complex
TGN38	Golgi Complex
COX IV	Mitochondria
NeuN	Nucleus
PDI	Endoplasmic Reticulum

Anti-sera for HSP-70 was used for IF to evaluate potential differences in stress response using the 2VO/HT model comparing CA1 and CA3. Same experimental groups listed above, were used.

Experimental Procedures

Materials

Antisera for α-tubulin (T6199) and neurofilament (NF) H/M (N2912) were purchased from Sigma-Aldrich (St. Louis, MO). Antisera for acidic protein rich in leucine, a HuR accessory protein (APRIL; ab4224), cytochrome C oxidase subunit 4, a mitochondrial marker (COX IV; ab16056) and PABP (ab21060) were purchased from Abcam (San Francisco, CA). Antisera for protein disulfide isomerase, a marker of the endoplasmic reticulum (PDI; MA3-019) and the trans-Golgi marker TGN38 (MA3-063) were purchased from Thermo Scientific

(Rockford, IL). A marker of the cis-Golgi, GM130 (610822), was purchased from BD Biosciences (Sparks, MD). HuR (sc-5261), TIA-1(sc-1751), and TTP (sc-8458) antisera were purchased from Santa Cruz Biotechnology, Inc (Santa Cruz, CA). Anti-NeuN, used here as a marker for neuronal nuclei, (MAB377) was purchased from Millipore (Billerica, MA). Antisera for pp32, another HuR accessory protein (ADI-905-234-100) was purchased from Enzo Life Sciences (Farmingdale, NY). HSP-70 antiserum (SPA-820) was from Stressgen (Ann Arbor, MI). Anti-eIF4G directed against a fragment corresponding to nucleotides 288-1811 of the rat sequence (previously described in (Kimball et al., 2003; DeGracia et al., 2006). Alexa FluorR 488 donkey anti-goat IgG, Alexa FluorR 555 donkey anti-rabbit IgG, Alexa FluorR 555 donkey anti-mouse, Alexa FluorR 555 donkey anti-goat IgG, used for IF histochemistry were purchased from Molecular Probes (Eugene, OR). All other chemicals were reagent grade.

Animal Model

All animal experiments were approved by the Wayne State University Animal Investigation Committee and were conducted following the *Guide for the Care and Use of Laboratory Animals* (National Research Council, revised 2011). All efforts were made to reduce animal suffering and minimize the total number of animals used. Normothermic global forebrain ischemia of 10 min duration was induced in male Long Evans rats using the 2VO/HT model of Smith et al., (1984), as previously described. Exclusion criteria and survival rates were as previously reported. Experimental groups (n = 5/group) were: sham-operated, NICs, 10 min ischemia and reperfusion durations of: 15 min (15mR), 1 hr (1hR), 8 hr (8hR), 16 hr (16hR), 36 hr (36hR) and 48 hr (48hR).

Tissue Slice Preparation and Double IF/FISH

At appropriate times, animals were transcardially perfused, brains dissected, and 50 μm slices through the dorsal hippocampus were obtained via vibratome and stored at -20^{o}C in

cryostat solution until used. IF was performed alone, using HSP-70, (1:200). Double IF/FISH was performed exactly as previously described, using 50 ng/ml of a 5'-biotinylated 50-mer oligo-dT probe (Integrated DNA Technologies, Inc., Coralville, IA). Antisera dilutions were: α-tubulin, (1:100); APRIL, (1:100); COX IV, (1:50); eIF4G, (1:50); GM130, (1:100); HuR, (1:25); NeuN, (1:500); NF H/M, (1:300); PABP, (1:250); PDI, (1:200); pp32, (1:250); TGN38, (1:200); TIA-1, (1:150); TTP, (1:25).

Validation of antisera stainings included (not shown): (1) loss of signal with omission of primary antisera, (2) graded loss of signal with antisera dilution, and (3) agreement with published descriptions of antisera neuronal staining patterns where available [e.g. ER and Golgi (Takeda et al., 2001); NeuN and α-tubulin (Gu et al., 2009); neurofilament H/M (Kim et al., 2002); poly(A) mRNAs (Martone et al., 1996b), TTP (Stoecklin et al., 2004) and HuR homologs (Gao and Keene, 1996). We previously validated the specificity of TIA-1 (Kayali et al., 2005) and eIF4G staining (DeGracia et al., 2006).

Slides were examined on an Axioplan 2 Imaging System (Carl Zeiss, Oberkochen, Germany) equipped with an ApoTome. Excitation at 488 nm and 568 nm, and emission at 518 nm and 600 nm were used for Alexa 488 (green) and Alexa 555 (red), respectively. Optical sectioning was performed using the 63X oil immersion objective to generate z-stacks as previously described. Fluorescent micrographs shown in the figures are orthographic projections of 3.5 μm z-stacks (10 x 0.35 μm optical sections), unless otherwise stated.

Semi-Quantitative Analysis of Colocalization

For TIA-1/poly(A) double staining, SGs were counted using the "yellow channel". "Yellow channels" were constructed from orthographic projections of acquired z-stacks of CA1. Orthographic projections were used to amplify colocalization signals. Colocalization of paired antigens in discreet spots was quantified in BioImage Intelligent Quantifier. The total number of

spots per image was determined and normalized to the number of cells in each image, and averages taken for each experimental group to give values for the "number of spots per cell". A semi-quantitative measure of the colocalization of TIA-1 with poly(A) was achieved by taking the integrated density of the entire yellow channel, normalized to the number of cells in each image to produce a value of "density per cell". These measurements were made using NIH ImageJ (Abramoff et al., 2004). Groups (n = 5–6 per group) were compared by ANOVA followed by Tukey post hoc testing with statistical significance set at $p < 0.05$. Below in Figure 18, Images A-F, collectively illustrate channel manipulation through a step-by-step process. A full description of channel manipulation is in Chapter 2, *Data Analysis*.

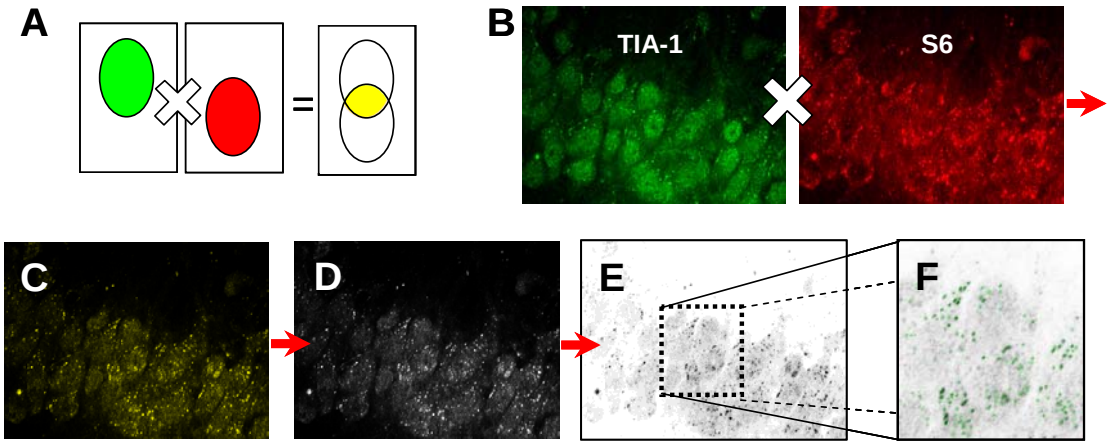

Figure 18. Diagram and fluorescent images provide examples of channel manipulation. Multiplication of red and green color channels depicted both graphically (A) and histologically (B). Multiplication of the channels gives an intersection showing only the colocalization of the two channels (C) that can then be converted into a gray-scale image (D). The image seen in D can then be inverted (E), the dense, dark spots can be highlighted in green (F) and imported into software to be counted (Kayali et al., 2005).

Western Blot Validation of Antisera

To further validate antibody specificity, Western blots were performed for each of the organelle and cytoskeletal antigens on either unfractionated non-ischemic brain homogenates (NeuN) or on the supernatant following centrifugation at 750 x g, 4°C (the remaining antisera). SDS-PAGE gels contained 50 µg of protein per lane, determined by Lowry assay. Conditions

for each Western blot are listed in Table 3, which includes primary antisera: dilution, buffer, incubation time, incubation temperature, and type of membrane for electroblot transfer, (NC, nitrocellulose; PDVF, polydivinylflouride). The base buffer for all primary antisera incubations was Tween-20 plus Tris buffered saline (TTBS). Other than the primary antisera incubation conditions, Western blots were performed as previously described.

Table 3. Conditions for each Western blot including: antisera, dilution, primary buffer (1^{o} buffer), time, temperature and membrane used.

Antisera	Dilution	1°Buffer	Time	Temperature	Membrane
APRIL	1:500	5%	1 hour	25° C	PVDF
α-Tubulin	1:1000	10%	1 hour	25° C	PVDF
COX IV	1:150	5%	overnight	4° C	PVDF
GM130	1:500	5%	1 hour	25° C	PVDF
NeuN	1:1000	5%	overnight	4° C	NC
NF H/M	1:1000	5%	overnight	4° C	NC
PDI	1:1000	2%	overnight	4° C	NC
pp32	1:333	N/A	overnight	4° C	NC
TGN38	1:250	5%	overnight	4° C	PVDF

Results

Microscope Observations

I preface the description of the microscopy results by stating that all descriptive observations occurred at 100% frequency in each group. The exact number of animals in each group (in parentheses) were: NIC(6), 1hR(6), 8hrR(6), 16hR(6), 36hR(5) and 48hR(5). Here, I systematically compared hippocampal regions CA1 and CA3. In the course of these observations, I also evaluated the hippocampal hilus and dentate gyrus as well as the cerebral cortex. Because these other brain regions: (1) did not show cell death in the ischemia model, and (2) behaved identically to CA3 as described below, only CA3 results are used to represent all other ischemia-resistant brain regions mentioned above.

Double IF/FISH

I previously showed that 10 min of 2VO/HT forebrain ischemia, in rat caused selective

CA1 cell death at 3 days reperfusion and that mRNA granules were present in CA1 neurons to 48 hR and in CA3 neurons to 16 hR. Identical results were obtained in the present study across the reperfusion time course (data not shown). For simplicity, the microscopic data will be presented within two groups: (1) ribonomic related antigens and (2) nonribonomic antigens (organelle, cytoskeletal and HuR transport antigens).

Ribonomic Related Antigens

The co-staining pairs (see ahead) shown within the NIC group, revealed punctate cytoplasmic poly(A) staining colocalized with eIF4G, TIA-1 and to a lesser extent with PABP and TTP, but not with HuR. Each of these components has previously been shown to be components of SGs (Anderson and Kedersha, 2006). Therefore, the punctate cytoplasmic poly(A) staining represented SGs, supporting our previous observations of SGs in neurons of the normal brain (Kayali et al., 2005; DeGracia et al., 2006, 2007).

Colocalization was assessed by double labeling with IF and FISH, of poly(A) with the following mRNA binding proteins: (1) eIF4G, a subunit of the eIF4F complex that delivers mRNA to the 40S subunit during translation initiation (Gingras et al., 1999), (2) poly(A) binding protein (PABP), which binds the 3' poly(A) tail, and contributes to a number of translation functions (Mangus et al., 2003), (3) TIA-1, a component of SGs (Anderson and Kedersha, 2002b), (4) TTP, a component of P-bodies (Stoecklin et al., 2004), and (5) HuR, an mRNA binding protein known to stabilize adenine and uridine rich element (ARE)-containing mRNAs (Keene, 1999). These costaining pairs are shown in Figures 19 and 20, in which arrows point to mRNA granules and arrowheads are used to point to SGs.

eIF4G and PABP & Poly(A)

eIF4G and PABP are described together because their staining patterns were the same across experimental groups (Figure 19). In CA1 and CA3 of NICs, eIF4G and PABP staining

were cytoplasmic as we previously showed for eIF4G (DeGracia et al., 2006). For both antisera, the cytoplasmic staining took two forms in the NICs: a diffuse staining and a punctate staining. Both the diffuse and the punctate cytoplasmic staining of each protein colocalized with the equivalent cytoplasmic staining of poly(A), producing in each case a diffuse yellow cytoplasm containing yellow punctate particles (Figure 19A and 19B, NIC samples). For eIF4G the diffuse colocalization likely represented their binding to mRNAs undergoing translation initiation. PABP diffuse colocalization likely represented PABP associated with mRNAs on translating cytoplasmic ribosomes. The punctate cytoplasmic staining represented colocalization with poly(A) mRNA in SGs (Figure 19A and 19B, arrowheads).

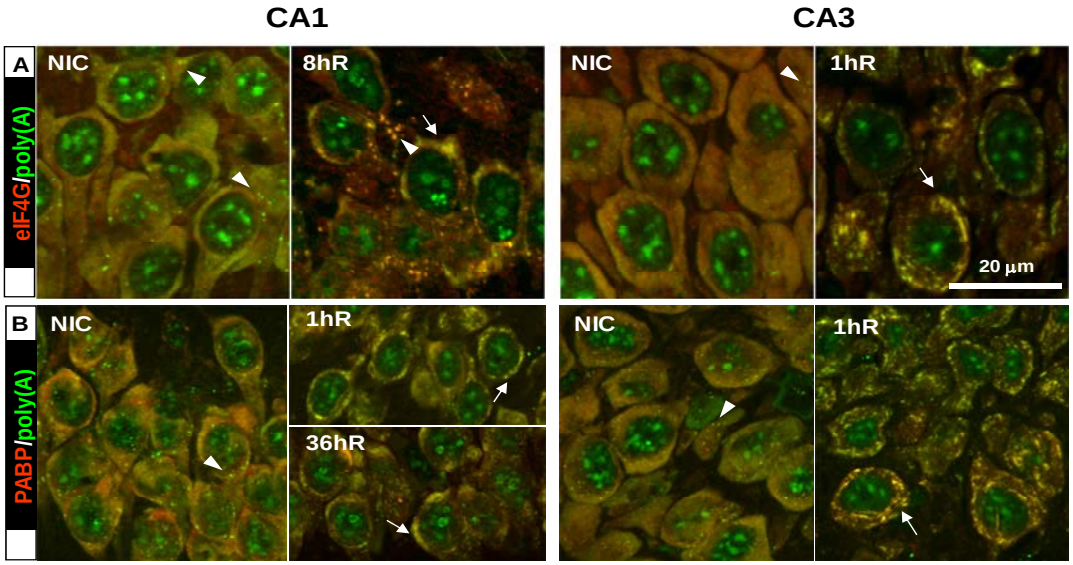

Figure 19. Ribonomic structural proteins that colocalized with mRNA granules during reperfusion. Co-staining of (A)eIF4G and poly(A), and (B)PABP and poly(A). Fluorescent colors associated with each staining pair are indicated in row labels. Merged fluorescent photomicrographs or representative samples (n= 5-6 per group) from experimental groups as indicated. Orthographic projections were derived as described previously. Scale bar = 20 µm and applies to all panels. Arrows point to mRNA granules, arrowheads point to SGs.

Following reperfusion, eIF4G and PABP clearly colocalized with the mRNA granules in both CA1 and CA3. In each costaining pair, the mRNA granules showed an intense yellow color in merged images (Figure 19A and 19B, reperfused, arrows). In all samples in which mRNA

granules were observed, they colocalized with eIF4G and PABP. In the individual channels for eIF4G and PABP, prominent cytoplasmic granules were present, similar to those we previously reported for eIF4G (DeGracia et al., 2006). At 36hR and 48hR in CA3, the costaining patterns for both proteins with poly(A) reverted to that seen in NICs (not shown).

TIA-1 & Poly(A)

The TIA-1 staining pattern obtained when costaining with poly(A) FISH was identical to that which we previously described (Kayali et al., 2005). That is, TIA-1 was predominantly nuclear, with punctate cytoplasmic staining. In NICS, the punctate TIA-1 staining colocalized with the punctate poly(A) staining (Figure 20, NIC CA1 and CA3, arrowheads), providing our main evidence that the punctate poly(A) staining represented SGs. Nuclear TIA-1 staining did not significantly colocalize with nuclear poly(A) staining in any control or reperfused samples.

During reperfusion, there was no colocalization of TIA-1 with the mRNA granules (Figure 20, reperfused, arrows), indicating that the mRNA granules were not SGs. In fact, the mRNA granules (Figure 20, arrows) and SGs (Figure 20, arrowheads) were mutually visualized in the neurons with poly(A)/TIA-1 costaining. The SGs formed small, circular, yellow colocalizations of TIA-1 and poly(A), whereas the mRNA granules were larger, irregularly shaped and stained only green for poly(A).

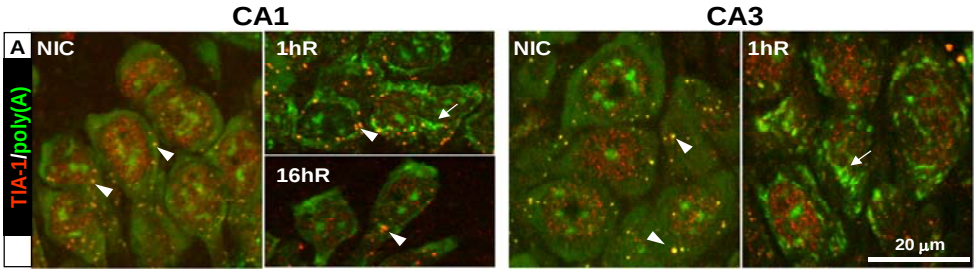

Figure 20. Results from TIA-1/poly(A) co-staining. Costaining of TIA-1 and poly(A). Fluorescent colors are associated with staining pair, as indicated in row labels. Merged fluorescent photomicrographs of representative samples (n= 5-6 per group) from experimental groups as indicated. Orthographic projections were derived as described previously. Scale bar = 20µm and applies to each panel. Arrows point to mRNA granules, arrowheads to SGs.

In order to count stress granules and compare the results using the 2VO/HT model to those obtained using CA/R model (Kayali et al., 2005), I used the double label IF technique, co-staining TIA-1 and S6. The same animal groups were used, as described above, plus one additional group: 10 min ischemia followed by 10 min reperfusion. The results are found in Figure 21, and show at 10 mins reperfusion, in both CA1 and CA3, stress granule numbers increase significantly as compared to control (nucleus does not contain SGs and thus was used here as a normalizer). However, at 1 hR the number of SGs decreased in both CA1 and CA3, and were no longer significantly different.

These results reveal that SGs are more prolific at 10 min reperfusion as compared to any of the remaining reperfusion time points studied. This also confirms that the CA/R model produces a more severe injury as compared to the 2VO/HT model thus explaining the variation in outcomes observed.

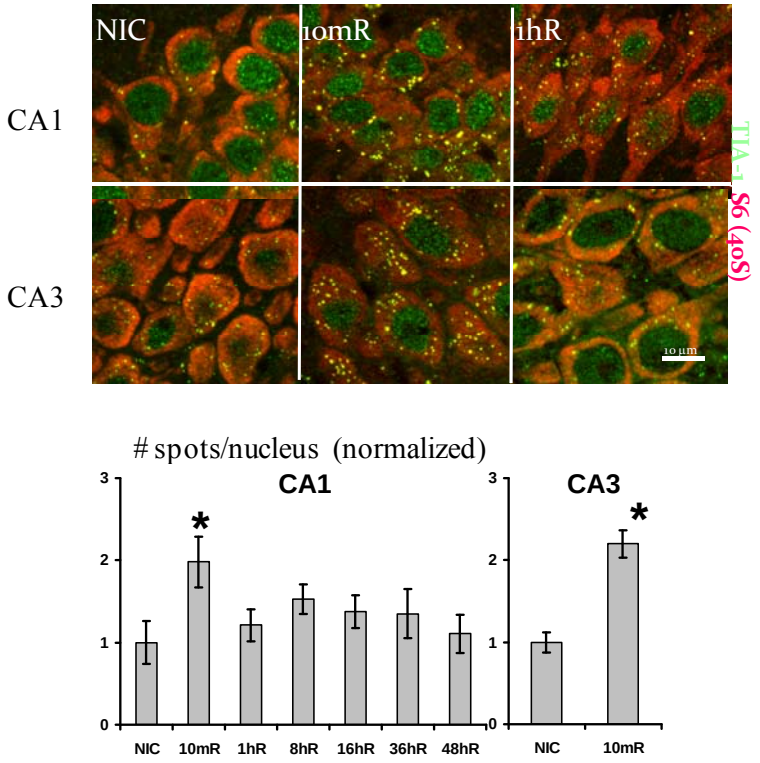

Figure 21. Results from TIA-1/S6 co-staining. Top Image: Fluorescent colors are associated with staining pair, as indicated in row labels. Merged fluorescent photomicrographs of representative samples (n= 5-6 per group) from experimental groups as indicated. Orthographic projections were derived as described previously. Scale bar = 10µm and applies to each panel. Lower Image: Counting of SGs in CA1 vs. CA3.

TTP & Poly(A)

I report here, to my knowledge, the first immunomapping of TTP in reperfused brain, and an assessment of its costaining with poly(A) (Figure 22A). In NICs, the TTP staining was similar to that of TIA-1 in that it was predominantly nuclear, in agreement with published TTP staining in other cell types (Stoecklin et al., 2004). However, in NICs, TTP did not significantly colocalize with the SG staining component of poly(A) (Figure 22A, NIC, arrowheads), suggesting it is not a major constituent of SGs in control neurons, but rather the distinct cytoplasmic sites known as P-bodies.

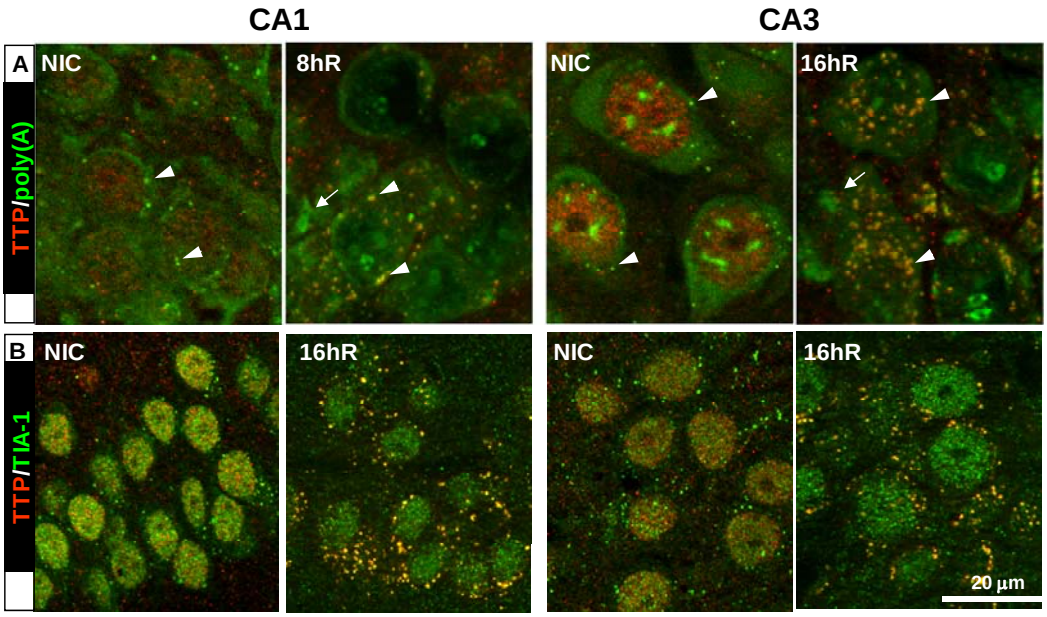

Figure 22. Ribonomic structural proteins that did not colocalize with mRNA granules during reperfusion. Costaining of: (A) TTP and poly(A); (B) TTP and TIA-1. Fluorescent colors associated with each staining pair are indicated in row labels. Merged fluorescent photomicrographs of representative samples (n= 5-6 per group) from experimental groups as indicated. Orthographic projections were derived as described previously. Scale bar = 20 µm and applies to all panels. Arrows point to mRNA granules, arrowheads point to SGs.

In reperfused CA1 and CA3 neurons showing mRNA granules, TTP did not colocalize with the mRNA granules (Figure 22A, arrows). However, in both CA1 and CA3, colocalization of TTP in poly(A) SGs, was observed starting at 8hR and peaking at 16hR (Figure 22A, reperfused, arrowheads). Increased colocalization of TTP and poly(A) in cytoplasmic SGs

corresponded with a decrease in the nuclear TTP signal. This colocalization decreased at 36hR, and was no longer evident at 48hR in both CA1 and CA3 (data not shown). This data suggests that: (1) TTP exported from the nucleus and entered cytoplasmic SGs during reperfusion, but that (2) TTP interaction with cytoplasmic SGs was reversible.

To confirm that TTP entered SGs, double-labeling IF with TIA-1 and TTP was performed (Figure 22B). I observed a redistribution of TTP out of the nucleus and into TIA-1 containing SGs in both CA1 and CA3 neurons by 16hR. Since TTP behaved identically in CA1 and CA3 (Figure 22A and 22B), it was determined that TTP changes did not correlate with selective vulnerability. However, the redistribution of TTP that was seen here, does correspond with observations made by (Kedersha et al., 2005), in which following the dissociation of polysomes, mRNA that is released is sorted and remodeled at SGs. From there, selected transcripts can be delivered from SGs to P-bodies for degradation. This account of SG and P-body association is consistent with my findings.

HuR and Poly(A)

Again, to my knowledge, this is the first investigation of HuR immunomapping, and an assessment of its colocalization with poly(A) mRNAs following brain reperfusion (Figure 23). In NICs, HuR showed a staining pattern in neurons essentially identical to that previously reported for its homolog HuB (Gao and Keene, 1996). HuR was mainly localized in the nucleus, but did show a diffuse cytoplasmic staining that was less intense, as compared to the nuclear staining. It was also noted, in the interneurons of CA1 (Figure 23, NIC, CA1, large arrow) and CA3 (not shown), the cytoplasmic HuR staining was much more intense than in the pyramidal cells. In pyramidal neurons, the colocalization of HuR and poly(A) resulted in an "olive" colored cytoplasm, representing a small degree of colocalization between cytoplasmic HuR and the diffuse component of the poly(A) cytoplasmic signal. Additionally, the HuR nuclear signal

showed “holes” within which the poly(A) nuclear staining tended to fit, almost like pieces of a puzzle, so there was no overlap between HuR and poly(A) nuclear staining patterns.

Upon reperfusion, different patterns of HuR/poly(A) colocalization were obtained for the CA1 and CA3. At 1hR, 8hrR and 16hR in CA1, HuR remained mainly nuclear and there was no colocalization with the cytoplasmic mRNA granules. At 36hR and 48hR in CA1, HuR showed colocalization with the cytoplasmic mRNA granules. In CA3, HuR colocalized with mRNA granules at the 1hR, 8hR and 16hR time points observed in CA3 neurons. At 36hR and 48hR in CA3, the colocalization pattern reverted back to that of the NIC group. Therefore, there was at least a 35 hour delay in HuR colocalizing with the mRNA granules in CA1 compared to CA3.

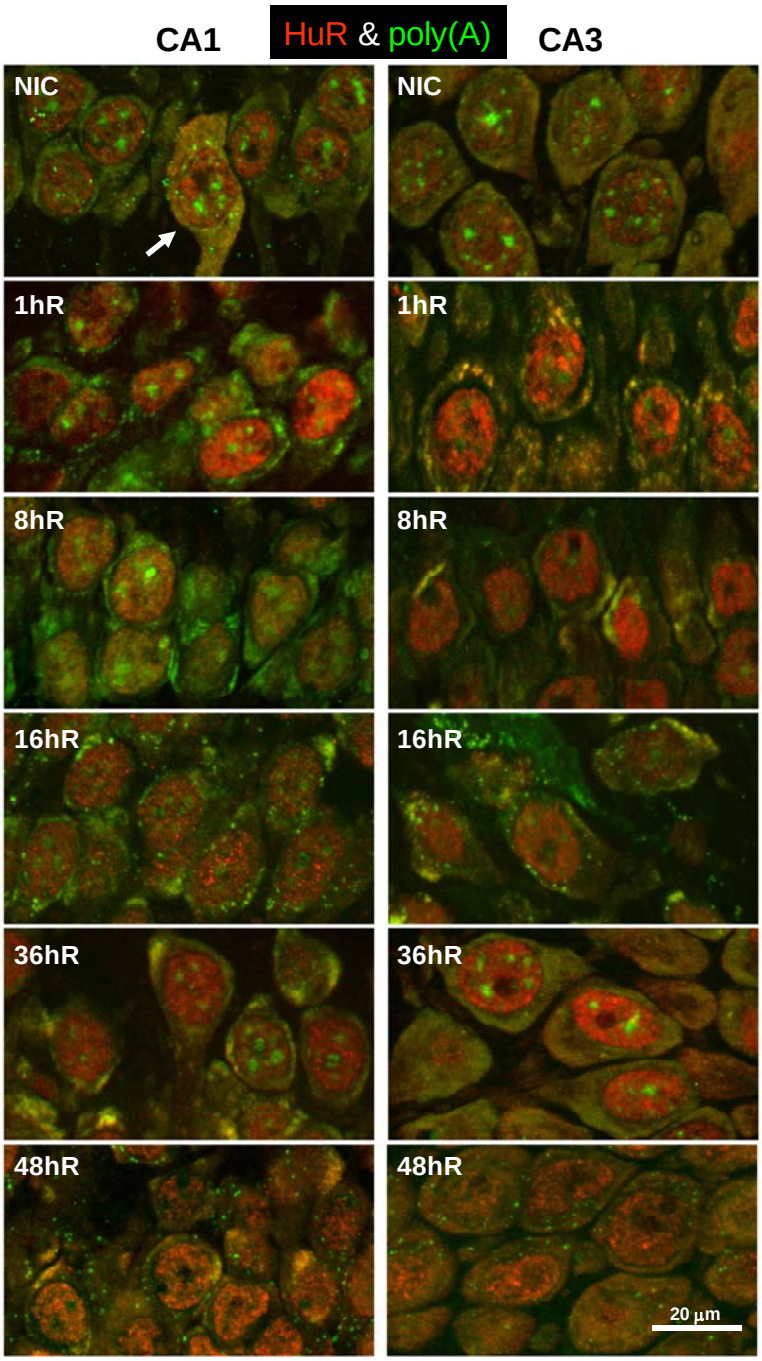

Figure 23. IF/FISH for HuR and poly(A). In NIC and 1hR-48hR. Merged fluorescent photomicrographs of CA1 and CA3 pyramidal layers of representative samples (n= 5-6 per group) from experimental groups as indicated. Orthographic projections were derived as previously described. Arrow points to CA1 interneuron. Scale bar = 20µm and applies to all panels.

HSP-70 Translation

Immunostaining for HSP70 is shown in Figure 24. When observed, HSP70 staining was extremely pronounced, resulting in what had been previously described as a "Golgi-like" staining pattern (Simon et al., 1991), in which the entire cell body, including extensive dendritic branching became labeled. In CA3, robust HSP70 staining occurred at the 8hR and 16hR time points. By 36hR in CA3, a much weaker HSP70 signal was obtained, confined predominantly to the nucleus and punctuate, cytoplasmic foci. By 48hR, the CA3 HSP70 signal was very weak.

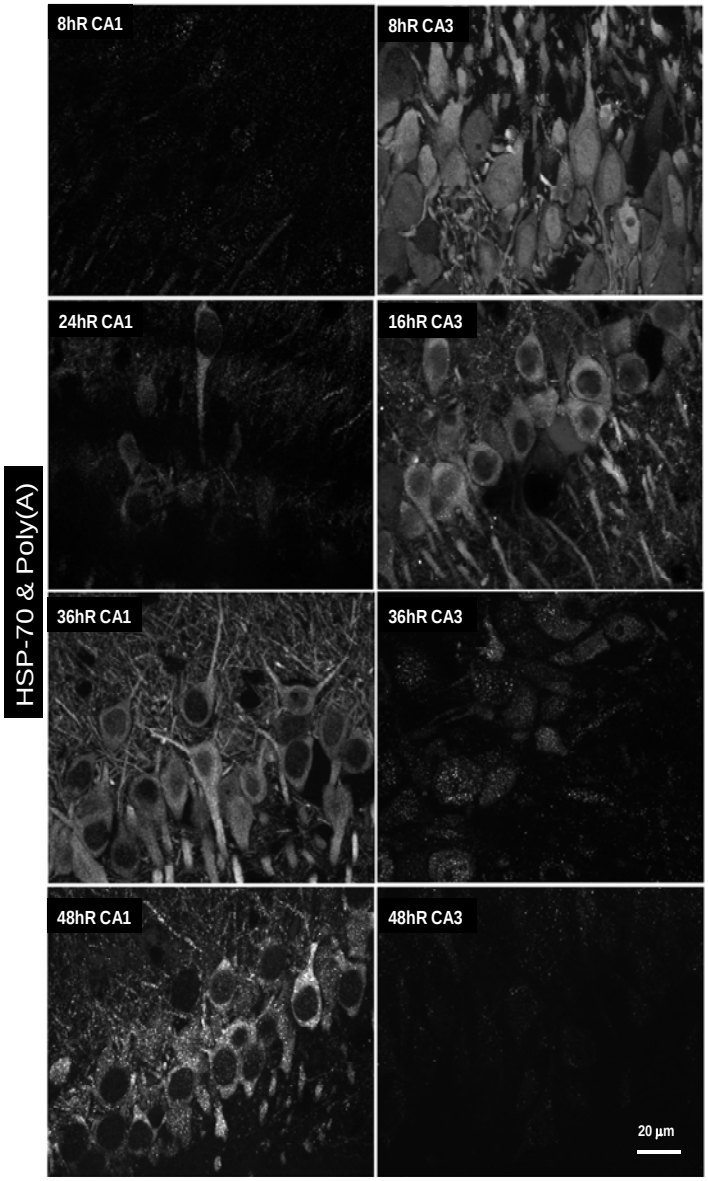

Figure 24. IF photomicrographs of HSP-70. In CA1 and CA3 pyramidal layer of representative samples (n= 5-6 per group) from experimental groups as indicated. Orthographic projections were derived as previously described. Scale bar =20 µm applies to all panels.

In contrast, in CA1 at 8hR, HSP70 staining was very weak. By 24hR in CA1, staining was detectable but still relatively weak. By 36hR, CA1 neurons were strongly stained with HSP70, which persisted at 48hR. These results are consistent with recent quantification from our laboratory, of HSP70 transcription and translation by PCR and Western blot, respectively, of microdissected CA1 and CA3 (Figure 25). There it showed, a similar, early translation of HSP70 in CA3 (by 8hR) and a much delayed translation in CA1 (seen by 30hR in that study) (Roberts et al., 2007).

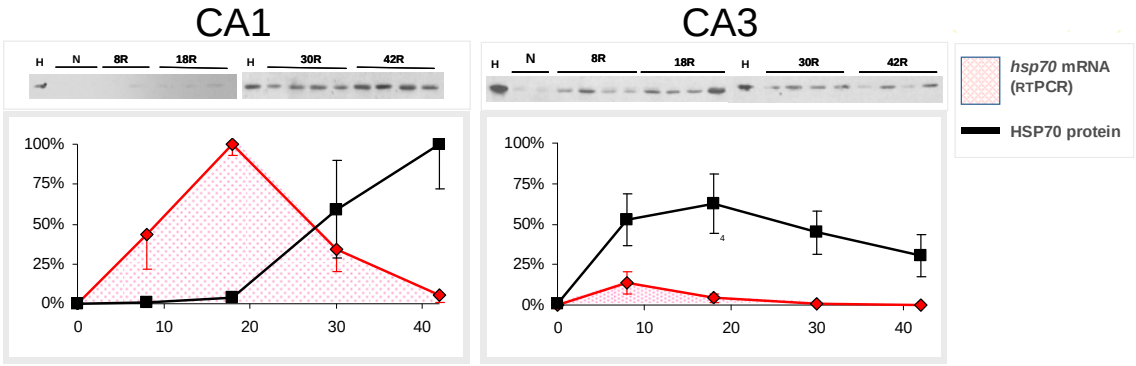

Figure 25. Differences between HSP70 translation in CA3 vs. CA1. Top left is the Western blots of HSP70 in microdissected CA1, on the right CA3 (as labeled). Below the Western blots, is the densitometry of HSP70 (for each region labeled above) normalized to GAPDH (not shown). Tukey post hoc $p<0.05$ compared with NIC, n=4 in each experimental group. Data obtained from Roberts et al., 2007.

Here the results from my data indicate a one-to-one correlation; samples that showed HuR in the mRNA granules also showed robust translation of HSP70 protein, with the exception of the 1hR CA3. In the latter case, previous studies have shown that hippocampal neurons do not begin synthesis of *hsp70* mRNA until at least several hours into reperfusion (Vass et al., 1988; DeGracia et al., 1993; Roberts et al., 2007)(Vass et al., 1988; Roberts et al., 2007), precluding synthesis of the protein at this early time point. As *hsp70* mRNA stability is regulated by a 3'-UTR ARE sequence (Laroia et al., 1999), the correlation between the colocalization of HuR in the mRNA granules and appearance of HSP70 protein in the same neurons is likely of functional significance.

Other Antigens: Organelles, Cytoskeltal and HuR Transport Proteins

Figures 26 and 27 illustrate representative photomicrographs of double IF/FISH staining in NIC and 1hR CA1 and CA3. Only 1hR samples are shown because the qualitative pattern of colocalization (or lack thereof) for a given antigen with the mRNA granules did not change over the reperfusion time course. Additionally, similar colocalization patterns were seen in cerebral cortical, thalamic and hilar neurons that evidenced mRNA granules following reperfusion (data not shown).

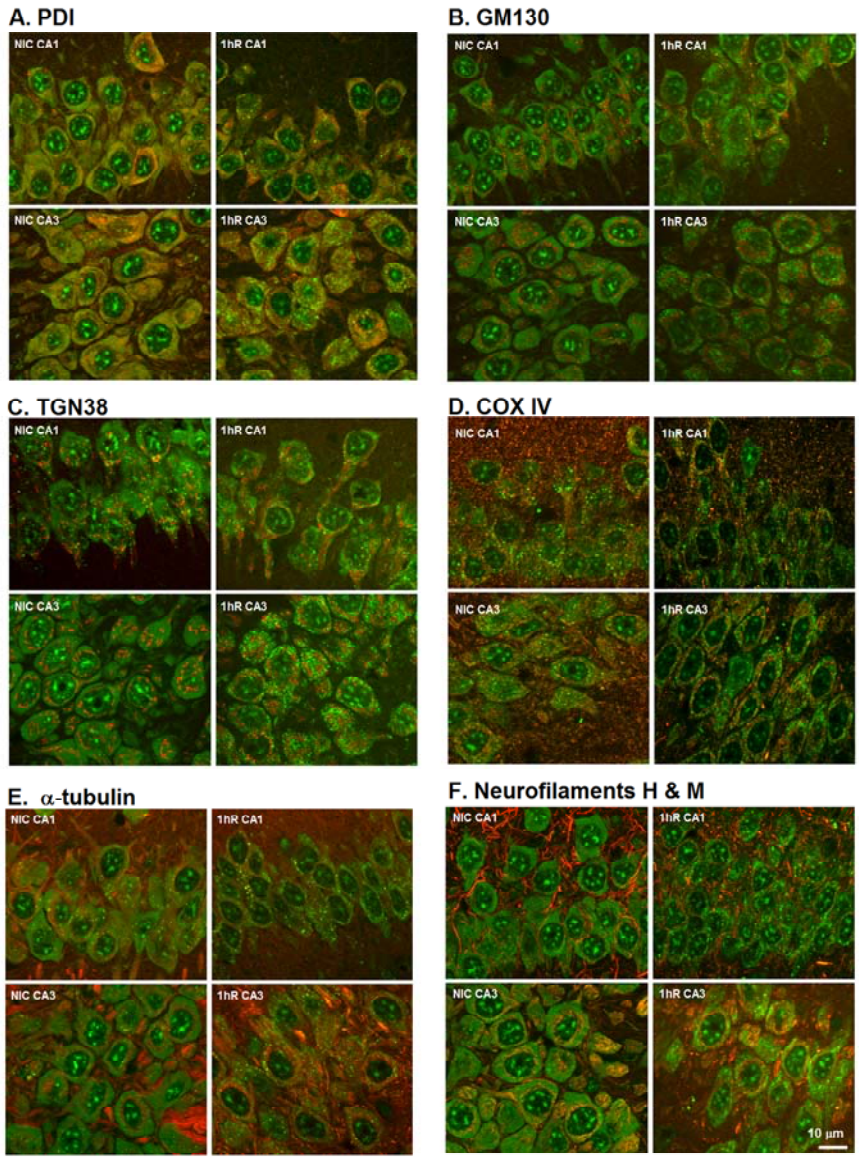

Figure 26. Representative photomicrographs of poly(A) mRNAs and organelle or cytoskeltal protein markers. Figures are labeled indicating nonischemic control (NIC) from one hour reperfusion (1hR), in hippocampal layers CA1 and CA3. All images were acquired under 63X oil immersion and are orthographic projections of ten sequential 0.35 μm optical slices. Scale bar in lower right most panel = 10 μm and applies to each image. Each image is a 1/3rd crop from the original photomicrograph.

Figure 26 shows double-labeling of poly(A) mRNAs and antisera detecting intracellular organelles. Only the antisera for PDI showed slight colocalization with poly(A) in the NIC samples, as indicated by the slight yellowish hue of the NIC cytoplasm (Figure 26A, NIC CA1 and CA3), likely indicative of ER-localized translation. However, at 1hR, the mRNA granules were distinctly green against the red PDI staining, thus the mRNA granules did not colocalize with ER (Figure 26A, 1hR CA1 and CA3). Markers of cis and trans- Golgi apparatus, GM130 and TGN38, respectively, showed no colocalization in NICs or at 1hR (Figures 26B and 1C). A lack of colocalization also held for the mitochondria marker COX IV (Figure 26D), and two cytoskeleton components, α-tubulin (Figure 26E) and NF-H/M (Figure 26F). Thus, the mRNA granules did not colocalize with any of the organelle or cytoskeletal protein markers tested.

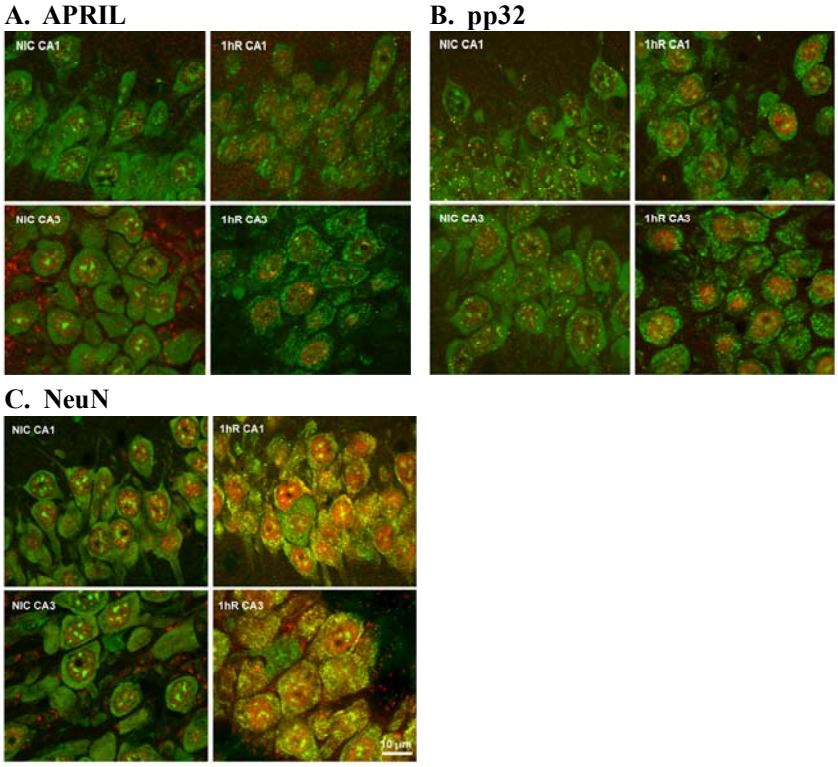

Figure 27. Representative photomicrographs of poly(A) mRNAs and mRNA binding systems. Indicated in the figure, nonischemic control (NIC) and one hour of reperfusion (1hR) in hippocampal layers CA1 and CA3. All images were acquired under 63X oil immersion and are orthographic projections of ten sequential 0.35 µm optical slices. Scale bar in lower right most panel = 10 µm and applies to each image. Each image is a 1/3rd crop from the original photomicrograph.

I previously showed that the mRNA binding protein HuR colocalized with mRNA granules in CA3 but not CA1 pyramidal neurons at 1hR. Steitz and colleagues (Gallouzi et al., 2003), have shown that HuR interacts with two protein ligands, APRIL and pp32, during CRM1-dependent nucleocytoplasmic transport of HuR-bound mRNAs. I observed no colocalization of APRIL (Figure 27A) or pp32 (Figure 27B) with the mRNA granules in the reperfused samples. Unexpectedly, the well-known neuronal nuclear marker NeuN strongly colocalized with the mRNA granules in both CA1 and CA3 during reperfusion (Figure 27C).

For all of the organelle antisera, cytoskeletal markers and HuR transport proteins used above, Western blots on brain homogenate proteins produced single bands at the correct molecular weights (Figure 28).

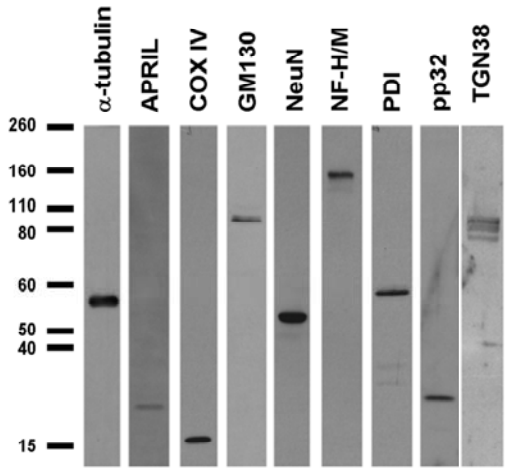

Figure 28. Western blots validating the specificity of the antisera. Antisera used was for identifying organelles, cytoskeletal proteins and HuR transport proteins for validation of microscope data. Positions of molecular weight standards are indicated to the left. Abbreviations for anti-sera are given in Materials and Methods.

The results of the double labeling revealed mRNA granules: (1) do not colocalize with SGs, P-bodies, or PAs, (2) do colocalize with PABP and eIF4G, and (3) do not colocalize with organelles (with the exception of the nuclear marker NeuN), cytoskeltal proteins or HuR transport proteins. A summary of these results are found in Table 4. First column lists the antigens double labeled with poly(A) using IF/FISH and the second column answers the question, does this antibody colocalize with mRNA granules?

Table 4. Summarizes double labeling results using IF/FISH.

Antigen	Coloc. w/poly(A)?
eIF4G	YES
PABP	YES
NeuN	YES
TIA-1	NO
TTP	NO
α-tubulin	NO
April	NO
COX IV	NO
GM130	NO
NF H/M	NO
PDI	NO
pp32	NO
TGN38	NO

CHAPTER 4

mRNA Granules Are Causally Linked to Post-Ischemic Translation Arrest

Overview

Hypothesis #4: Formation of the ribonomic structures are causally linked to post-ischemic translation arrest.

Rationale

A decrease in cerebral blood flow (CBF) to about 0.55 ml/g/min, or about 50% of normal CBF, will trigger the inhibition of neuronal protein synthesis (Hossmann, 2006). Given the relationship I showed above, between inhibition of protein synthesis and the formation of the mRNA granules, I predicted that the mRNA granules should form at the same blood flow rates known to induce inhibition of protein synthesis. To induce changes in CBF, I employed endothelin-1 (ET-1).

ET-1 is one of the most potent vasoconstricting agents known. It is a peptide produced by the vascular endothelium that binds the endothelin receptors, ET_A and ET_B (Sato et al., 1995). In smooth muscle, both receptors are Gq-coupled (Arai et al., 1990; Sakurai et al., 1990). When activated, IP_3 causes the release of ER calcium to induce smooth muscle contraction and vasoconstriction (Arai et al., 1990; Sakurai et al., 1990).

It has been shown via functional magnetic resonance imaging (MRI), that ET-1 administered intraventricularly produces dose-dependent, apparently graded, decreases in local CBF as shown in Figure 29 (Jamison et al., 2011).

Another well known agent used to inhibit protein synthesis is cycloheximide (CHX). CHX is a glutarimide antibiotic that has been well established as an inhibitor of protein initiation as well as elongation (Grollman, 1966). In fact, CHX "freezes" nascent polypeptides in place, thereby not releasing them from the ribosome, nor dissociating any part of the whole

polyribosomal structural unit (Pestka, 1971). Therefore, if animals were treated with CHX prior to I/R, one would predict CHX would prevent polysome disaggregation, and without free mRNA, the mRNA granules would not form. However, if CHX was given shortly after reperfusion (~10-15 mins), during acute TA when eIF2α(P) levels are the highest (Roberts et al., 2007), polysomes would be in an already dissociated state (Hossmann, 1993; DeGracia et al., 2008b), thus one would expect the post-administration of CHX to produce mRNA granules.

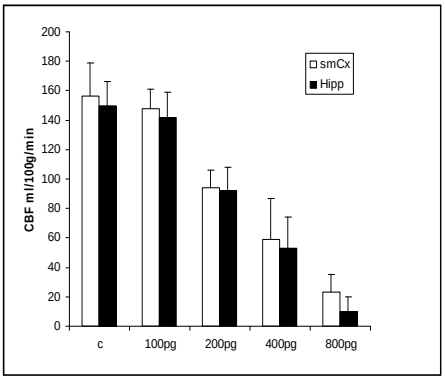

Figure 29. Effect of ET-1 on cerebral blood flow, as measured by MRI. ET-1 administered intraventricularly in hippocampus (Hipp) and sensorimotor (smCx) cortex of the rat (Jamison et al., 2011).

Both CHX and ET-1, are pharmacologic agents that are recognized for their effects on TA, albeit through very different mechanisms. Here, these agents were used in different capacities to link the mRNA granules with TA. For ET-1, it was used to reduce CBF to TA threshold. For CHX, it was to directly investigate the link between polysomal structure and mRNA granule formation.

Experimental Overview

Both CHX and ET-1, are pharmacologic agents that are recognized for their effects on TA, albeit through very different mechanisms. Here, these agents were used in different capacities to link the mRNA granules with TA. For ET-1, it was used to reduce CBF to TA threshold. For CHX, it was to directly investigate the link between polysomal structure and mRNA granule formation.

Experimental Overview

Using a stereotaxic frame, ET-1 was administered, through intraventricular injection, in

male Long Evans rats. The experimental groups consisted of ET-1 administered at 100 pg, 200pg, 400pg, or 800pg verses saline-treated controls. The specific number of animals per experimental group are listed below. Animals were sacrificed 4 hours following the ET-1 injections. Each animal was perfusion fixed and had tissue slices prepared, as described previously. FISH was used to detect for mRNA granules. If the mRNA granules form at blood flow rates that induce inhibition of protein synthesis, this will reinforce the functional link between mRNA granules and TA.

The second group of animals were administered CHX either 15 min before or 15 min after global forebrain ischemia was induced in male Long Evans rats for 10 min using the 2VO/HT model described previously. Both the pre and post-treated CHX groups were reperfused for 1 hr, (1hR). Identical groups were repeated using saline vehicle. Animals were perfusion fixed and had tissue slices prepared for staining. Tissue slices were double labeled using FISH to detect poly(A) mRNAs and IF to detect HuR proteins.

Hypothesis 3 was tested by administering two mechanistically different pharmacologic agents to see if either could induce mRNA granules and thus provide a causal link between injury and mRNA granule formation.

Experimental Procedures

Materials

Alexa 488-labeled streptavidin (S32354) was obtained from Invitrogen (Carlsbad, CA). Biotinylated goat anti-streptavidin (BA-0500) was purchased from Vector Laboratories (Burlingame, CA). Alexa FluorR 555 anti-mouse IgG, used for IF histochemistry, was purchased from Molecular Probes (Eugene, OR). HuR (sc-5261) antiserum was purchased from Santa Cruz Biotechnology, Inc. (Santa Cruz, CA). A 5'-biotinylated 50-mer oligo-dT probe was made by Integrated DNA Technologies, Inc. (Coralville, IA). Prehybridization and hybridization

buffers were obtained from the mRNA locator In Situ Hybridization Kit (Ambion, Austin, TX). Cycloheximide and endothelin-1 were purchased from Sigma (St. Louis, MO). All other chemicals were reagent grade.

Animal Model

ET-1 Treatment

Male Long-Evans rats were anesthetized with ketamine and xylazine (100 and 10 mg/kg, respectively), heads shaved and then symmetrically fixed by ear bars, front teeth, and nosebar into a stereotaxic frame. A 1-inch incision was made down the midline of the scalp and the exposed skull was cleared of tissue. Coordinates for injection into the lateral ventricle were: posterior 20.80 mm, lateral 21.5 mm, ventral 23.8 mm, all relative to Bregma (Paxinos and Watson, 1998). Bilateral holes were drilled and a 21-guage needle lowered sequentially into the lateral ventricles. ET-1 or vehicle was injected 10 µl over 10 sec, and the needle left in place for an additional 1 min. ET-1 treatment was randomly assigned to animals in five experimental groups: (i) vehicle (normal saline) only; (ii) 100 pg; (iii) 200 pg; (iv) 400 pg; and (v) 800 pg endothelin-1. These injection amounts corresponded to 25, 50, 100, and 200 mM ET-1, respectively. Following ET-1 injection, rats were released from the stereotaxic frame and the wound sealed by staples. Animals were returned to their cages for 4 hr, at which time, they were perfusion fixed for tissue staining (n=3–5 per experimental group).

Cycloheximide Treatment

Global forebrain ischemia was induced in male Long Evans rats for 10 min using the 2VO/HT model of Smith et al. (1984), as previously described. Rats were maintained normothermic during both I/R periods. Post-surgical animals displaying necrosis or sustained seizure activity were excluded from the study. Animals were administered CHX (1.5 mg/kg I.P.) either 15 min before (C-pre; n = 6) or 15 min after (C-post; n = 5) the 10 min ischemia period.

Both the C-pre and C-post groups were reperfused for 1 hr, (1hR). Identical groups were repeated using saline vehicle administration for the pretreatment (v-pre; n = 5) and post treatment (v-post; n = 5) groups. The dose of CHX used here, has been shown in previous studies to be a protein synthesis blocker in forebrain ischemia models (Papas et al., 1992). Animals were perfusion fixed as previously described.

Tissue Staining

For ET-1 animals, only FISH was used to detect mRNA granules. IF/FISH was used to double label HuR/Poly(A) mRNAs in the animals pre and post treated with CHX.

Data Analysis

For blood flow measurements, multiple experimental groups were compared by analysis of variance followed by Tukey post hoc analysis. For measurements of cortical neuron loss after ET-1 treatment, visualized by poly(A) mRNA FISH staining, estimates of percentage cell loss and percent of area in which cell loss occurred were performed by evaluating the entire cerebral cortex in the tissue slice at 10X. Cell loss was confirmed by viewing at 40X to distinguish cell loss from weak staining. The percent of damaged area and of cell loss were both compared by analysis of variance followed by Tukey post hoc if necessary. The majority of results reported here are descriptive and based on three-dimensional reconstruction of tissue using an ApoTome-equipped microscope as described. Photomontages were manually constructed in Photoshop CS (Adobe Systems, San Jose, CA).

For the CHX group, only the CA3 pyramidal neurons are shown because of their prominent formation of mRNA granules. Therefore, all photomicrographs were collected at the lateral-most bend of CA3 in the dorsal hippocampus. The same microscope field for both the left and right CA3 were photographed giving two images per animal. Stacks of optically sectioned tissue slices were acquired under a 63X oil immersion lens, where each pixel

represented spatial dimensions of x = 0.1 µm, y = 0.1 µm, and z = 0.35 µm. Acquired z stacks were used for the construction of maximum intensity orthographic projections in NIH Image J (Abramoff et al., 2004).

Results

ET-1 and Cerebral Blood Flow

Figure 29 shows the result of local cerebral blood flow measurements in cerebral cortex and hippocampus in vehicle-treated and from 100-800 pg ET-1 (Jamison et al., 2011). The 100 pg dose had no effect on blood flow in either region. A dose dependent decrease in blood flow was observed from 200 pg to 800 pg ET-1. Blood flow was reduced by one third and one half with 200 and 400 pg ET-1, respectively, and no difference in decrease occurred between cerebral cortex or hippocampus. At 800 pg ET-1, cortical blood flow was decreased 80%, and hippocampal blood flow was decreased 94%.

The graded decrease in blood flow led to the hypothesis that one would observe graded effects in brain tissue injury following ET-1 administration. However, results from my *in situ* studies described below indicated that the graded changes in blood flow were only apparent, and likely represented averages of inhomogeneous patterns of blood flow reduction.

ET-1 Induced Cortical Damage

Figure 30 shows coronal sections of the ET-1 injection site at -0.8 mm posterior to the

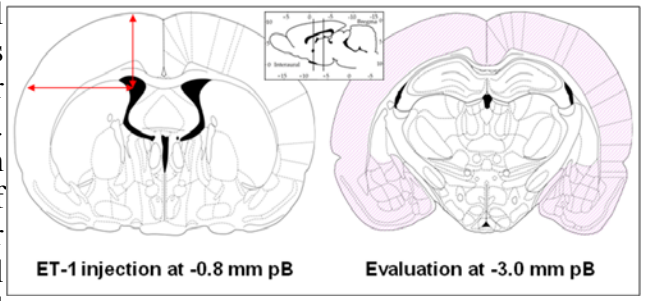

Figure 30. Diagram depicting the coronal sections used for ET-1 and its coordinate sites for injection. Particular section identified for microscope analysis using poly(A) mRNA FISH. Arrows mark lateral and ventral injection coordinates. Right image shows extent of cerebral cortex evaluated and served as 100% for area measurements in Table 5. Inset: midsagittal section showing locations of two coronal sections. Images adapted from Paxinos and Watson (2005). pB, posterior to Bregma.

Bregma and the level of brain section chosen for evaluation at -3.0 mm posterior to Bregma containing the dorsal hippocampus. Ventral and lateral injection coordinates are indicated by red arrows on the left image. Slices were evaluated 2.2 mm posterior to the site of ET-1 injection to avoid damage due to the injection site. I excluded slices showing cortical damage that had obviously resulted from the injection tract into the brain. As described below, damage occurred heterogeneously throughout the entire area of the cerebral cortex.

Table 5 lists averages for the total area of cerebral cortex at -3.0 mm pB, displaying evidence of cell damage or death following ET-1 injection, as evaluated by poly(A) mRNA FISH staining. Table 5 also lists the decrease in the number of cells, expressed as a percentage of controls, in areas displaying cellular damage. The criteria for designating an area as "damaged" included: (1) decreased density of cells, (2) altered cell morphology from controls, usually, but not exclusively, in the form of cell shrinkage and distortion, and (3) a significant decrease in cell staining compared to undamaged areas. The values in Table 5 are only rough indicators of cell damage because of the heterogeneity reported below.

Table 5. Average percent cell death and damaged cortical area, following ET-1 treatment.

	n	# Animals with Cortical Damage	% Area Damaged (Mean ± SD)	% Decrease in Cell Number (Mean ± SD)
200 pg ET-1	3	1	10.0 ± 17.3 *	20.0 + 34.6
400 pg ET-1	5	5	48.1 ± 17.8	54.0 + 5.5
800 pg ET-1	3	3	67.5 ± 10.9	58.2 + 14.4

ANOVA $p = 0.007$ (% area damaged); ANOVA $p = 0.068$ (% decrease in cell number). *, post hoc $p < 0.05$ compared to respective experimental groups. SD, standard deviation.

There was a trend toward a dose-dependent increase in the area of cerebral cortex showing cell damage from 200-800 pg ET-1. However, for 200 pg only one of three animals showed evidence of damage at -3.0 mm posterior to Bregma. It is possible that other slices in the 200 pg samples showed damage, but we did not observe them due to our adherence to fixed

coordinates for analysis. All of the 400 pg and 800 pg treated animals showed evidence of cerebral cortical damage at -3.0 mm posterior to Bregma. The respective percent area damaged did not clear statistically because the 400 pg samples showed wide variation, ranging from 18% to 63% of cortical area damaged. The 800 pg samples showed less variation, ranging from 60%-80% damaged area. For all three experimental groups, the percentage decrease in cells within the damaged areas averaged about 50% and there was no statistical difference amongst the groups.

Assessment of Cortical Histology Following ET-1 Treatment

Histological assessment of cortical damage by poly(A) mRNA staining showed the heterogeneity in damage distribution. Figure 31 shows poly(A) mRNA staining for each ET-1 dose under both low (10X) and high (40X) power objectives. The 100 pg group was excluded from poly(A) mRNA staining because this group showed no decrease in cerebral blood flow (Figure 29). Figure 32 includes the single 200 pg ET-1 treated animal that displayed cortical damage (Figure 32 insert A) with areas of normal-looking, viable cells surrounding it (Figure 32 insert B). Non-ischemic control layer II cortical neurons (Figure 31 B), had the same three general features of poly(A) mRNA staining reported previously in Chapter 2, for hippocampal neurons : (1) diffuse and relatively homogeneous poly(A) mRNA staining throughout the entire cytoplasm, (2) occasional small and circular intense poly(A) mRNA cytoplasmic staining that I previously showed were stress granules, and (3) the presence, inside the area of the nucleus, of several intense, roughly circular structures ranging from 0.5 – 2 μm against a weak background of diffuse poly(A) mRNA staining.

As the image progresses in Figure 31, layers II and III of the cerebral cortex were most strongly affected. The 200 pg sample shows decreased cell density and cell shrinkage (Figure 31 C and D) as compared to controls (Figure 31 A and B). The 400 pg samples showed greater

numbers of shrunken cells and areas devoid of cell staining.

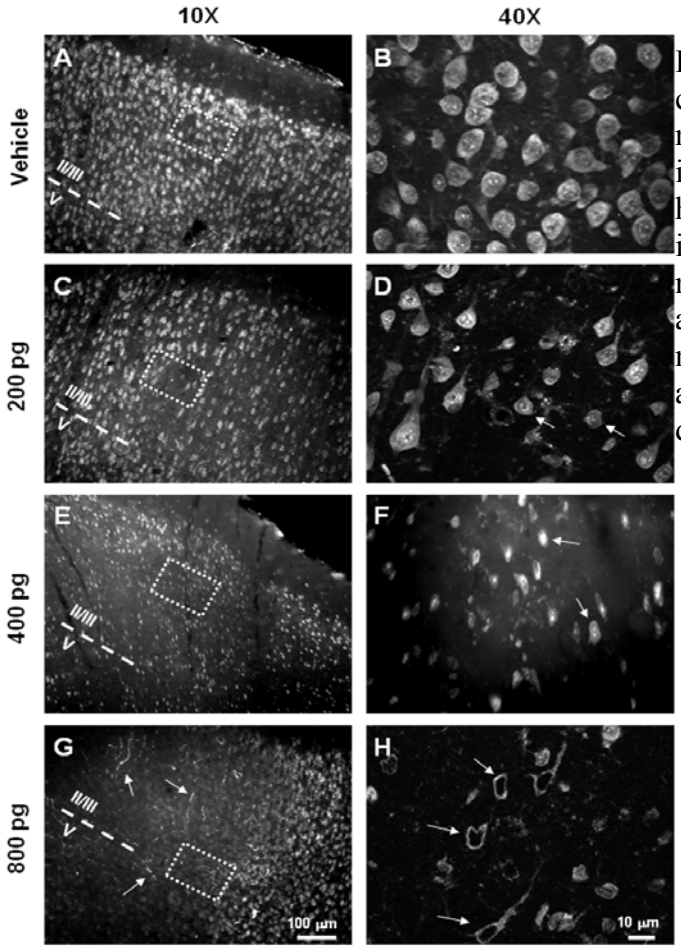

Figure 31. Photomontage of the cerebral cortex assessed by poly(A) mRNA FISH following 200 pg ET-1 intraventricular injection. Inset: red highlighted section depicts where 10X images were taken. Blue lines on inset mark the area of injection 2.8 mm anterior to the coronal section. Area A marks area of maximal damage and areas B mark adjacent areas of lesser damage.

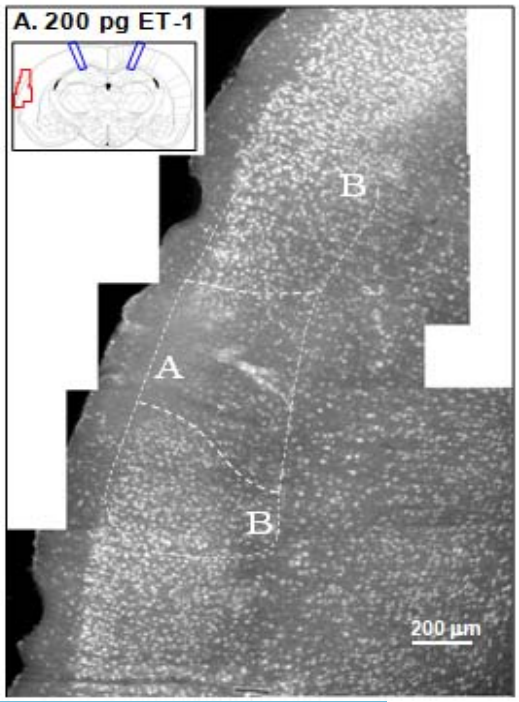

Figure 32. Histological view of the effects of ET-1 on the cerebral cortex. Histological assessment using poly(A) mRNA FISH. Left column: low power (10X objective) photomicrographs. Right column: high power (40X objective) photomicrographs. ET-1 doses as specified to the left. Images of 40X are from areas marked by white dashed boxes indicated on respective 10X images. Arrows in (D) and (F) point to shrunken neurons identified in the text as ischemic cell change. Arrows in (G) point to microclots in capillaries. Arrows in (H) point to neurons lacking poly(A) mRNA nuclear staining. Scale bar in (G) applies to all images at 10X and scale bar in (H) applies to all images at 40X.

In the 800 pg samples, the damage extended into other cerebral cortical layers, and the areas devoid of cell staining were generally larger than the 400 pg group. Occasionally, microclots were observed in which red blood cells trapped in capillaries were stained by the poly-T probe (Figure 31 G, arrows).

With respect to poly(A) mRNA staining at high magnification, mRNA granules were not observed in any of the neurons following any dose of ET-1. Instead, one of two general patterns were observed. In the first, poly(A) mRNA staining of shrunken and distorted cells was reminiscent of that of controls with an apparently homogenous cytoplasm and intense nuclear poly(A) mRNA staining (Figure 31 F, arrows). However, in the second poly(A) mRNA staining pattern, we observed in many cases that cells were devoid of nuclear poly(A) mRNA staining and that such cells, though distorted to some extent, were generally not shrunken (Figure 31 H, arrows).

Effect of Cycloheximide On mRNA Granule Formation

Poly(A) and HuR cytoplasmic staining were assessed in rats either pretreated or post-treated with CHX. Both the pretreated and post-treated groups were reperfused for 1 hr, (1hR). Figure 33 shows the classic example of NICs, where HuR is mostly nuclear and poly(A) reflects the common homogenous cytoplasmic staining that has been described previously. In the vehicle treated animal, pyramidal neurons contained the yellow speckled cytoplasmic staining, indicating the presence of mRNA granules, as described previously. The CHX pretreated (C-pre) group had an appearance similar to NICs, with smooth cytoplasmic staining. However the C-pre group had a more yellowish hue indicating more HuR had transported out from the nucleus into the cytoplasm, as compared to the NIC. Also there were bright green round punctate poly(A) staining, which I have previously identified as stress granules, but no mRNA granules were seen. The post-treated CHX (C-post) group, the cytoplasm is extremely granular,

filled with the intensely stained mRNA granules.

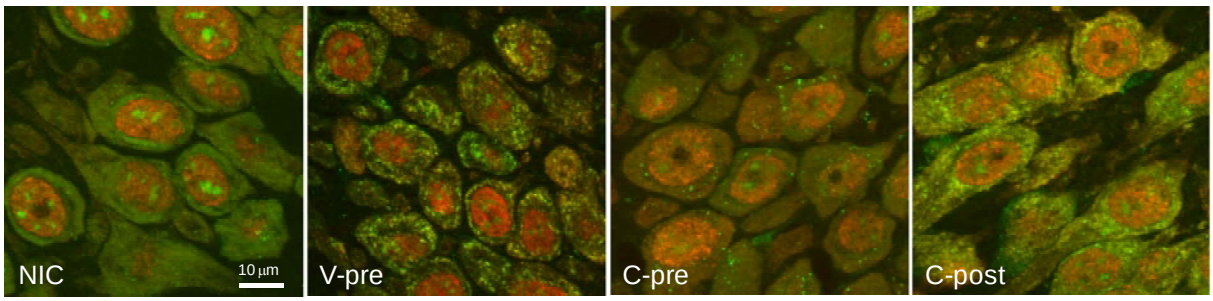

Figure 33. Effects of pre and post-treatments of cycloheximide in CA3 neurons at 1hR. CHX given 15 mins before or after 10 mins ischemia. Formation of mRNA granules assessed at 1hr brain reperfusion. (A) Merged images of pA (green) and HuR (red) double-labeling of individual samples as indicated. Samples are non-ischemic, sham-operated control (NIC), vehicle pretreated 1hR (v-pre), CHX pretreated 1h reperfused (C-pre), and CHX post-treatment 1h reperfused (C-post). All images are 1/3rd crops of original images. Scale bar applies to all images.

From these results it was determined that CHX pretreatment inhibited poly(A) mRNA granules, while CHX post-treatment did not prevent mRNA granule formation. The CHX results support the above model and indicate that mRNA granule formation depends on the dissociation of polysomes to free-up polysome-bound mRNAs. The increase in unbound mRNA molecules can then serve as the substrate driving the formation of RNPs into complexes, such as the mRNA granules.

CHAPTER 5

Discussion

Summary of Results

In the preceding sections, I have described my studies involving persistent TA following global brain I/R. To summarize the main findings:

- A novel discovery was made; cytoplasmic poly(A) containing mRNAs redistributed to form **mRNA granules** in reperfused neurons.
- mRNA granules sequester mRNA away from both the small and large ribosomal subunits, providing a novel mechanism of prolonged TA in post-ischemic neurons. More specifically, the presence of mRNA granules in post-ischemic neurons correlated precisely with in vivo TA. In CA3, mRNA granules abated by 16hR, whereas mRNA granules persisted in selectively vulnerable CA1 neurons and remained until the cells underwent DND.
- The colocalization of mRNA granules with known mRNA binding proteins PABP, eIF4G and HuR suggests that mRNA granules are ribonomic complexes, involved in mRNA regulation that may itself be related to or a subset of the ELAV/Hu granule.
- I observed a correlation between HuR colocalized to mRNA granules and translation of HSP-70. This correlation suggests mRNA granules are involved in post-transcriptional stress gene regulation in reperfused neurons.
- Through further characterization of mRNA granules, I determined: (1) mRNA granules are not SGs, P-bodies, polysomes or any other organelle marker tested.
- mRNA granules colocalized with NeuN in the cytoplasm.
- mRNA granules were mechanistically linked to polysome dissociation.

I now discuss the relation of this work, to other studies in the brain ischemia field and

how these findings provide new insights into the response of neurons to global brain ischemia injury.

mRNA Granules and Ribonomics

Subcellular redistribution of translational machinery or ribonomics, plays an important role in translation regulation in pathological circumstances (reviewed in Anderson and Kedersha, 2006). Because brain I/R results in a profound TA in selectively vulnerable neurons (Hossmann, 1993), the purpose of the first study was to assess if changes in the subcellular distribution of mRNA and translation regulators, into mRNP complexes, contributed to prolonged TA in vulnerable neurons. The second study focused on identifying the histological composition of the mRNA granules and further considered their intracellular properties, while the final experiments discussed in Chapter 4, looked to specific pharmacologic agents to induce their formation. Below, I discuss how the results gathered from these experiments have substantially advanced the understanding of post-ischemic TA.

Subcellular Structures in Reperfused Neurons

To date, four subcellular structures have been identified in reperfused neurons: (1) ubiquitin-protein clusters (ubi-protein clusters), (2) protein aggregates (PAs) (Hu et al., 2000; Liu et al., 2005a; Liu et al., 2005b), (3) SGs (Kayali et al., 2005; DeGracia et al., 2007), and (4) aggregates of eIF4G (DeGracia et al., 2006). The question to consider: How do these mRNPs relate to mRNA granules?

Ubi-protein clusters and PAs appear to be related as they are both marked by ubiquitin immunostaining *in situ* (Hu et al., 2000). Ubi-protein clusters form early in reperfusion in all post-ischemic neurons, but are reversible in resistant neurons (Hu et al., 2000; DeGracia et al., 2007). In vulnerable neurons at later reperfusion, the ubiquitin immunostaining transforms to take the form of PAs, suggesting that the PAs somehow derive from the ubi-protein clusters

(DeGracia and Hu, 2007). Under the microscope, the ubi-protein clusters are large (~2-5 microns) irregular domains of ubiquitin staining, and the PAs are punctate ubiquitin-containing particles of 200-500 nm, best visualized using EM. Thus, the particles marked by ubiquitin immunoreactivity persist in vulnerable neurons and become smaller as reperfusion progresses (Hu et al., 2000; reviewed in DeGracia and Hu, 2007). However, the mRNA granules observed here became larger with reperfusion duration (Figure 11). Additionally, PAs were shown to colocalize with TIA-1 at 48 hR (DeGracia et al., 2007). However, TIA-1 did not colocalize with mRNA granules at any of the time points observed. The data therefore suggests that mRNA granules are not the same as ubi- protein clusters, nor PAs.

It can also be concluded that the mRNA granules are not SGs. Again, the morphology of the two particles are very different: SGs form circular punctate structures, but the mRNA granules are instead irregular domains occupying wide areas of cytoplasm. The mRNA granules lacked TIA-1 (Figure 20), the self-aggregating component of SGs (Gilks et al., 2004). Finally, we could simultaneously visualize both the mRNA granules and SGs in the same neuron, proving their distinct identities (Figure 20).

It was previously shown, following I/R using the CA/R model, the formation of aggregates of eIF4G that persisted in CA1 pyramidal neurons (DeGracia et al., 2006). Using the 2VO/HT model to induce ischemia, I also observed aggregates of eIF4G that precisely colocalized with mRNA granules (Figure 19). The morphology of the eIF4G aggregates were identical in both studies, using two distinct models; this suggests that eIF4G aggregates are markers of mRNA granule formation. If validated, the mRNA granules would provide a mechanism of prolonged TA common to both the CA/R and 2VO/HT models.

mRNA Granules

Although many forebrain I/R investigations have looked at changes in individual mRNAs

with *in situ* hybridization or PCR, few studies have evaluated markers of total mRNA following brain I/R. In one such study, (Matsumoto et al., 1990) showed a subcellular redistribution of mRNA by gradient centrifugation, and concluded mRNA transport was altered following brain I/R. This suggested that mRNA transport may contribute to the TA associated with selective vulnerability. The observations I presented above, support this suggestion. However, the Matsumoto et al. (1990) study offered no rationale underlying the change in mRNA distribution.

The understanding of translation regulation in reperfused neurons that I have presented here, does provide one plausible explanation. Phosphorylation of eIF2□ occurs with the onset of reperfusion (Kumar et al., 2003) resulting in translation initiation inhibited, polysome dissociation, and resultant TA. Focus on ribosome regulation has diverted attention from the issue of what happens to mRNA when polysomes dissociate. My data suggests that the mRNA granules form in response to polysome dissociation, possibly to sequester, preserve and silence neuronal "housekeeping" mRNAs. In this role, the mRNA granules are likely part of a protective mechanism, as they formed in all post-ischemic neurons.

The translational control literature offers further insight into the potential nature of the mRNA granules. A recent report showed that glucose deprivation (and not amino acid deprivation) in yeast, lead to a redistribution of cytoplasmic mRNAs in structures termed EGP granules. EGP granules were found to contain eIF4E, eIF4G and PABP, but lacked the P-body markers and decapping enzymes, Dcp1p and Dcp2p (Hoyle et al., 2007). The mRNA granules also colocalized with eIF4G and PABP, but not the P-body marker TTP. Given that ischemia is a form of severe neuronal glucose deprivation, the mRNA granules identified here may be the neuronal counterpart of the yeast EGP granules. It was suggested by Hoyle et al. (2007) that EGP granules may serve a function analogous to SGs, which is to route mRNAs to appropriate compartments within the cell (Anderson and Kedersha. 2006). However, the colocalization of

HuR in the mRNA granules (Figure 23) suggests a different, but related function.

Several laboratories have identified ELAV/Hu granules, which also are granular cytoplasmic mRNA formations that contain HuR or its homolog HuB (Keene, 1999). Evidence suggests that the ELAV/Hu granules partition functionally related mRNAs, allowing for their coordinated regulation in terms of translation, silencing or degradation (Keene and Lager, 2005). This type of functional mRNA coordination has been observed following cell stress, in which well-known immediate early genes (IEGs) such as *c-fos* and *c-myc* are translated. Many of the stress-induced mRNAs contain an ARE sequence (Atasoy et al., 1998; Brennan et al., 2000; Chen et al., 2002), including the mRNA for HSP70 (Laroia et al., 1999). HuR, a RNA binding protein, has been identified by its ability to bind to ARE sequences, thus shuttling select early response gene mRNAs from the nucleus out to the cytosol for translation (Cherry et al., 2006).

It is well established that many stress genes are induced following reperfusion (Nowak, 1993; Kogure and Kato, 1993; Akins et al., 1996; Koistinaho and Hökfelt, 1997). (Amadio et al., 2008), report HuR binding to HSP-70 following hydrogen peroxide induced cell stress. Thus, in addition to mRNA granules silencing "housekeeping" mRNAs, the correlation between HuR/mRNA granule colocalization and HSP70 translation suggests that the mRNA granules may also function to coordinate stress gene expression in the reperfused brain. Or, in other words, mRNA granules may represent a morphological correlate of the selective regulation of stress-induced mRNAs, while normal neuronal translation is silenced.

Differences Between CA1 and CA3

It is well established that, following the durations of ischemia used in the 2VO/HT model, CA1 pyramidal neurons show a profound and irreversible TA (Hossmann, 1993) and that there is either a delay in or no translation of HSP70 (Vass et al., 1988; Simon et al., 1991; Nowak, 1993). It has been proposed that these are linked insofar as the TA in CA1 will preclude

synthesis of HSP70 (White et al., 2000). However, it is well established that HSP70 is translated under conditions where general protein synthesis is inhibited (Panniers, 1994). In fact, exclusive synthesis of HSPs in reperfused hippocampus has been reported (Kiessling et al., 1986). Additionally, induced stress proteins such as HSP70 are crucial to recovery of general translation (DiDomenico et al., 1982; Van Nieuwenhoven et al., 2001; Ron, 2002; Gilks et al., 2004). Therefore, the direction of causality is not that TA prevents HSP70 translation in CA1, but the reverse: delayed synthesis of HSP70 prevents translation recovery, and hence causes prolonged TA. The differential behavior of the mRNA granules between CA1 and CA3 described here, provides a deeper level linking these two events.

The results just presented, have lead us to ask the following questions: (1) Why is there a delay in HuR entering the mRNA granules in CA1? (2) How does HuR in the mRNA granule facilitate HSP70 translation? (3) By what mechanism does HSP70 protein contribute to mRNA granule dissipation and general translation recovery?

HuR and mRNA Granules

HuR exports from the nucleus following cellular stress, to effect regulation of cytoplasmic ARE-containing mRNAs in compartmentalized structures (Cherry et al., 2006). The delayed accumulation of HuR in the mRNA granules of CA1 pyramidal neurons, could be due to a transportation defect in HuR. Alternatively, there could be successful nuclear export, but some biochemical alteration in the cytoplasm precludes HuR from entering the mRNA granules. Future work needs to address these issues.

In spite of the delay in HuR entering the mRNA granules, it is well established that there is copious transcription of *hsp70* mRNA in both CA1 and CA3 at the duration of ischemia using the present model (Figure 25). If, in CA3, the *hsp70* mRNA is translated because of some process marked by HuR entering the mRNA granules, then what happens to *hsp70* mRNA in

CA1 neurons? It thus becomes essential to compare the subcellular distribution and protein interactions of *hsp70* mRNA in CA1 and CA3 following I/R. The results presented in Chapter 3, leads to the prediction that *hsp70* mRNA will have differential binding partners and/or different subcellular localizations in CA1 as compared to CA3, occurring between 8hR - 36hR.

Finally, there is the issue of how precisely HuR can regulate the translation of an ARE-containing mRNA, such as *hsp70*. (Antic and Keene, 1998b) showed that interaction of Hu granules with microtubules, and polysomes with microfilaments, was important for translation of mRNAs in Hu granules. As cytoskeleton alterations occur in reperfused CA1 (Siesjö, 1994; Yokota et al., 1995), this provided another potential marker that could be used in IF/FISH to further elucidate and characterize mRNA granules. Thus in Chapter 3, I present results from histochemical methods used to further assess the colocalization properties of the mRNA granules formed in reperfused neurons. The results from this study determined: (1) the mRNA granules present in the reperfused CA1 and CA3 neurons did not colocalize with markers of major intracellular organelles, cytoskeleton or HuR binding proteins, and (2) mRNA granules did colocalize with NeuN out in the cytoplasm.

In spite of mRNA granules in CA3 neurons colocalizing with HuR at 1hR (Figure 23), there was no colocalization with the HuR accessory proteins APRIL and pp32, suggesting that the function of HuR in the mRNA granules may be distinct from its role in nuclear to cytoplasmic transport of mRNAs mediated in conjunction with APRIL and pp32 (Gallouzi et al., 2003).

Unexpectedly, the mRNA granules strongly colocalized with NeuN outside of the nucleus following brain I/R (Figure 27C). This result is consistent with a recent study that identified NeuN as an mRNA splicing factor, FOX-3 (Kim et al., 2002). The colocalization of NeuN and the mRNA granules suggests, NeuN may function similarly to other mRNA binding

proteins, such as HuR (Gorospe, 2003) or TIA-1 (Anderson and Kedersha, 2006); suggesting NeuN may reside in the nucleus under normal conditions, but export out into the cytoplasm under conditions of cell stress, in order to contribute to the genetic reprogramming to a stress response phenotype (DeGracia et al. 2008).

mRNA Granules; Involved in Damage Response or Stress Response

Since I showed that mRNA granules are very likely the mechanism of prolonged TA in reperfused neurons, I sought additional means to confirm the link between TA and mRNA granules. The purpose of the pharmacological studies was to manipulate known triggers and see if they had the expected effects on mRNA granules. ET-1 was used to lower cerebral perfusion to a blood flow rate known to inhibit protein synthesis. CHX was used because it is a well-known agent that prevents dissociation of polysomes.

ET-1 and mRNA Granules

Inhibition of protein synthesis has been shown to occur after blood flow reductions to about 0.55 ml/gm/min (Hossman 2006), which we observed at 400 pg ET-1 (Figure 29). I sought to confirm whether mRNA granule formation occurred at the threshold of protein synthesis inhibition. However, I did not observe mRNA granules at any ET-1 dose. The histological results suggest an explanation for this apparent discrepancy. I observed discreet areas of damaged cerebral cortex interspersed amongst regions showing little or no damage (e.g. Figure 32A), with the damaged area showing a trend of increasing as a function of ET-1 dose (Table 5). Such heterogeneous damage implies that blood flow reduction was equally heterogeneous. The apparent graded decrease in blood flow with ET-1 dose can be explained by an increasing recruitment of cortical areas with little or no blood flow, corresponding to the increased area of cortical damage (Table 5). The MRI measurements would then represent averages of these heterogeneous blood flow patterns over the volumes used for detection.

Mechanistically, this would imply that ET-1 affected discreet blood vessels differentially. Once a vessel became constricted by ET-1, blood flow would be reduced in that vessel, which may have limited the bulk flow of ET-1 throughout the vasculature.

Thus, ET-1 proved unsuitable to generate a homogeneous graded decrease in cerebral blood flow, preventing the use of ET-1 as a means to assess if the blood flow threshold for the formation of mRNA granules was the same as that, which induces the inhibition of protein synthesis.

Cycloheximide and mRNA granules

CHX is a glutarimide antibiotic and well-known protein synthesis inhibitor. Specifically, CHX prevents the release of the deacylated tRNA from the large 60S ribosome, halting elongation and preventing polysome disassembly (Pestka, 1971). Thus, it was predicted that pretreatment of CHX would prevent mRNA granulation, whereas CHX post-treatment would induce their formation. These predictions were confirmed. That CHX pretreatment, but not post-treatment, inhibited the formation of mRNA granules indicates that mRNA granule formation requires polysome dissociation.

A Model of Post Ischemic Stress Responses and TA

My results can be combined with other results in the literature to develop a novel, new model of how stress responses are activated in reperfused neurons. This new model in turn suggests new hypotheses to test for the cause of DND.

During ischemia, there is no protein synthesis because ATP levels go to zero. However, ATP returns rapidly with reperfusion. Increased ATP is a substrate for kinases, and allow the alpha subunit of eIF2 to become phosphorylated, as was studied extensively by Dr. DeGracia (DeGracia et al 1996; 1997). Phosphorylation of eIF2□ causes polysome dissociation, explaining the original 1971 observation of Kleihaus and Hossmann. I showed above that SGs

increase at 10 min reperfusion, and it would follow that the increase in SGs is concurrent with polysome dissociation because free mRNA levels will increase greatly. Work from Kedersha and Anderson have shown that SGs form any condition leading to polysome dissociation (Anderson and Kedersha, 2002b). However, the SG increase was very transitory, and was only observed at 10 min. Therefore, it must precede the formation of the mRNA granules, which I observed only as early as 1 hr reperfusion. The early formation of mRNA granules possibly serve to sequester existing mRNAs. In line with the Keene idea of an mRNA operon (Mansfield and Keene, 2009), this might reflect the first step in genetic reprogramming; the shutting off of existing translation in preparation for some new set of mRNAs that will eventually be translated.

This idea is supported by the correlation between HuR and mRNA granule colocalization. This observation suggests the mRNA granules play a role in the reprogramming of the neuron to a stress response phenotype. It was observed that this did not occur until ~ 36-48 hr in CA1, suggesting that translation of HSP70 protein, by this time, is too late to help salvage the CA1 neuron, and it then dies, perhaps by the protein aggregate mechanism advocated by Dr. Hu (Hu et al., 2000).

Therefore, this new model suggests that there is some defect in the ribonomic regulation in CA1 neurons that prevents it from translating HSP70 protein, in spite of the extremely large amount of mRNA in the CA1 neurons. This provides a new pathway that requires investigation.

Limitations of the Present Studies

The following are limitations relevant to the studies presented here:

1. The main technique used in my studies was microscopy. Therefore, I could only correlate my observations with molecular changes such as TA and synthesis of HSP70.
2. Biochemical and molecular biology of the mRNA granules was not performed.
3. The CHX was only conducted to 1hr reperfusion and therefore, the effect on outcome of

inhibiting mRNA granules, or whether or not they form later than 1 hr was not studied.

4. Intraventricular administration of ET-1 proved unsuitable for controlling cerebral blood flow.

Future Directions

My dissertation work provides many new directions for future investigation. Some of the most prominent are:

1. What is the molecular biology of the mRNA granules? How do they form? What do they do after they form? What is their composition? Does their composition change with time? Questions of the molecular composition involve both protein and mRNA composition. The technique RNA immunoprecipitation (IP) first IPs a specific mRNA binding protein under conditions that preserve the mRNA-protein interaction, and then the mRNAs can be isolated, amplified and analyzed in mass by microarrays. I observed PABP, eIF4G, HuR and NeuN to colocalize with the mRNA granules. Any of these could be used as the IP protein. HuR would be the most informative because of its differential colocalization between CA1 and CA3. RNA IP can also be used to isolate the proteins in the complex, which could be analyzed by proteomics. Thus, there are many possible molecular studies waiting to be performed.

2. What is the status of mRNA granules in other forms of ischemia? Monique Lewis has shown they are also prominent following focal cerebral ischemia. What is the status of mRNA granules in preconditioning, where preconditioning is first subjecting a rat to a sublethal, 2 min global ischemia. After two days, if a 10 min ischemia is given to the same rat, the CA1 neurons do not die. Therefore, it would be of great interest to study mRNA granules in preconditioning. Specifically, does HuR colocalize early (~1 hr) in CA1 after preconditioning as it does in CA3 at 10 min of ischemia and 1 hr reperfusion?

3. Other methods of reducing brain blood flow can be tried to see if the mRNA granules

form at the same threshold as TA, as shown by Hossmann. One such method is to use a more graded hypotension, as used in the 2VO/HT model, to see if blood flow can be titrated and graded to produce the required 50% threshold.

4. Once the details of the mRNA granule system are identified, a long-term goal is to use them as targets for neuroprotection therapy. It is possible that a drug intervention early in the time course of reperfusion could cause HuR to enter the mRNA granules in CA1 neurons and allow them to translate HSP70 protein. How this might be carried out is unknown lacking knowledge of the detailed molecular biology, but it is one of the most exciting long-term prospects of my work in this dissertation.

Conclusion

In this dissertation, I have discovered a new mechanism for prolonged post-ischemic TA that correlated exactly with *in vivo* translation rates and correlated precisely with cell outcome. Through the extensive colocalization studies, my results indicate that the mRNA granules are ribonomic structures involved with mRNA regulation. This is important because it now shifts the focus on mRNA metabolism and away from exclusive focus on ribosome molecular biology that has been the main line of work in this area. I have identified new pathways to investigate for understanding why there is selective delayed death in post-ischemic neurons, however my work also gives insight into why resistant neurons survive. Further study of these pathways in resistant neurons may offer new therapeutic targets that promote survival following brain ischemia.

I conclude giving a special thanks and my appreciation to all the individuals in the field who have laid the foundation for my work reported here. It is my hope that the insights and knowledge gained here will provide future investigators with the tools and ideas to keep advancing our understanding of neuronal death after brain ischemia and reperfusion. Through

this ongoing process, we may one day find effective ways to stop cellular death in the brain following stroke and cardiac arrest. My work here suggests we have reason to be optimistic.

REFERENCES

1. Abramoff MD, Magalhaes PJ, Ram SJ (2004) Image Processing with ImageJ. Biophotonics International 11:36-42
2. Akins PT, Liu PK, Hsu CY (1996) Immediate early gene expression in response to cerebral ischemia. Friend or foe? Stroke 27:1682-1687 Available at: [Accessed December 2, 2011].
3. Amadio M, Scapagnini G, Laforenza U, Intrieri M, Romeo L, Govoni S, Pascale A (2008) Post-transcriptional regulation of HSP70 expression following oxidative stress in SH-SY5Y cells: the potential involvement of the RNA-binding protein HuR. Curr. Pharm. Des. 14:2651-2658 Available at: [Accessed December 1, 2011].
4. American Heart Association (2009) Heart Disease and Stroke Statistics. Dallas, Texas: AMA.
5. Anderson P, Kedersha N (2002)(a) Stressful initiations. J. Cell. Sci 115:3227-3234 Available at: [Accessed November 24, 2009].
6. Anderson P, Kedersha N (2002)(b) Visibly stressed: the role of eIF2, TIA-1, and stress granules in protein translation. Cell Stress Chaperones 7:213-221 Available at: [Accessed December 2, 2011].
7. Anderson P, Kedersha N (2006) RNA granules. J. Cell Biol 172:803-808 Available at: [Accessed November 24, 2009].
8. Antic D, Keene JD (1998)(a) Messenger ribonucleoprotein complexes containing human ELAV proteins: interactions with cytoskeleton and translational apparatus. J. Cell. Sci. 111 (Pt 2):183-197 Available at: [Accessed November 15, 2011].
9. Antic D, Keene JD (1998)(b) Messenger ribonucleoprotein complexes containing human ELAV proteins: interactions with cytoskeleton and translational apparatus. J. Cell. Sci.

111 (Pt 2):183-197 Available at: [Accessed December 2, 2011].

10. Arai H, Hori S, Aramori I, Ohkubo H, Nakanishi S (1990) Cloning and expression of a cDNA encoding an endothelin receptor. Nature 348:730-732 Available at: [Accessed December 1, 2009].

11. Atasoy U, Watson J, Patel D, Keene JD (1998) ELAV protein HuA (HuR) can redistribute between nucleus and cytoplasm and is upregulated during serum stimulation and T cell activation. J. Cell. Sci. 111 (Pt 21):3145-3156 Available at: [Accessed December 2, 2011].

12. Beckman JS, Beckman TW, Chen J, Marshall PA, Freeman BA (1990) Apparent hydroxyl radical production by peroxynitrite: implications for endothelial injury from nitric oxide and superoxide. Proc. Natl. Acad. Sci. U.S.A 87:1620-1624 Available at: [Accessed November 8, 2009].

13. Benveniste H, Jørgensen MB, Diemer NH, Hansen AJ (1988) Calcium accumulation by glutamate receptor activation is involved in hippocampal cell damage after ischemia. Acta Neurol. Scand 78:529-536 Available at: [Accessed November 8, 2009].

14. Bessert DA, Skoff RP (1999) High-resolution in situ hybridization and TUNEL staining with free-floating brain sections. J. Histochem. Cytochem. 47:693-702 Available at: [Accessed October 11, 2011].

15. Bonneau AM, Sonenberg N (1987) Involvement of the 24-kDa cap-binding protein in regulation of protein synthesis in mitosis. J. Biol. Chem 262:11134-11139 Available at: [Accessed November 13, 2009].

16. Boron W (2005) Medical physiology : a cellular and molecular approach Updated ed. Philadelphia Penns.: Elsevier Saunders.

17. Brengues M, Teixeira D, Parker R (2005) Movement of eukaryotic mRNAs between

polysomes and cytoplasmic processing bodies. Science 310:486-489 Available at: [Accessed November 12, 2011].

18. Brennan CM, Gallouzi IE, Steitz JA (2000) Protein ligands to HuR modulate its interaction with target mRNAs in vivo. J. Cell Biol. 151:1-14 Available at: [Accessed December 2, 2011].

19. Bu X, Haas DW, Hagedorn CH (1993) Novel phosphorylation sites of eukaryotic initiation factor-4F and evidence that phosphorylation stabilizes interactions of the p25 and p220 subunits. J. Biol. Chem 268:4975-4978 Available at: [Accessed November 13, 2009].

20. Burda J, Martín ME, García A, Alcázar A, Fando JL, Salinas M (1994) Phosphorylation of the alpha subunit of initiation factor 2 correlates with the inhibition of translation following transient cerebral ischaemia in the rat. Biochem. J 302 (Pt 2):335-338 Available at: [Accessed November 11, 2009].

21. Burry RW, Smith CL (2006) HuD distribution changes in response to heat shock but not neurotrophic stimulation. J. Histochem. Cytochem. 54:1129-1138 Available at: [Accessed November 15, 2011].

22. Cardell M, Siesjö BK, Wieloch T (1991) Changes in pyruvate dehydrogenase complex activity during and following severe insulin-induced hypoglycemia. J. Cereb. Blood Flow Metab 11:122-128 Available at: [Accessed November 9, 2009].

23. Carpenter B, MacKay C, Alnabulsi A, MacKay M, Telfer C, Melvin WT, Murray GI (2006) The roles of heterogeneous nuclear ribonucleoproteins in tumour development and progression. Biochim. Biophys. Acta 1765:85-100 Available at: [Accessed November 15, 2011].

24. Chen C-YA, Xu N, Shyu A-B (2002) Highly selective actions of HuR in antagonizing

AU-rich element-mediated mRNA destabilization. Mol. Cell. Biol. 22:7268-7278 Available at: [Accessed December 2, 2011].

25. Cherry J, Karschner V, Jones H, Pekala PH (2006) HuR, an RNA-binding protein, involved in the control of cellular differentiation. In Vivo 20:17-23 Available at: [Accessed November 29, 2011].

26. Cummings BS, McHowat J, Schnellmann RG (2000) Phospholipase A(2)s in cell injury and death. J. Pharmacol. Exp. Ther 294:793-799 Available at: [Accessed November 30, 2009].

27. Davis DP, Patel PM (2003) Ischemic preconditioning in the brain. Curr Opin Anaesthesiol 16:447-452 Available at: [Accessed November 17, 2009].

28. DeGracia DJ (2004) Acute and persistent protein synthesis inhibition following cerebral reperfusion. J. Neurosci. Res 77:771-776 Available at: [Accessed October 4, 2009].

29. DeGracia DJ, Hu BR (2007) Irreversible translation arrest in the reperfused brain. J. Cereb. Blood Flow Metab 27:875-893 Available at: [Accessed June 25, 2009].

30. DeGracia DJ, Jamison JT, Szymanski JJ, Lewis MK (2008)(a) Translation arrest and ribonomics in post-ischemic brain: layers and layers of players. J. Neurochem 106:2288-2301 Available at: [Accessed November 15, 2010].

31. DeGracia DJ, Jamison JT, Szymanski JJ, Lewis MK (2008)(b) Translation arrest and ribonomics in post-ischemic brain: layers and layers of players. J. Neurochem. 106:2288-2301 Available at: [Accessed December 2, 2011].

32. DeGracia DJ, Jamison JT, Szymanski JR, Marshall MK (2008)(c) Translation Arrest and Ribonomics In Post-ischemic Brain: Layers and Layers of Players. J Neurochem 106:2288-2301

33. DeGracia DJ, Kreipke CW, Kayali FM, Rafols JA (2007)(a) Brain endothelial HSP-70

stress response coincides with endothelial and pericyte death after brain trauma. Neurol. Res 29:356-361 Available at: [Accessed December 12, 2009].

34. DeGracia DJ, Kumar R, Owen CR, Krause GS, White BC (2002) Molecular pathways of protein synthesis inhibition during brain reperfusion: implications for neuronal survival or death. J. Cereb. Blood Flow Metab 22:127-141 Available at: [Accessed October 4, 2009].

35. DeGracia DJ, Neumar RW, White BC, Krause GS (1996) Global brain ischemia and reperfusion: modifications in eukaryotic initiation factors associated with inhibition of translation initiation. J. Neurochem 67:2005-2012 Available at: [Accessed November 13, 2009].

36. DeGracia DJ, O'Neil BJ, Frisch C, Krause GS, Skjaerlund JM, White BC, Grossman LI (1993) Studies of the protein synthesis system in the brain cortex during global ischemia and reperfusion. Resuscitation 25:161-170 Available at: [Accessed December 2, 2011].

37. DeGracia DJ, Rafols JA, Morley SJ, Kayali F (2006) Immunohistochemical mapping of total and phosphorylated eukaryotic initiation factor 4G in rat hippocampus following global brain ischemia and reperfusion. Neuroscience 139:1235-1248 Available at: [Accessed December 2, 2011].

38. DeGracia DJ, Rudolph J, Roberts GG, Rafols JA, Wang J (2007)(b) Convergence of stress granules and protein aggregates in hippocampal cornu ammonis 1 at later reperfusion following global brain ischemia. Neuroscience 146:562-572 Available at: [Accessed November 24, 2009].

39. DeGracia DJ, Sullivan JM, Neumar RW, Alousi SS, Hikade KR, Pittman JE, White BC, Rafols JA, Krause GS (1997) Effect of brain ischemia and reperfusion on the localization of phosphorylated eukaryotic initiation factor 2 alpha. J. Cereb. Blood Flow Metab

17:1291-1302 Available at: [Accessed November 17, 2009].

40. Dember LM, Kim ND, Liu KQ, Anderson P (1996) Individual RNA recognition motifs of TIA-1 and TIAR have different RNA binding specificities. J. Biol. Chem 271:2783-2788 Available at: [Accessed November 24, 2009].

41. Demopoulos HB, Flamm ES, Pietronigro DD, Seligman ML (1980) The free radical pathology and the microcirculation in the major central nervous system disorders. Acta Physiol Scand Suppl 492:91-119 Available at: [Accessed November 10, 2009].

42. Dennis EA (1994) Diversity of group types, regulation, and function of phospholipase A2. Journal of Biological Chemistry 269:13057-13060 Available at: [Accessed November 30, 2009].

43. Deshpande J, Bergstedt K, Lindén T, Kalimo H, Wieloch T (1992) Ultrastructural changes in the hippocampal CA1 region following transient cerebral ischemia: evidence against programmed cell death. Exp Brain Res 88:91-105 Available at: [Accessed November 30, 2009].

44. DiDomenico BJ, Bugaisky GE, Lindquist S (1982) Heat shock and recovery are mediated by different translational mechanisms. Proc. Natl. Acad. Sci. U.S.A. 79:6181-6185 Available at: [Accessed December 2, 2011].

45. Duncan RF, Hershey JW (1989) Protein synthesis and protein phosphorylation during heat stress, recovery, and adaptation. J. Cell Biol 109:1467-1481 Available at: [Accessed November 13, 2009].

46. Eckstein M, Stratton SJ, Chan LS (2005) Cardiac Arrest Resuscitation Evaluation in Los Angeles: CARE-LA. Ann Emerg Med 45:504-509 Available at: [Accessed November 4, 2009].

47. Fan H, Penman S (1970) Regulation of protein synthesis in mammalian cells. II.

Inhibition of protein synthesis at the level of initiation during mitosis. J. Mol. Biol 50:655-670 Available at: [Accessed November 13, 2009].

48. Farber JL (1982) Biology of disease: membrane injury and calcium homeostasis in the pathogenesis of coagulative necrosis. Lab. Invest 47:114-123 Available at: [Accessed November 30, 2009].

49. Feigenblum D, Schneider RJ (1996) Cap-binding protein (eukaryotic initiation factor 4E) and 4E-inactivating protein BP-1 independently regulate cap-dependent translation. Mol. Cell. Biol 16:5450-5457 Available at: [Accessed November 13, 2009].

50. Forcina MS, Farhat AY, O'Neill WW, Haines DE (2009) Cardiac arrest survival after implementation of automated external defibrillator technology in the in-hospital setting. Crit. Care Med 37:1-8

51. Freeman BA, Crapo JD (1982) Biology of disease: free radicals and tissue injury. Lab. Invest 47:412-426 Available at: [Accessed November 30, 2009].

52. Fukuda T, Adachi E, Kawashima S, Yoshiya I, Hashimoto PH (1990) Immunohistochemical distribution of calcium-activated neutral proteinases and endogenous CANP inhibitor in the rabbit hippocampus. J. Comp. Neurol 302:100-109 Available at: [Accessed November 8, 2009].

53. Gallouzi I-E, Brennan CM, Steitz JA (2003) Protein ligands mediate the CRM1-dependent export of HuR in response to heat shock. RNA 9:1410 Available at: [Accessed December 2, 2011].

54. Gao FB, Keene JD (1996) Hel-N1/Hel-N2 proteins are bound to poly(A)+ mRNA in granular RNP structures and are implicated in neuronal differentiation. J. Cell. Sci. 109 (Pt 3):579-589 Available at: [Accessed December 2, 2011].

55. García L, Burda J, Hrehorovská M, Burda R, Martín ME, Salinas M (2004) Ischaemic

preconditioning in the rat brain: effect on the activity of several initiation factors, Akt and extracellular signal-regulated protein kinase phosphorylation, and GRP78 and GADD34 expression. J. Neurochem 88:136-147 Available at: [Accessed November 17, 2009].

56. Gilks N, Kedersha N, Ayodele M, Shen L, Stoecklin G, Dember LM, Anderson P (2004) Stress granule assembly is mediated by prion-like aggregation of TIA-1. Mol. Biol. Cell 15:5383-5398 Available at: [Accessed December 2, 2011].

57. Gillardon F, Kiprianova I, Sandkühler J, Hossmann KA, Spranger M (1999) Inhibition of caspases prevents cell death of hippocampal CA1 neurons, but not impairment of hippocampal long-term potentiation following global ischemia. Neuroscience 93:1219-1222 Available at: [Accessed November 30, 2009].

58. Gingras AC, Raught B, Sonenberg N (1999) eIF4 initiation factors: effectors of mRNA recruitment to ribosomes and regulators of translation. Annu. Rev. Biochem 68:913-963 Available at: [Accessed November 12, 2009].

59. Goll DE, Thompson VF, Li H, Wei W, Cong J (2003) The calpain system. Physiol. Rev 83:731-801 Available at: [Accessed November 8, 2009].

60. Gorospe M (2003) HuR in the mammalian genotoxic response: post-transcriptional multitasking. Cell Cycle 2:412-414 Available at: [Accessed November 29, 2011].

61. Grollman AP (1966) STRUCTURAL BASIS FOR INHIBITION OF PROTEIN SYNTHESIS BY EMETINE AND CYCLOHEXIMIDE BASED ON AN ANALOGY BETWEEN IPECAC ALKALOIDS AND GLUTARIMIDE ANTIBIOTICS*. Proc Natl Acad Sci U S A 56:1867-1874

62. Grøndahl T, Langmoen IA (1998) Confocal laser scanning microscopy used to monitor intracellular Ca2+ changes in hippocampal CA 1 neurons during energy deprivation. Brain Res 785:58-65 Available at: [Accessed November 8, 2009].

63. Gu W, Brännström T, Rosqvist R, Wester P (2009) Cell division in the cerebral cortex of adult rats after photothrombotic ring stroke. Stem Cell Res 2:68-77 Available at: [Accessed December 2, 2011].

64. Gueydan C, Droogmans L, Chalon P, Huez G, Caput D, Kruys V (1999) Identification of TIAR as a protein binding to the translational regulatory AU-rich element of tumor necrosis factor alpha mRNA. J. Biol. Chem 274:2322-2326 Available at: [Accessed November 24, 2009].

65. Haghighat A, Mader S, Pause A, Sonenberg N (1995) Repression of cap-dependent translation by 4E-binding protein 1: competition with p220 for binding to eukaryotic initiation factor-4E. EMBO J 14:5701-5709 Available at: [Accessed November 13, 2009].

66. Harding HP, Novoa I, Bertolotti A, Zeng H, Zhang Y, Urano F, Jousse C, Ron D (2001) Translational regulation in the cellular response to biosynthetic load on the endoplasmic reticulum. Cold Spring Harb. Symp. Quant. Biol 66:499-508 Available at: [Accessed November 24, 2009].

67. Hellen CUT, Sarnow P (2001) Internal ribosome entry sites in eukaryotic mRNA molecules. Genes & Development 15:1593 -1612 Available at: [Accessed September 27, 2011].

68. Hertz L (2008) Bioenergetics of cerebral ischemia: a cellular perspective. Neuropharmacology 55:289-309 Available at: [Accessed November 6, 2009].

69. Hoehner TJ, Garritano AM, Dilorenzo RA, O'Neil BJ, Kumar K, Koehler J, Nayini NR, Huang RR, Krause GS, Aust SD (1987) Brain cortex tissue Ca, Mg, Fe, Na, and K following resuscitation from cardiac arrest in dogs. Am J Emerg Med 5:19-23 Available at: [Accessed November 10, 2009].

70. Hossmann K-A (2006) Pathophysiology and therapy of experimental stroke. Cell. Mol. Neurobiol 26:1057-1083 Available at: [Accessed December 1, 2009].

71. Hossmann KA (1993) Disturbances of cerebral protein synthesis and ischemic cell death. Prog. Brain Res 96:161-177 Available at: [Accessed October 4, 2009].

72. Hossmann KA, Kleihues P (1973) Reversibility of ischemic brain damage. Arch. Neurol 29:375-384 Available at: [Accessed September 6, 2011].

73. Hoyle NP, Castelli LM, Campbell SG, Holmes LEA, Ashe MP (2007) Stress-dependent relocalization of translationally primed mRNPs to cytoplasmic granules that are kinetically and spatially distinct from P-bodies. J. Cell Biol. 179:65-74 Available at: [Accessed December 2, 2011].

74. Hu BR, Janelidze S, Ginsberg MD, Busto R, Perez-Pinzon M, Sick TJ, Siesjö BK, Liu CL (2001) Protein aggregation after focal brain ischemia and reperfusion. J. Cereb. Blood Flow Metab 21:865-875 Available at: [Accessed November 24, 2009].

75. Hu BR, Martone ME, Jones YZ, Liu CL (2000) Protein aggregation after transient cerebral ischemia. J. Neurosci 20:3191-3199 Available at: [Accessed August 21, 2009].

76. Hu BR, Wieloch T (1993) Stress-induced inhibition of protein synthesis initiation: modulation of initiation factor 2 and guanine nucleotide exchange factor activities following transient cerebral ischemia in the rat. J. Neurosci 13:1830-1838 Available at: [Accessed November 17, 2009].

77. Jamison JT, Lewis MK, Kreipke CW, Rafols JA, DeGracia DJ (2011) Polyadenylated mRNA staining reveals distinct neuronal phenotypes following endothelin 1, focal brain ischemia, and global brain ischemia/ reperfusion. Neurol. Res. 33:145-161 Available at: [Accessed December 3, 2011].

78. Jenkins LW, Povlishock JT, Lewelt W, Miller JD, Becker DP (1981) The role of

postischemic recirculation in the development of ischemic neuronal injury following complete cerebral ischemia. Acta Neuropathol 55:205-220 Available at: [Accessed September 6, 2011].

79. Jones RM, Branda J, Johnston KA, Polymenis M, Gadd M, Rustgi A, Callanan L, Schmidt EV (1996) An essential E box in the promoter of the gene encoding the mRNA cap-binding protein (eukaryotic initiation factor 4E) is a target for activation by c-myc. Mol. Cell. Biol 16:4754-4764 Available at: [Accessed November 13, 2009].

80. Kass IS, Lipton P (1986) Calcium and long-term transmission damage following anoxia in dentate gyrus and CA1 regions of the rat hippocampal slice. J. Physiol. (Lond.) 378:313-334 Available at: [Accessed November 8, 2009].

81. Kayali F, Montie HL, Rafols JA, DeGracia DJ (2005) Prolonged translation arrest in reperfused hippocampal cornu Ammonis 1 is mediated by stress granules. Neuroscience 134:1223-1245 Available at: [Accessed November 23, 2009].

82. Kedersha N, Anderson P (2002) Stress granules: sites of mRNA triage that regulate mRNA stability and translatability. Biochem. Soc. Trans 30:963-969 Available at: [Accessed November 24, 2009].

83. Kedersha N, Chen S, Gilks N, Li W, Miller IJ, Stahl J, Anderson P (2002) Evidence that ternary complex (eIF2-GTP-tRNA(i)(Met))-deficient preinitiation complexes are core constituents of mammalian stress granules. Mol. Biol. Cell 13:195-210 Available at: [Accessed November 24, 2009].

84. Kedersha N, Cho MR, Li W, Yacono PW, Chen S, Gilks N, Golan DE, Anderson P (2000) Dynamic shuttling of TIA-1 accompanies the recruitment of mRNA to mammalian stress granules. J. Cell Biol 151:1257-1268 Available at: [Accessed November 24, 2009].

85. Kedersha N, Stoecklin G, Ayodele M, Yacono P, Lykke-Andersen J, Fritzler MJ, Scheuner D, Kaufman RJ, Golan DE, Anderson P (2005) Stress granules and processing bodies are dynamically linked sites of mRNP remodeling. J. Cell Biol 169:871-884 Available at: [Accessed November 24, 2009].

86. Kedersha NL, Gupta M, Li W, Miller I, Anderson P (1999) RNA-binding proteins TIA-1 and TIAR link the phosphorylation of eIF-2 alpha to the assembly of mammalian stress granules. J. Cell Biol 147:1431-1442 Available at: [Accessed November 23, 2009].

87. Keene JD (1999) Why is Hu where? Shuttling of early-response-gene messenger RNA subsets. Proc. Natl. Acad. Sci. U.S.A. 96:5-7 Available at: [Accessed December 2, 2011].

88. Keene JD (2001) Ribonucleoprotein infrastructure regulating the flow of genetic information between the genome and the proteome. Proc. Natl. Acad. Sci. U.S.A. 98:7018-7024 Available at: [Accessed November 15, 2011].

89. Keene JD (2007) RNA regulons: coordination of post-transcriptional events. Nat. Rev. Genet. 8:533-543 Available at: [Accessed November 15, 2011].

90. Keene JD, Lager PJ (2005) Post-transcriptional operons and regulons co-ordinating gene expression. Chromosome Res. 13:327-337 Available at: [Accessed December 2, 2011].

91. Kiessling M, Dienel GA, Jacewicz M, Pulsinelli WA (1986) Protein synthesis in postischemic rat brain: a two-dimensional electrophoretic analysis. J. Cereb. Blood Flow Metab. 6:642-649 Available at: [Accessed December 2, 2011].

92. Kim O-J, Ariano MA, Lazzarini RA, Levine MS, Sibley DR (2002) Neurofilament-M interacts with the D1 dopamine receptor to regulate cell surface expression and desensitization. J. Neurosci. 22:5920-5930 Available at: [Accessed December 2, 2011].

93. Kimball SR, Horetsky RL, Ron D, Jefferson LS, Harding HP (2003) Mammalian stress granules represent sites of accumulation of stalled translation initiation complexes. Am. J.

Physiol., Cell Physiol. 284:C273-284 Available at: [Accessed December 2, 2011].

94. Kirino T (1982) Delayed neuronal death in the gerbil hippocampus following ischemia. Brain Res 239:57-69 Available at: [Accessed October 27, 2009].

95. Kirino T, Tamura A, Sano K (1984) Delayed neuronal death in the rat hippocampus following transient forebrain ischemia. Acta Neuropathol 64:139-147 Available at: [Accessed November 24, 2009].

96. Kleihues P, Hossmann KA (1971) Protein synthesis in the cat brain after prolonged cerebral ischemia. Brain Res 35:409-418 Available at: [Accessed June 23, 2009].

97. Kogure K, Kato H (1993) Altered gene expression in cerebral ischemia. Stroke 24:2121-2127 Available at: [Accessed December 2, 2011].

98. Koistinaho J, Hökfelt T (1997) Altered gene expression in brain ischemia. Neuroreport 8:i-viii Available at: [Accessed December 2, 2011].

99. Krause GS, White BC, Aust SD, Nayini NR, Kumar K (1988) Brain cell death following ischemia and reperfusion: a proposed biochemical sequence. Crit. Care Med 16:714-726 Available at: [Accessed November 6, 2009].

100. Kumar R, Krause GS, Yoshida H, Mori K, DeGracia DJ (2003) Dysfunction of the unfolded protein response during global brain ischemia and reperfusion. J. Cereb. Blood Flow Metab. 23:462-471 Available at: [Accessed December 2, 2011].

101. Laroia G, Cuesta R, Brewer G, Schneider RJ (1999) Control of mRNA decay by heat shock-ubiquitin-proteasome pathway. Science 284:499-502 Available at: [Accessed December 2, 2011].

102. Lipton P (1999) Ischemic cell death in brain neurons. Physiol. Rev 79:1431-1568 Available at: [Accessed November 8, 2009].

103. Liu CL, Ge P, Zhang F, Hu BR (2005) Co-translational protein aggregation after transient

cerebral ischemia. Neuroscience 134:1273-1284 Available at: [Accessed August 21, 2009].

104. Lloyd-Jones D et al. (2009) Heart disease and stroke statistics--2009 update: a report from the American Heart Association Statistics Committee and Stroke Statistics Subcommittee. Circulation 119:480-486 Available at: [Accessed November 4, 2009].

105. Lyden P, Wahlgren NG (2000) Mechanisms of action of neuroprotectants in stroke. J Stroke Cerebrovasc Dis 9:9-14 Available at: [Accessed November 30, 2009].

106. MacManus JP, Buchan AM (2000) Apoptosis after experimental stroke: fact or fashion? J. Neurotrauma 17:899-914 Available at: [Accessed November 30, 2009].

107. MacManus JP, Graber T, Luebbert C, Preston E, Rasquinha I, Smith B, Webster J (2004) Translation-state analysis of gene expression in mouse brain after focal ischemia. J. Cereb. Blood Flow Metab 24:657-667 Available at: [Accessed December 1, 2009].

108. Mangus DA, Evans MC, Jacobson A (2003) Poly(A)-binding proteins: multifunctional scaffolds for the post-transcriptional control of gene expression. Genome Biol. 4:223 Available at: [Accessed December 2, 2011].

109. Mansfield KD, Keene JD (2009) The ribonome: a dominant force in co-ordinating gene expression. Biol. Cell 101:169-181 Available at: [Accessed November 15, 2011].

110. Martone ME, Pollock JA, Jones YZ, Ellisman MH (1996)(a) Ultrastructural localization of dendritic messenger RNA in adult rat hippocampus. J. Neurosci. 16:7437-7446 Available at: [Accessed October 11, 2011].

111. Martone ME, Pollock JA, Jones YZ, Ellisman MH (1996)(b) Ultrastructural localization of dendritic messenger RNA in adult rat hippocampus. J. Neurosci. 16:7437-7446 Available at: [Accessed December 2, 2011].

112. Martín de la Vega C, Burda J, Nemethova M, Quevedo C, Alcázar A, Martín ME,

Danielisova V, Fando JL, Salinas M (2001) Possible mechanisms involved in the down-regulation of translation during transient global ischaemia in the rat brain. Biochem. J 357:819-826 Available at: [Accessed October 4, 2009].

113. Matsumoto K, Yamada K, Hayakawa T, Sakaguchi T, Mogami H (1990) RNA synthesis and processing in the gerbil brain after transient hindbrain ischaemia. Neurol. Res. 12:45-48 Available at: [Accessed December 1, 2011].

114. Matsumoto S, Shamloo M, Matsumoto E, Isshiki A, Wieloch T (2004) Protein kinase C-gamma and calcium/calmodulin-dependent protein kinase II-alpha are persistently translocated to cell membranes of the rat brain during and after middle cerebral artery occlusion. J. Cereb. Blood Flow Metab 24:54-61 Available at: [Accessed November 8, 2009].

115. McCabe MJ, Nicotera P, Orrenius S (1992) Calcium-dependent cell death. Role of the endonuclease, protein kinase C, and chromatin conformation. Ann. N. Y. Acad. Sci 663:269-278 Available at: [Accessed November 8, 2009].

116. McCord JM (1993) Oxygen-derived free radicals. New Horiz 1:70-76 Available at: [Accessed November 30, 2009].

117. Merrick WC (1990) Overview: mechanism of translation initiation in eukaryotes. Enzyme 44:7-16 Available at: [Accessed November 11, 2009].

118. Mies G, Paschen W, Hossmann KA (1990) Cerebral blood flow, glucose utilization, regional glucose, and ATP content during the maturation period of delayed ischemic injury in gerbil brain. J. Cereb. Blood Flow Metab 10:638-645 Available at: [Accessed November 9, 2009].

119. Montie HL, Haezebrouck AJ, Gutwald JC, DeGracia DJ (2005) PERK is activated differentially in peripheral organs following cardiac arrest and resuscitation.

Resuscitation 66:379-389 Available at: [Accessed December 1, 2009].

120. Morley SJ, McKendrick L (1997) Involvement of stress-activated protein kinase and p38/RK mitogen-activated protein kinase signaling pathways in the enhanced phosphorylation of initiation factor 4E in NIH 3T3 cells. J. Biol. Chem 272:17887-17893 Available at: [Accessed November 13, 2009].

121. Morley SJ, Pain VM (1995) Translational regulation during activation of porcine peripheral blood lymphocytes: association and phosphorylation of the alpha and gamma subunits of the initiation factor complex eIF-4F. Biochem. J 312 (Pt 2):627-635 Available at: [Accessed November 13, 2009].

122. Morley SJ, Traugh JA (1990) Differential stimulation of phosphorylation of initiation factors eIF-4F, eIF-4B, eIF-3, and ribosomal protein S6 by insulin and phorbol esters. J. Biol. Chem 265:10611-10616 Available at: [Accessed November 13, 2009].

123. Morley SJ, Traugh JA (1993) Stimulation of translation in 3T3-L1 cells in response to insulin and phorbol ester is directly correlated with increased phosphate labelling of initiation factor (eIF-) 4F and ribosomal protein S6. Biochimie 75:985-989 Available at: [Accessed November 13, 2009].

124. Muir KW, Buchan A, von Kummer R, Rother J, Baron J-C (2006) Imaging of acute stroke. Lancet Neurol 5:755-768 Available at: [Accessed October 4, 2009].

125. Murakami M, Nakatani Y, Atsumi G, Inoue K, Kudo I (1997) Regulatory functions of phospholipase A2. Crit. Rev. Immunol 17:225-283 Available at: [Accessed November 30, 2009].

126. Neumar RW, DeGracia DJ, Konkoly LL, Khoury JI, White BC, Krause GS (1998) Calpain Mediates Eukaryotic Initiation Factor 4G Degradation During Global Brain Ischemia. J Cereb Blood Flow Metab 18:876-881 Available at: [Accessed November 8,

2009].

127. Neumar RW, Meng FH, Mills AM, Xu YA, Zhang C, Welsh FA, Siman R (2001) Calpain activity in the rat brain after transient forebrain ischemia. Exp. Neurol 170:27-35 Available at: [Accessed November 8, 2009].

128. Van Nieuwenhoven FA, Martin X, Heijnen VV, Cornelussen RN, Snoeckx LH (2001) HSP70-mediated acceleration of translational recovery after stress is independent of ribosomal RNA synthesis. Eur. J. Cell Biol. 80:586-592 Available at: [Accessed December 2, 2011].

129. Nitatori T, Sato N, Waguri S, Karasawa Y, Araki H, Shibanai K, Kominami E, Uchiyama Y (1995) Delayed neuronal death in the CA1 pyramidal cell layer of the gerbil hippocampus following transient ischemia is apoptosis. J. Neurosci 15:1001-1011 Available at: [Accessed November 30, 2009].

130. Nover L, Scharf KD, Neumann D (1983) Formation of cytoplasmic heat shock granules in tomato cell cultures and leaves. Mol. Cell. Biol 3:1648-1655 Available at: [Accessed November 24, 2009].

131. Nowak TS Jr (1993) Synthesis of heat shock/stress proteins during cellular injury. Ann. N. Y. Acad. Sci. 679:142-156 Available at: [Accessed December 2, 2011].

132. Oldfield S, Jones BL, Tanton D, Proud CG (1994) Use of monoclonal antibodies to study the structure and function of eukaryotic protein synthesis initiation factor eIF-2B. Eur. J. Biochem 221:399-410 Available at: [Accessed November 11, 2009].

133. O'Neil BJ, McKeown TR, DeGracia DJ, Alousi SS, Rafols JA, White BC (1999) Cell death, calcium mobilization, and immunostaining for phosphorylated eukaryotic initiation factor 2-alpha (eIF2alpha) in neuronally differentiated NB-104 cells: arachidonate and radical-mediated injury mechanisms. Resuscitation 41:71-83 Available at: [Accessed

November 8, 2009].

134. Panniers R (1994) Translational control during heat shock. Biochimie 76:737-747 Available at: [Accessed December 2, 2011].

135. Papas S, Crépel V, Hasboun D, Jorquera I, Chinestra P, Ben-Ari Y (1992) Cycloheximide Reduces the Effects of Anoxic Insult In Vivo and In Vitro. Eur. J. Neurosci. 4:758-765 Available at: [Accessed December 1, 2011].

136. Paxinos G, Watson C (1998) The rat brain in stereotaxic coordinates 4th ed. New York: Academic Press.

137. Perlmutter LS, Siman R, Gall C, Seubert P, Baudry M, Lynch G (1988) The ultrastructural localization of calcium-activated protease "calpain" in rat brain. Synapse 2:79-88 Available at: [Accessed November 8, 2009].

138. Pestka S (1971) Inhibitors of ribosome functions. Annu. Rev. Microbiol. 25:487-562 Available at: [Accessed December 1, 2011].

139. Pulsinelli WA, Duffy TE (1983) Regional energy balance in rat brain after transient forebrain ischemia. J. Neurochem 40:1500-1503 Available at: [Accessed November 9, 2009].

140. Rami A (2003) Ischemic neuronal death in the rat hippocampus: the calpain-calpastatin-caspase hypothesis. Neurobiol. Dis 13:75-88 Available at: [Accessed November 8, 2009].

141. Roberts GG, Di Loreto MJ, Marshall M, Wang J, DeGracia DJ (2007) Hippocampal cellular stress responses after global brain ischemia and reperfusion. Antioxid. Redox Signal 9:2265-2275 Available at: [Accessed December 12, 2009].

142. Roger VL et al. (2011) Heart disease and stroke statistics--2011 update: a report from the American Heart Association. Circulation 123:e18-e209 Available at: [Accessed September 6, 2011].

143. Ron D (2002) Translational control in the endoplasmic reticulum stress response. J. Clin. Invest. 110:1383-1388 Available at: [Accessed December 2, 2011].

144. Rosenwald IB, Lazaris-Karatzas A, Sonenberg N, Schmidt EV (1993)(a) Elevated levels of cyclin D1 protein in response to increased expression of eukaryotic initiation factor 4E. Mol. Cell. Biol 13:7358-7363 Available at: [Accessed November 13, 2009].

145. Rosenwald IB, Rhoads DB, Callanan LD, Isselbacher KJ, Schmidt EV (1993)(b) Increased expression of eukaryotic translation initiation factors eIF-4E and eIF-2 alpha in response to growth induction by c-myc. Proc. Natl. Acad. Sci. U.S.A 90:6175-6178 Available at: [Accessed November 13, 2009].

146. Rowlands AG, Panniers R, Henshaw EC (1988) The catalytic mechanism of guanine nucleotide exchange factor action and competitive inhibition by phosphorylated eukaryotic initiation factor 2. J. Biol. Chem 263:5526-5533 Available at: [Accessed November 11, 2009].

147. Saido TC, Sorimachi H, Suzuki K (1994) Calpain: new perspectives in molecular diversity and physiological-pathological involvement. FASEB J 8:814-822 Available at: [Accessed November 30, 2009].

148. Sairanen T, Ristimäki A, Karjalainen-Lindsberg ML, Paetau A, Kaste M, Lindsberg PJ (1998) Cyclooxygenase-2 is induced globally in infarcted human brain. Ann. Neurol 43:738-747 Available at: [Accessed November 8, 2009].

149. Sakurai T, Yanagisawa M, Takuwa Y, Miyazaki H, Kimura S, Goto K, Masaki T (1990) Cloning of a cDNA encoding a non-isopeptide-selective subtype of the endothelin receptor. Nature 348:732-735 Available at: [Accessed December 1, 2009].

150. Sato K, Oka M, Hasunuma K, Ohnishi M, Sato K, Kira S (1995) Effects of separate and combined ETA and ETB blockade on ET-1-induced constriction in perfused rat lungs.

Am. J. Physiol 269:L668-672 Available at: [Accessed December 1, 2009].

151. Sattler R, Tymianski M (2001) Molecular mechanisms of glutamate receptor-mediated excitotoxic neuronal cell death. Mol. Neurobiol 24:107-129 Available at: [Accessed November 30, 2009].

152. Schmued LC, Albertson C, Slikker W Jr (1997) Fluoro-Jade: a novel fluorochrome for the sensitive and reliable histochemical localization of neuronal degeneration. Brain Res. 751:37-46 Available at: [Accessed October 11, 2011].

153. Schwartz DC, Parker R (2000) mRNA decapping in yeast requires dissociation of the cap binding protein, eukaryotic translation initiation factor 4E. Mol. Cell. Biol. 20:7933-7942 Available at: [Accessed November 15, 2011].

154. Siemkowicz E, Hansen AJ (1981) Brain extracellular ion composition and EEG activity following 10 minutes ischemia in normo- and hyperglycemic rats. Stroke 12:236-240 Available at: [Accessed November 8, 2009].

155. Siesjö BK (1994) Calcium-mediated processes in neuronal degeneration. Ann. N. Y. Acad. Sci. 747:140-161 Available at: [Accessed December 2, 2011].

156. Silver IA, Erecińska M (1990) Intracellular and extracellular changes of [Ca2+] in hypoxia and ischemia in rat brain in vivo. J. Gen. Physiol 95:837-866 Available at: [Accessed November 8, 2009].

157. Silver IA, Erecińska M (1992) Ion homeostasis in rat brain in vivo: intra- and extracellular [Ca2+] and [H+] in the hippocampus during recovery from short-term, transient ischemia. J. Cereb. Blood Flow Metab 12:759-772 Available at: [Accessed November 8, 2009].

158. Simon RP, Cho H, Gwinn R, Lowenstein DH (1991) The temporal profile of 72-kDa heat-shock protein expression following global ischemia. J. Neurosci. 11:881-889

Available at: [Accessed December 2, 2011].

159. Simon RP, Swan JH, Griffiths T, Meldrum BS (1984) Blockade of N-methyl-D-aspartate receptors may protect against ischemic damage in the brain. Science 226:850-852 Available at: [Accessed November 30, 2009].

160. Smith ML, Auer RN, Siesjö BK (1984) The density and distribution of ischemic brain injury in the rat following 2-10 min of forebrain ischemia. Acta Neuropathol 64:319-332 Available at: [Accessed November 7, 2009].

161. Sonenberg N, Dever TE (2003) Eukaryotic translation initiation factors and regulators. Curr. Opin. Struct. Biol 13:56-63 Available at: [Accessed November 12, 2009].

162. Sonenberg N, Hinnebusch AG (2009) Regulation of translation initiation in eukaryotes: mechanisms and biological targets. Cell 136:731-745 Available at: [Accessed November 11, 2009].

163. Stoecklin G, Stubbs T, Kedersha N, Wax S, Rigby WFC, Blackwell TK, Anderson P (2004) MK2-induced tristetraprolin:14-3-3 complexes prevent stress granule association and ARE-mRNA decay. EMBO J. 23:1313-1324 Available at: [Accessed December 2, 2011].

164. Sun GY, Xu J, Jensen MD, Simonyi A (2004) Phospholipase A2 in the central nervous system. Journal of Lipid Research 45:205 -213 Available at: [Accessed September 13, 2011].

165. Svitkin YV, Imataka H, Khaleghpour K, Kahvejian A, Liebig HD, Sonenberg N (2001) Poly(A)-binding protein interaction with elF4G stimulates picornavirus IRES-dependent translation. RNA 7:1743-1752 Available at: [Accessed November 14, 2009].

166. Takeda K, Inoue H, Tanizawa Y, Matsuzaki Y, Oba J, Watanabe Y, Shinoda K, Oka Y (2001) WFS1 (Wolfram syndrome 1) gene product: predominant subcellular localization

to endoplasmic reticulum in cultured cells and neuronal expression in rat brain. Hum. Mol. Genet. 10:477-484 Available at: [Accessed December 2, 2011].

167. Teixeira D, Parker R (2007) Analysis of P-body assembly in Saccharomyces cerevisiae. Mol. Biol. Cell 18:2274-2287 Available at: [Accessed November 15, 2011].

168. Temecula (2009) Sudden Cardiac Arrest. The City of Temecula Available at: http://www.cityoftemecula.org/temecula/Templates/Residents_3rdLevel_css.aspx?NRMODE=Published&NRNODEGUID={92ED7667-0F27-40EC-9E7E-4D3F49DDCAE5}&NRORIGINALURL=%2Ftemecula%2FResidents%2FPublicSafety%2FSuddenCardiacArrest%2F&NRCACHEHINT=NoModifyGuest.

169. Tenenbaum SA, Lager PJ, Carson CC, Keene JD (2002) Ribonomics: identifying mRNA subsets in mRNP complexes using antibodies to RNA-binding proteins and genomic arrays. Methods 26:191-198 Available at: [Accessed October 4, 2009].

170. Ulrich CM, Bigler J, Potter JD (2006) Non-steroidal anti-inflammatory drugs for cancer prevention: promise, perils and pharmacogenetics. Nat Rev Cancer 6:130-140 Available at: [Accessed November 30, 2009].

171. Valadkhan S (2007) The spliceosome: caught in a web of shifting interactions. Curr. Opin. Struct. Biol. 17:310-315 Available at: [Accessed November 15, 2011].

172. Vass K, Welch WJ, Nowak TS Jr (1988) Localization of 70-kDa stress protein induction in gerbil brain after ischemia. Acta Neuropathol. 77:128-135 Available at: [Accessed December 2, 2011].

173. Vries RG, Flynn A, Patel JC, Wang X, Denton RM, Proud CG (1997) Heat shock increases the association of binding protein-1 with initiation factor 4E. J. Biol. Chem 272:32779-32784 Available at: [Accessed November 13, 2009].

174. Wang X, Flynn A, Waskiewicz AJ, Webb BL, Vries RG, Baines IA, Cooper JA, Proud

CG (1998) The phosphorylation of eukaryotic initiation factor eIF4E in response to phorbol esters, cell stresses, and cytokines is mediated by distinct MAP kinase pathways. J. Biol. Chem 273:9373-9377 Available at: [Accessed November 13, 2009].

175. White BC, Grossman LI, Krause GS (1993) Brain injury by global ischemia and reperfusion: a theoretical perspective on membrane damage and repair. Neurology 43:1656-1665 Available at: [Accessed September 6, 2011].

176. White BC, Hildebrandt JF, Evans AT, Aronson L, Indrieri RJ, Hoehner T, Fox L, Huang R, Johns D (1985) Prolonged cardiac arrest and resuscitation in dogs: Brain mitochondrial function with different artificial perfusion methods. Annals of Emergency Medicine 14:383-388 Available at: [Accessed September 6, 2011].

177. White BC, Sullivan JM, DeGracia DJ, O'Neil BJ, Neumar RW, Grossman LI, Rafols JA, Krause GS (2000) Brain ischemia and reperfusion: molecular mechanisms of neuronal injury. J. Neurol. Sci. 179:1-33 Available at: [Accessed December 2, 2011].

178. Xie Y, Zacharias E, Hoff P, Tegtmeier F (1995) Ion channel involvement in anoxic depolarization induced by cardiac arrest in rat brain. J. Cereb. Blood Flow Metab 15:587-594 Available at: [Accessed November 8, 2009].

179. Yokota M, Saido TC, Tani E, Kawashima S, Suzuki K (1995) Three distinct phases of fodrin proteolysis induced in postischemic hippocampus. Involvement of calpain and unidentified protease. Stroke 26:1901-1907 Available at: [Accessed December 2, 2011].

180. Zhang F, Liu CL, Hu BR (2006) Irreversible aggregation of protein synthesis machinery after focal brain ischemia. J. Neurochem 98:102-112 Available at: [Accessed November 24, 2009].

181. Zhao H, Sapolsky RM, Steinberg GK (2006) Interrupting reperfusion as a stroke therapy: ischemic postconditioning reduces infarct size after focal ischemia in rats. J. Cereb.

Blood Flow Metab 26:1114-1121 Available at: [Accessed November 17, 2009].

ABSTRACT

MECHANISMS OF PERSISTENT TRANSLATION ARREST FOLLOWING GLOBAL BRAIN ISCHEMIA & REPERFUSION

by

JILL T. JAMISON

May 2012

Advisor: Donald J. DeGracia, Ph.D.

Major: Physiology

Degree: Doctor of Philosophy

The information presented here studies the mechanisms that underlie persistent TA following global brain I/R. To summarize the main findings I have discovered a new mechanism for prolonged post-ischemic TA that correlated exactly with *in vivo* translation rates and correlated precisely with cell outcome. Through the extensive colocalization studies, my results indicate that the mRNA granules are ribonomic structures involved with mRNA regulation. This finding is significant because it shifts the focus onto mRNA metabolism and away from ribosomal molecular biology. I have identified new pathways to investigate for understanding why there is selective delayed death in post-ischemic neurons, however my work also gives insight into why resistant neurons survive. The results were tested in a whole animal (male Long Evans rats) model of global brain I/R using *in situ* antibodies and mRNA staining methods, *in vivo* protein synthesis and Western blots. Results are collectively summarized below:

1. Cytoplasmic poly(A) containing mRNAs redistributed to form **mRNA granules** in reperfused neurons.
2. mRNA granules sequester mRNA away from both the small and large ribosomal subunits, providing a novel mechanism of prolonged TA in post-ischemic neurons.
3. mRNA granules are ribonomic structures.
4. mRNA granules, are neither stress granules, processing bodies, or polysomes.
5. mRNA granules were found to only colocalize with eIF4G, PABP and HuR, suggesting that mRNA granules may itself be related to or a subset of the ELAV/Hu granule.

6. HuR co-localized to mRNA granules and translation of HSP-70. This correlation suggests mRNA granules are involved in post-transcriptional stress gene regulation in reperfused neurons.
7. mRNA granules are causally linked to TA.

AUTOBIOGRAPHICAL STATEMENT

JILL T. JAMISON

EDUCATION:

Wayne State University	Detroit, MI	
Ph.D in Physiology	planned graduation date:	May 2012
Arizona State University		
BS in Psychology	April 2002	
St. Clair County Community College		
Associate Degree	May 1998	

PUBLICATIONS:

1. **Jamison, JT**., Szymanski, JJ., DeGracia, DJ. Lack of Colocalization of mRNA Granules and Organelles do not colocalize with mRNA granules in post-ischemic neurons. Neuroscience. 2011; Epub.
2. Szymanski, JJ., **Jamison, JT**., DeGracia, DJ. Texture analysis of poly-adenylated mRNA staining following global brain ischemia and reperfusion. Comput Methods Programs Biomed. 2011 Apr 6; Epub.
3. **Jamison JT**. Lewis MK, Kreipke CW. Rafols J. DeGracia DJ. Polyadenylated mRNA staining reveals distinct neuronal phenotypes following endothelin 1, focal brain ischemia, and global brain ischemia/ reperfusion. Neurological Research 2011;33(2):145-161.
4. DeGracia DJ, **Jamison JT**, Szymanski JJ, Lewis MK. Translation arrest and ribonomics in post-ischemic brain: layers and layers of players. J Neurochem. 2008;106(6):2288-301.
5. **Jamison JT**, Kayali F, Rudolph J, Marshall M, Kimball SR, DeGracia DJ. Persistent redistribution of poly-adenylated mRNAs correlates with translation arrest and cell death following global brain ischemia and reperfusion. Neuroscience. 2008;154(2):504-20.